Universidad Autónoma de Madrid

Programa de Doctorado en Biociencias Moleculares

Regulation of endothelial cell cycle dynamics by Notch during angiogenesis

Samuel Pontes Quero

Madrid, 2018

Programa de Doctorado en Biociencias Moleculares

Departamento de Bioquímica

Facultad de Medicina

Universidad Autónoma de Madrid

Regulation of endothelial cell cycle dynamics by Notch during angiogenesis

Doctoral Thesis

Samuel Pontes Quero

Licenciado en Biología

Madrid, 2018

Director: Dr. Rui Benedito

Centro Nacional de Investigaciones Cardiovasculares (CNIC)

Financial Support:

The laboratory of Dr. Rui Benedito is supported by the following grants:

- From the Spanish Ministry of Economy, Industry and Competitiveness (SAF2013-44329-P, SAF2013- 42359-ERC, and RYC-2013-13209).
- From the European Research Council (ERC- 2014-StG - 638028).

Samuel Pontes was supported by a PhD fellowship by the Fundación La Caixa (CX-SO-2013-02)

The CNIC is supported by the Ministerio de Economía, Industria y Competitividad (MEIC) and the Pro CNIC Foundation, and is a Severo Ochoa Center of Excellence (SEV-2015-0505)

This work was performed under the direction of Dr. Rui Benedito´s laboratory in the Developmental Biology and Repair Department at the Spanish National Center for Cardiovascular Research (CNIC) in Madrid.

The thesis director, Dr. Rui Benedito certifies that this thesis has been carried out under his supervision.

SUMMARY / RESUMEN

SUMMARY

The formation of new blood vessels by angiogenesis requires the precise coordination of endothelial cell differentiation, proliferation, migration and maturation to ensure that a proper vasculature is formed to satisfy the metabolic needs of the surrounding tissue. The Notch signaling pathway is a critical regulator of endothelial cell biology, participating in different processes of blood vessel formation from tip-cell specification to arterio-venous differentiation and blood vessel stabilization. Inhibition of this pathway during angiogenesis has been associated with increased proliferation of endothelial cells. However, this seemingly antiproliferative effect of Notch activation does not adjust well to the current tip-stalk cell model of molecular control of angiogenesis, in which proliferative stalk cells are defined as having higher Notch activity.

In this work we have tried to resolve this apparent paradox by characterizing in detail the effects of Notch on endothelial cell proliferation *In vivo*. We have used different pharmacological and classical genetic approaches in combination with newly developed mosaic genetic tools to evaluate, with high spatio-temporal resolution, endothelial cell cycle dynamics.

We have found that physiological Notch activation is required for maintaining endothelial cell proliferation by repressing excessive activation of pro-proliferative molecular mechanism. Inhibition of Notch activity induces and hyperproliferative response that is partially dependent on ERK activation. This response is, however, not sustained in time and leads to proliferative arrest, partially mediated by ERK overactivation and p21 upregulation. This cell-cycle arrest is associated with an increase in the expression of genes characteristic of sprouting tip cells. Thus, Notch can control a mechanism to differentiate between a proliferative and migratory cellular response.

Comparative trancriptomics revealed new putative Notch-repressed genes that promote cell cycle progression like Myc and Odc1. Functional analysis of these genes showed their absolute requirement for normal endothelial cell proliferation.

RESUMEN

La generación de nuevos vasos sanguíneos mediante angiogénesis requiere la precisa coordinación de procesos de diferenciación, proliferación, migración y maduración de células endoteliales para asegurar la correcta formación de una red vascular que satisfaga las necesidades metabólicas del tejido circundante. La vía de señalización de Notch es un regulador clave de la biología endotelial ya que participa en distintos procesos durante la formación de los vasos sanguíneos, incluyendo la especificación de células *tip* y *stalk*, la diferenciación arterio-venosa o la estabilización de la vasculatura. La inhibición de esta vía durante la angiogénesis se ha asociado con un incremento de la proliferación del endotelio. Sin embargo, este efecto antiproliferativo no se ajusta completamente al modelo actual de control molecular de la angiogénesis basado en la especificación de células *tip* y *stalk*, por el cual se considera que las células *stalk* proliferativas tienen mayor activación de Notch

En esta Tesis hemos tratado de resolver esta aparente paradoja mediante la caracterización de los efectos de Notch en la proliferación de células endoteliales *In vivo.* Para ello hemos empleado una combinación de métodos farmacológicos y genéticos clásicos con el desarrollo de nuevas herramientas genéticas para generar mosaicos funcionales y evaluar con gran resolución espacio-temporal la dinámica del ciclo celular en células endoteliales.

Hemos descubierto que la activación de Notch es necesaria para mantener el estado proliferativo de células endoteliales mediante la represión de una activación excesiva de señales pro-proliferativas. La excesiva proliferación tras la inhibición de Notch depende parcialmente de la activación de ERK. Esta respuesta, sin embargo, no se mantiene en el tiempo y conduce a una interrupción en la proliferación, que está parcialmente controlada por la sobreactivación de ERK y la sobreexpresión de la proteína p21. Esta detención del ciclo celular se asocia con la expresión de marcadores típicos de células *tip*. Por lo tanto Notch forma parte de un mecanismo que permite diferenciar entre células endoteliales con actividad proliferativa o migratoria. Análisis transcriptómicos comparativos también han revelado nuevos genes que promueven la proliferación y que podrían estar reprimidos por Notch, como Myc y Odc1. El análisis genético funcional de estos genes ha mostrado que son absolutamente esenciales para la proliferación normal de las células endoteliales.

TABLE OF CONTENTS

INDEX OF FIGURES AND TABLES

Figures

Tables

Supplementary RNAseq DATA is provided in the digital format of the thesis.

LIST OF ABBREVIATIONS

ADAM Angiopoietin-1 receptor

AF Angiogenic Front

AF# Alexa Fluor#

Akt Protein kinase B (PKB)

Angp Angiopoietin

APC Allophycocyanin

b-Gal beta-galactosidase

BAC Bacterial artificial chromosomes

bHLH: Basic-Helix-Loop-Helix

BM Basal lamina

BSA Bovine Serum ALbumin

CBF C-Repeat Binding Factors

Cdh5 Cadherin 5 / VE-Cadherin

CDK Cyclin dependent Kinase

CIp/Kip CDK interacting protein/Kinase inhibitory protein

CKI CDK inhibitor

CXCR4 C-X-C chemokine receptor type 4

DAPI 4',6-diamidino-2-phenylindole

Dll Delta-like

DMSO Dimethyl sulfoxide

DNA Deoxyribonucleic acid

E#: Embryonic Day #

EB: Embryoid Body

EC Endothelial cell

EdU 5-ethynyl-2-deoxyuridine

EGFP Enhanced GFP

ERG ETS-related gene

ERK Extracellular signal–regulated kinase

Esm1 Endothelial cell-specific molecule 1

FBS fetal bovine serum

Flk-1 VEGFR2/Kdr

Flt-1 Fms-like tyrosine kinase 1 (VEGFR-1)

Flt-4 Fms related tyrosin kinase 4 (VEGFR-3)

FP Fluorescent protein

GFP Green fluorescent protein

H2B Histone 2B

HA Human Influenza Hemagglutinin

HEKs Human embryonic kidney cells 293, HEK-293 cells

Hes Hairy/Enhancer of split Hey: Hairy Related genes

Hey Hairy and enhancer-of-split related with YRPW motif protein

HUVEC Human umbilical vein endothelial cell

iChr inducible chromatin

IF Immunofluorescence

Ig Immunoglobulin

iMb inducible membrane

Ink4 I**N**hibitors of CD**K4**

ISV Intersomitic Vessel

Kdr Kinase insert domain receptor. In zebrafish also Flk-1b or VEGFR-2.

LSL Lox-STOP-Lox

MADM Mosaic analysis with double markers

MAML1 Mastermind-like protein 1

MAPK Mitogen-activated protein kinase

MEF Mouse embryonic fibroblast

MEK Mitogen-activated protein kinase kinase

mESC mouse embryonic stem cell

NICD NOTCH intracellular domain

NRP Neuropilin

O/N Overnight

Oaz1 Ornithine decarboxylase antizyme

Odc1 Ornithine decarboxylase

P# Postnatal day #)

PBS Phosphate-buffered saline

PCR Polymerase chain reaction

PDGFb Platelet-derived growth factor-B

PEST: Proline, glutamic acid, serine and treonined enriched-domain

PFA Paraformaldehyde

PI3K Phosphatidylinositol-4,5-bisphosphate 3-kinase

PLGF Placental Growth Factor

PTEN Phosphatase and tensin homolog 2

qPCR Quantitative polymerase chain reaction

RBPJ Recombination Signal-Binding Protein 1 for J-Kappa sequence (CBF1 in mammals)

RT Room temperature

RTKs Tyrosine kinase receptors

SEM Standard error of the mean

SMC: Smooth muscle cell

Src Proto-oncogene tyrosine-protein kinase

SV40: Simian vacuolating virus 40

Tie2 Angiopoietin-1 receptor

VEGF Vascular endothelial growth factor

VEGFR Vascular endothelial growth factor receptor

WT: Wild type

INTRODUCTION

1 INTRODUCTION

1.1 The cardiovascular system

The evolution of complex multicellular organisms required the presence of a system devoted to nutrient and waste transport to overcome the inefficiency of a simple diffusion-based transport mechanism, when organisms size increased and surface:volume ratios decreased (Muñoz-Chápuli and Pérez-Pomares, 2010). In vertebrates the necessity for a transport system is already apparent during embryonic development, as the cardiovascular system is the first functional organ to be formed. This allows for the subsequent normal development of the remaining organs and systems (Chung and Ferrara, 2011). In addition to its transport function it is now acknowledged that the cells that form the cardiovascular system have also an essential paracrine regulatory role that influence the development and homeostasis of other organs (Udan, Culver and Dickinson, 2013; Rafii, Butler and Ding, 2016).

The cardiovascular system in vertebrates is formed by the heart and the network of vessels connected to it that extends throughout their bodies. The vasculature is functionally subdivided in three types of blood vessels that exhibit differences at the structural, cellular and molecular levels. Arteries are the vessels that carry blood out from the heart and progressively decrease in size until they reach the vascular networks in the tissues. This vascular network is formed by the smallest vessels, the capillaries, and is where the nutrient and waste exchange occur between blood and the tissues. Finally, from capillaries, blood is transported back to the heart by increasingly bigger veins (Potente and Mäkinen, 2017). The distinct functions of the three types of vessels are related with their structural differences. Arteries have a thinner diameter and are covered by a thick layer of smoot muscle cells (SMC)s to provide and regulate vascular tension, whereas capillaries have a more permeable structure to diffuse nutrients and waste products, and veins tend to have a larger diameter and valves to offer low resistance and enable unidirectional blood flow.

All three types of vessels are formed by layer of endothelial cells (ECs) arranged as a squamous epithelium (the endothelium) forming the inner lining of the vessels. Surrounding the endothelium other cell types can be associated to the basal lamina (BM), secreted by the ECs, to give support and functionally differentiate the vessels. In capillaries, pericytes stabilize the endothelium and also contribute to its circulatory dynamics. When compared with veins, arteries have a thicker layer of SMCs (Media) and a distinct extracellular matrix (Adventitia), which is in accordance with their different functional roles in the circulatory system (Fig. 1.1).

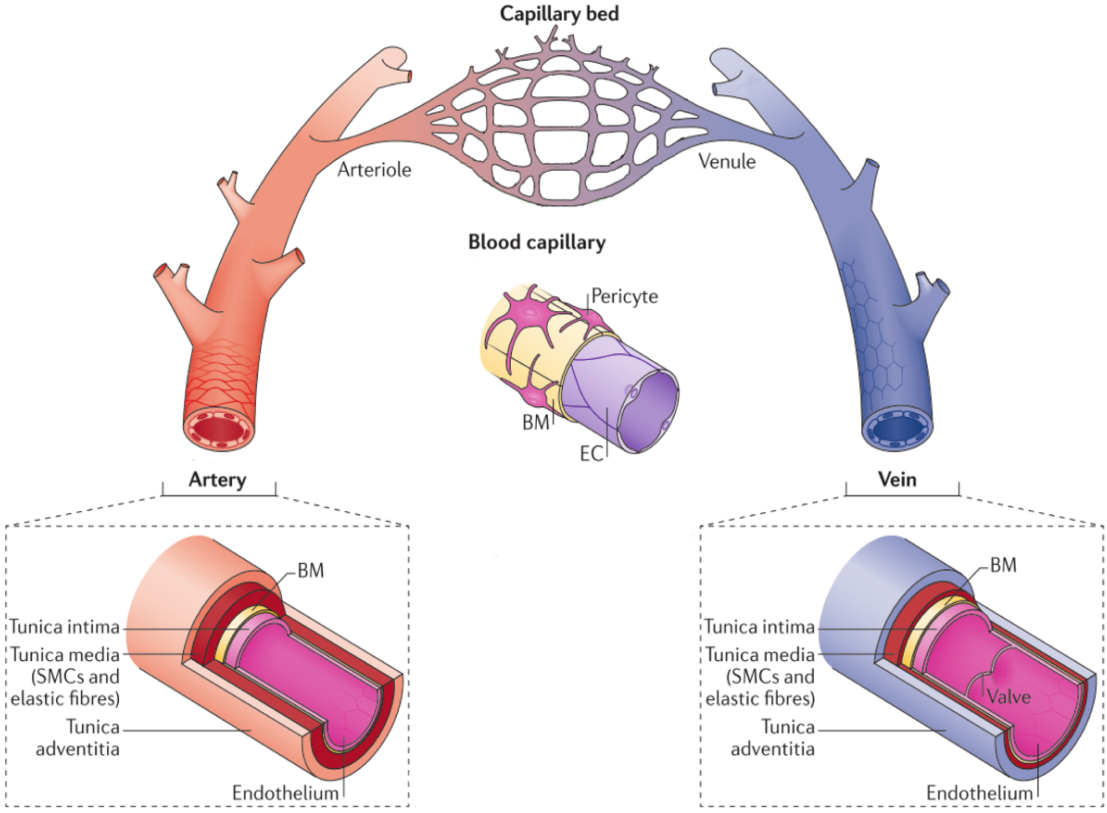

Figure 1.1. Organization of the vascular system. Hierarchical organization of the blood vascular system formed by three main types of blood vessels: arteries, capillaries and veins. Arteries and veins of smaller caliber that connect with the capillary network are denominated arterioles and venules respectively. The three types of vessels are internally lined by ECs and their associated BM. This is denominated tunica intima in larger vessels. Additional cells are associated with the ECs: perycites in capillaries and SMCs in arteries and veins. These larger vessels have and additional layer of supportive connective tissue. Note bigger size of the elastic SMC layer in arteries (Modified from Potente & Mäkinen, 2017).

1.2 The development of the vascular system

During development there are two main processes that give rise to new blood vessels: vasculogenesis and angiogenesis. Vasculogenesis mainly occurs at early stages in embryonic development and involves *de novo* formation of endothelial cells from undifferentiated mesodermal precursors called angioblasts (Risau and Flamme, 1995). In mice this process occurs prominently in the yolk sac, associated to early hematopoiesis, giving rise to primitive vascular plexus filled with blood precursors called blood islands. Vasculogenesis also occurs in several places along the antero-posterior axis of the embryo from lateral mesoderm derived cells, generating several immature primary vascular plexus (Drake and Fleming, 2000) (Fig. 1.2 Left).

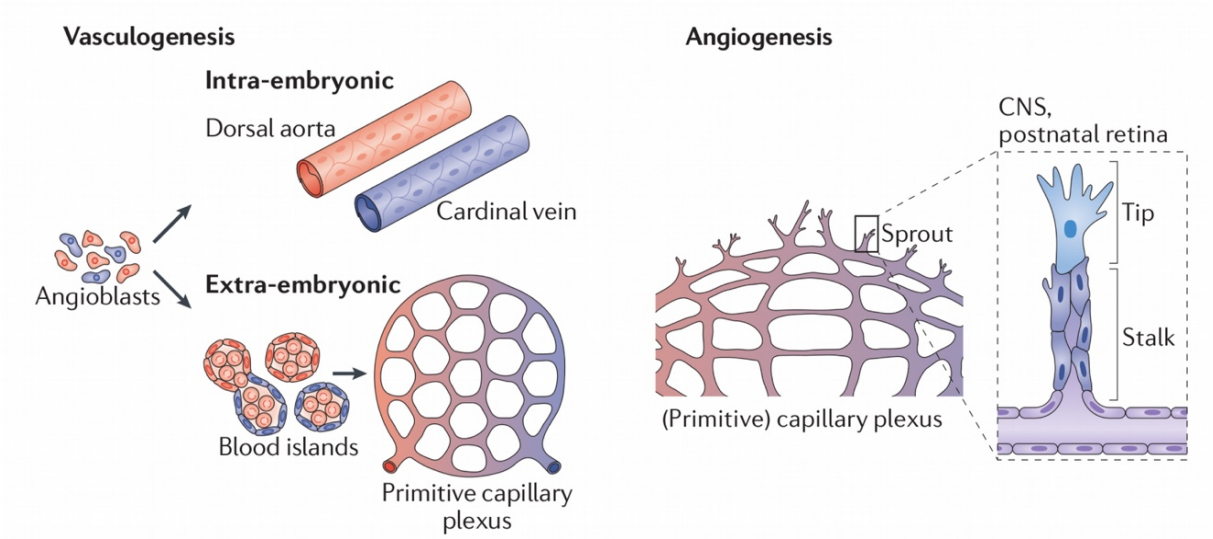

Figure 1.2. Mechanisms of vessel formation. Blood vessel are generated by two different mechanisms: vasculogenesis (left) and angiogenesis (right). During vasculogenesis mesodermal precursors called angioblast coalesce in different parts of the embryo to form primitive vascular networks and the principal blood vessels of the embryo. From the primitive capillary plexus formed, sprouting angiogenesis occurs through the selection of migratory sprouts composed by migratory tip cells and trailing proliferative stalk cells (Modified from Potente & Mäkinen ,2017).

Angiogenesis occurs later as it involves the formation of new vessels from preexisting ones, without additional endothelial cell differentiation (Fig. 1.2 Right). Angiogenesis not only occurs during development but it is also important during normal physiological processes in adult animals, like the female reproductive cycle and wound repair. Moreover, blood vessel formation is involved in pathological process like tumor progression or ischemic cardiovascular disease (Carmeliet and Jain, 2011).

Two mechanistically different types of angiogenesis have been described: sprouting and intussusceptive angiogenesis. While sprouting angiogenesis is the main type involved in the expansion of vascular networks towards avascular areas, intussusceptive angiogenesis has been more associated with posterior remodeling and maturation of these networks in response to blood flow dynamics (Burri, Hlushchuk and Djonov, 2004).

1.3 Sprouting angiogenesis

Sprouting angiogenesis is the main mechanism by which blood vessels expand to tissues that require vascularization. It is first initiated through paracrine signaling from the hypoxic tissue that is close to capillaries. This activates endothelial cells in blood vessels and instructs them to form vascular sprouts composed by a few ECs that have been denominated tip cells (Potente, Gerhardt and Carmeliet, 2011). These sprouts form at variable intervals along the vascular front and are able to locally modify the extracellular matrix and to migrate towards the avascular areas of the tissue. However, in order for sprouting angiogenesis to be efficient, and result in the formation of a honeycomb like capillary network, vascular loops and side-connections need to occur. These occur when two sprouts contact during their migration, through a process called as anastomosis. After this process, they lumenize to give rise to a new vessel branch. At the same time, surrounding endothelial cells generally denominated stalk cells proliferate to supply more cells to the newly forming immature vessel network that advances until the initial pro-angiogenic signals disappear (Fig. 1.3).

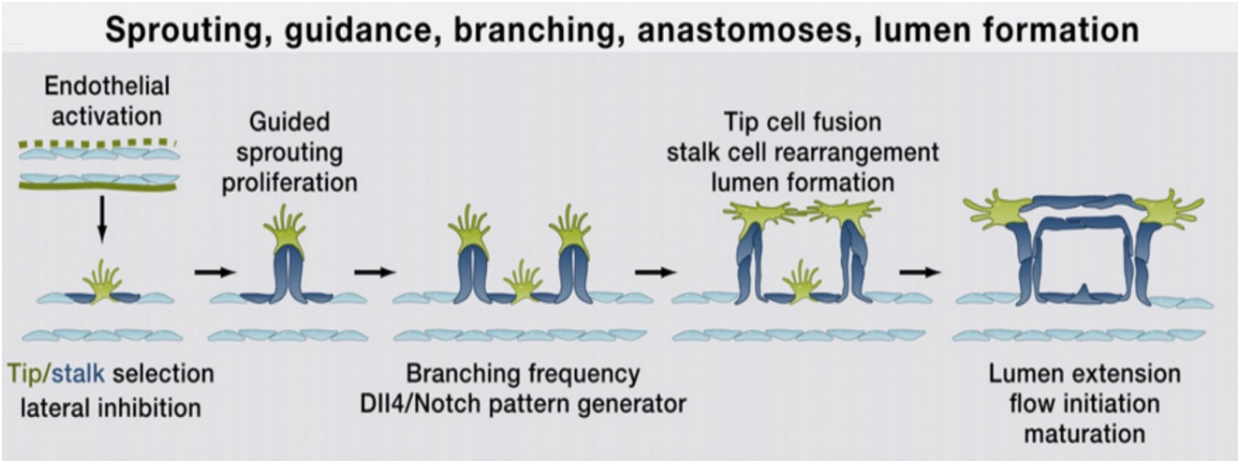

Figure 1.3. Sprouting angiogenesis. Sprouting angiogenesis starts when proangiogenic signals, mainly VEGF, secreted by hypoxic tissues are detected by the endothelial cells. This induces to the selection of tip cell along the vascular front that start to migrate (Green) and are followed by proliferating cells (Blue). When tip cells from adjacent sprouts contact they form a new vessel branch. This process occurs recursively until the tissue is fully vascularized (Modified from Potente, Gerhardt and Carmeliet, 2011).

In parallel to the formation of new vessels at the angiogenic front, the vessels already formed start a process of maturation, recruiting perycites and SMCs, and remodeling to achieve the final blood flow dynamics that better suits the surrounding tissue needs. This is achieved by the pruning of some branches of the maturing vascular network and stabilization of others as well as progressive specialization into arterial and venous endothelial cells gives rise to the final hierarchical organization of the mature vasculature (Potente, Gerhardt, and Carmeliet 2011).

1.4 *In vivo* models of sprouting angiogenesis

Two main systems have been widely used to study the molecular mechanisms that regulate angiogenesis *In vivo*: the vascularization of the mouse postnatal retina and the formation of intersomitic and brain vessels during zebrafish embryonic development. Each system has a different set of advantages and caveats but in conjunction both have been instrumental to identify and study several molecular and cellular mechanisms of angiogenesis.

The formation of intersomitic vessels (ISV) in zebrafish is a process that can be easily genetically targeted with morpholinos and live-imaged at high resolution with confocal microscopes. While the analysis of the development of these vessels has provided important insights into the regulatory signals and dynamics of angiogenesis they constitute a particular system of angiogenesis as sprouts form directly from arteries or veins, and the single sprouts follow a very defined path of migration and proliferate minimally. These differences call for caution when interpreting and extrapolating results obtained using this system to other vascular beds like the mouse retinal or tumor vasculature (Ellertsdóttir *et al.*, 2010).

1.4.1 Postnatal vascularization of mouse retina

Two different vascular networks provide vascular supply to the eye at different stages of development. During embryonic development, the hyaloid vasculature is composed of vessels that transverse the vitreous from the optic nerve towards the anterior part of the eye. These vessels however start regressing after birth to allow for normal vision (Stahl *et al.*, 2010).

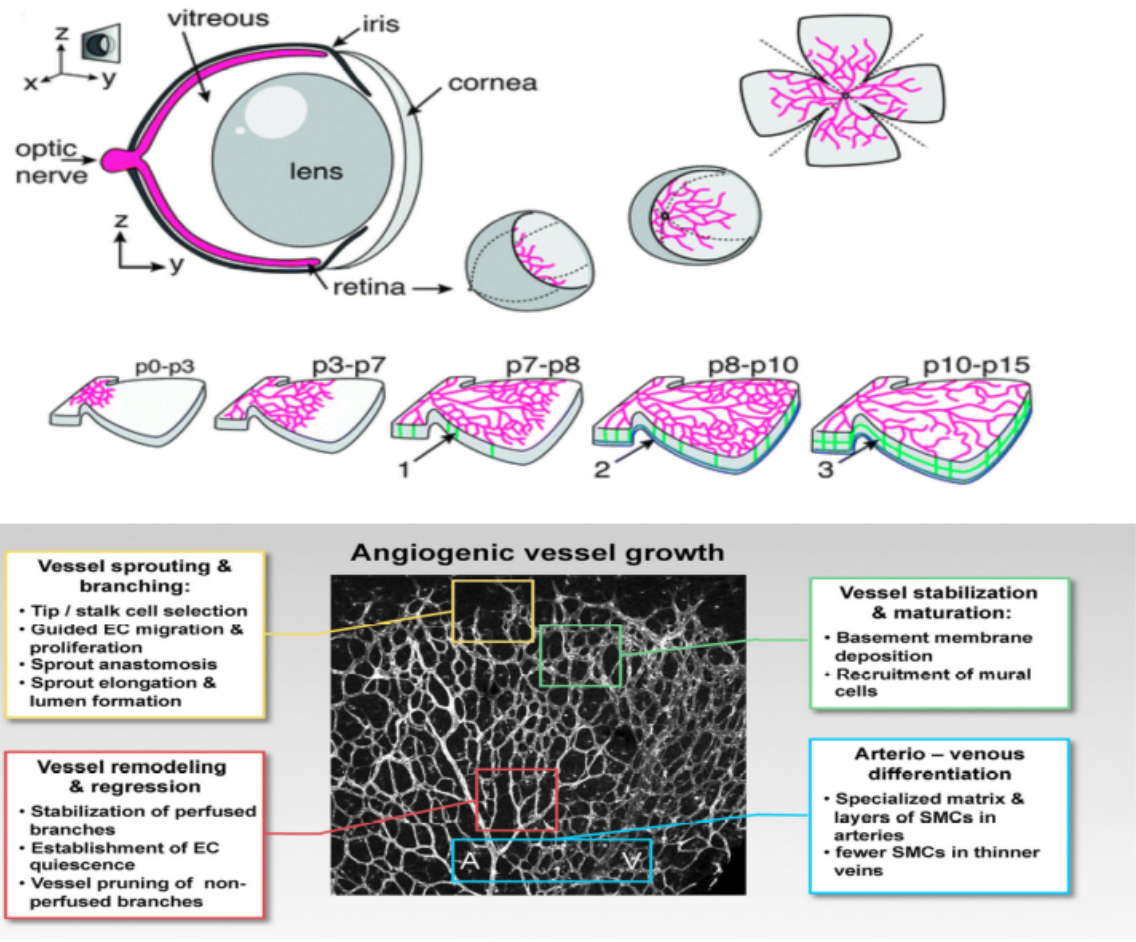

Figure 1.4. Mouse retinal vascularization. Endothelial cells enter the retina through the optic nerve opening and expand radially during the first postnatal week. Migration to deeper layer of the retina occurs from P7 and progress until the end of the second postnatal week. During the first week the stereotyped patterning of the expanding vascular plexus allows the analysis of different aspects of angiogenesis (Adapted from Milde *et al*., 2013 and Oellerich and Potente, 2012).

After birth, intraretinal vascularization commences, to substitute for the regressing hyaloid vasculature. Angiogenic endothelial cells enter the retina through the optic nerve area at the center of the retina. During the first postnatal week, expansion of the vasculature occurs in a two-dimensional and superficial plane towards the retinal periphery. ECs migrate over an

underlying astrocyte network through the process of sprouting angiogenesis, and proliferate to expand the vasculature (Fig. 1.4). As angiogenesis progresses, the vascular network closer to the center starts to mature and remodel, forming differentiated arterial, venous and capillary areas. From postnatal day (P) 7, in the maturing areas closer to the center, additional sprouting occurs towards the deeper layers of the retina. This leads to the formation of two additional interconnected parallel plexus. Remodeling and differentiation of these two networks proceeds until the retinal vasculature reaches full maturity around 6 weeks of age (Milde *et al.*, 2013).

The fundamental advantage in using this system is that during the first postnatal week, the two dimensional expansion of the vasculature allows for the straightforward global analysis of the full developing vascular network in a relatively thin confocal optical section. The relatively fixed and stereotyped vascular patterning of this network also facilitates the phenotypic analysis after genetic and pharmacological interventions. Moreover, it is possible to study different aspects of angiogenesis at the same time as remodeling and maturation can be analyzed in parallel to sprouting and proliferation in the same retina (Milde *et al.*, 2013).

1.5 Molecular regulation of vascular development

Several signaling pathways have been involved in the regulation of vascular development, however due to limitations of space, I will mention only the ones directly studied in this thesis. Particularly the VEGF and Notch signaling pathways have been found to strongly influence different aspects of endothelial cell biology.

1.5.1 The VEGF signaling pathway

Vascular Endothelial Growth Factor (VEGFs) compose a family of five secreted glycoproteins (VEGF A-D and placental growth factor, PLGF) that participate in numerous aspects of vascular and endothelial biology. They act by binding to three possible VEGF tyrosine kinase receptors (RTKs), VEGFR1 (Flt1), VEGFR2 (Flk1/Kdr) and VEGFR3 (Flt4) (Olsson *et al.*, 2006) (Fig. 1.5).

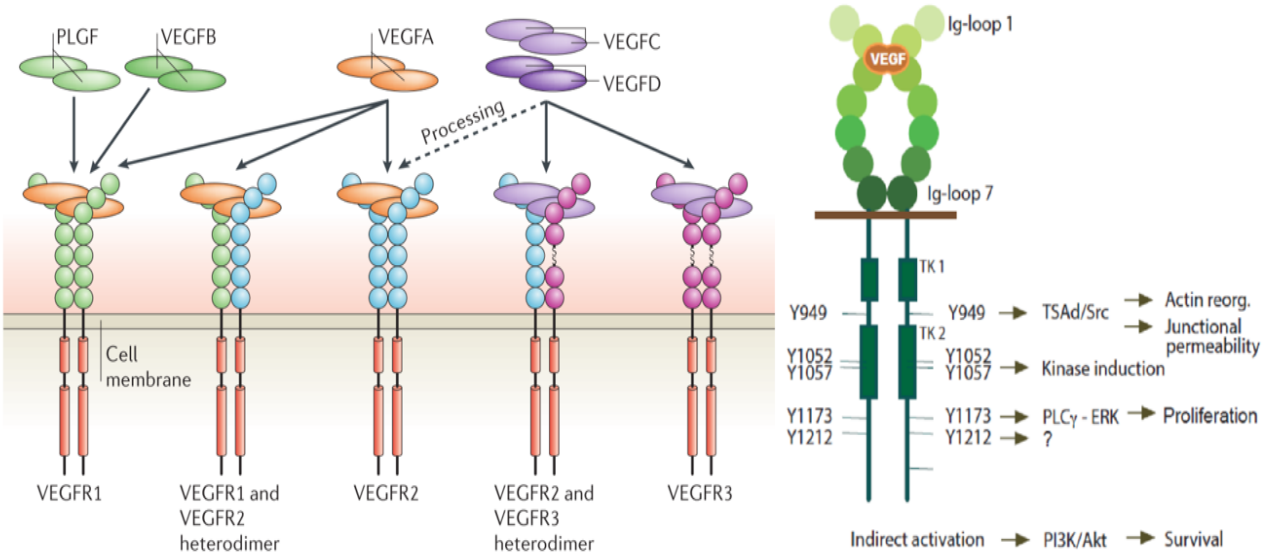

Figure 1.5. VEGF signaling pathway. The VEGF signaling family of ligands and receptors is composed of five secreted glycoproteins (VEGF A-D and placental growth factor, PLGF) with different specificities for three types of RTKs (VEGFR1-3) that can form homo- or heterodimers. Downstream signaling pathways that can be activated by VEGFR2 include the MAPK and PI3K/Akt pathways among others (Adapted from Olsson *et al.*, 2006 and Claesson-Welsh, 2016).

Ligand binding promotes the dimerization of the receptors and auto- or cross- phosphorylation in tyrosine residues. This in turn leads to the recruitment of different adapter proteins harboring SH2 domains and the activation of several downstream cascades including the PI3K/AKT and MAPK signaling pathways (Claesson-Welsh, 2016). VEGFRs can also bind to other co-receptors like neuropilins (NRP1 and 2) that can modulate their signaling output**.** VEGF signaling can be regulated at different levels: differential expression of ligands and receptors, ligand availability in the extracellular space, differential affinity between ligands and receptors and receptor membrane trafficking among others (Vempati, Popel and Mac Gabhann, 2014; Simons, Gordon and Claesson-Welsh, 2016).

Genetic elimination of the different members of the family has revealed differential roles in regulating vascular development. VEGFA signaling through VEGFR2 has been proposed as the main regulator of vascular development. VEGFR2 is highly expressed in ECs, particularly at stages of vessel formation and expansion. VEGFA can be expressed by a variety of cells, generally in response to conditions of hypoxia or lack of nutrients (Coultas, Chawengsaksophak, and Rossant,

2005). Animals with homozygous deletion of the VEGFR2 gene die very early during development due to severe defects in the initial stages of vasculogenesis and hematopoiesis (Shalaby *et al.*, 1995)**.** Heterozygous VEGFA mutants die of similar defects slightly later, also because of defects on EC differentiation and blood island formation (Carmeliet *et al.,* 1996; Ferrara *et al.*, 1996)**,** showing how the VEGF signaling dose must be tightly controlled.

In contrast, VEGFR1 elimination leads to hypervascularization due to increased EC proliferation and sprouting (Fong *et al*., 1995). These animals also die during development but it seems that VEGFR1 acts as a negative regulator of angiogenesis. This appears to be due to two aspects of the biology of VEGFR1. One is that its affinity towards VEGFA is much higher than that of VEGFR2 but its kinase activity is much weaker (Papadopoulos *et al.*, 2012). The other is that VEGFR1 presents an alternative splicing form that lack the transmembrane domain and is secreted (Kearney *et al.*, 2004). Due to this, both soluble and membrane VEGFR1 can act as a VEGF sink, blocking its binding to VEGFR2 and modulating in this way vascular VEGF signaling.

The other receptor, VEGFR3, is mainly activated by the ligands VEGFC and VEGFD (Olsson *et al.,* 2006) and is expressed in lymphatic vessels being the most important receptor for lymphangiogenesis. However, it is also expressed in blood ECs, and important for vascular development as its deletion its embryonic or postnatal deletion results in severe vascular defects (Dumont *et al.*, 1998).

1.5.2 The Notch signaling pathway

Notch signaling is a conserved pathway, essential in the regulation of a wide range of biological processes, from developmental morphogenesis and stem cell maintenance to tissue homeostasis and disease.

In mammals it is formed by four Notch receptors (Notch 1-4) and five ligands named Delta Like (Dll)1, Dll3, Dll4, Jagged1 and Jagged2 (Fig 1.6). Ligands and receptors are transmembrane proteins, thus constituting a juxtacrine signaling system that requires close physical interaction between sender and receiver cells (Bray, 2006).

Upon ligand binding, a series of proteolytic reactions occurs near the membrane of the receiving cell that lead to the processing of the receptor. The last of these cleavages is mediated by a γ-secretase complex that releases the Notch Intra Cellular Domain, NICD. This protein translocates to the nucleus and forms a complex with a DNA binding protein called CSL/RBPJk and the transcriptional coactivator MAML1 (Kopan and Ilagan, 2009). This complex regulates the transcription of different targets genes including the family of basic helix-loop-helix (bHLH) transcriptional repressors Hes/Hey and the Notch ligand Dll4 among others (Iso, Kedes, and Hamamori, 2003).

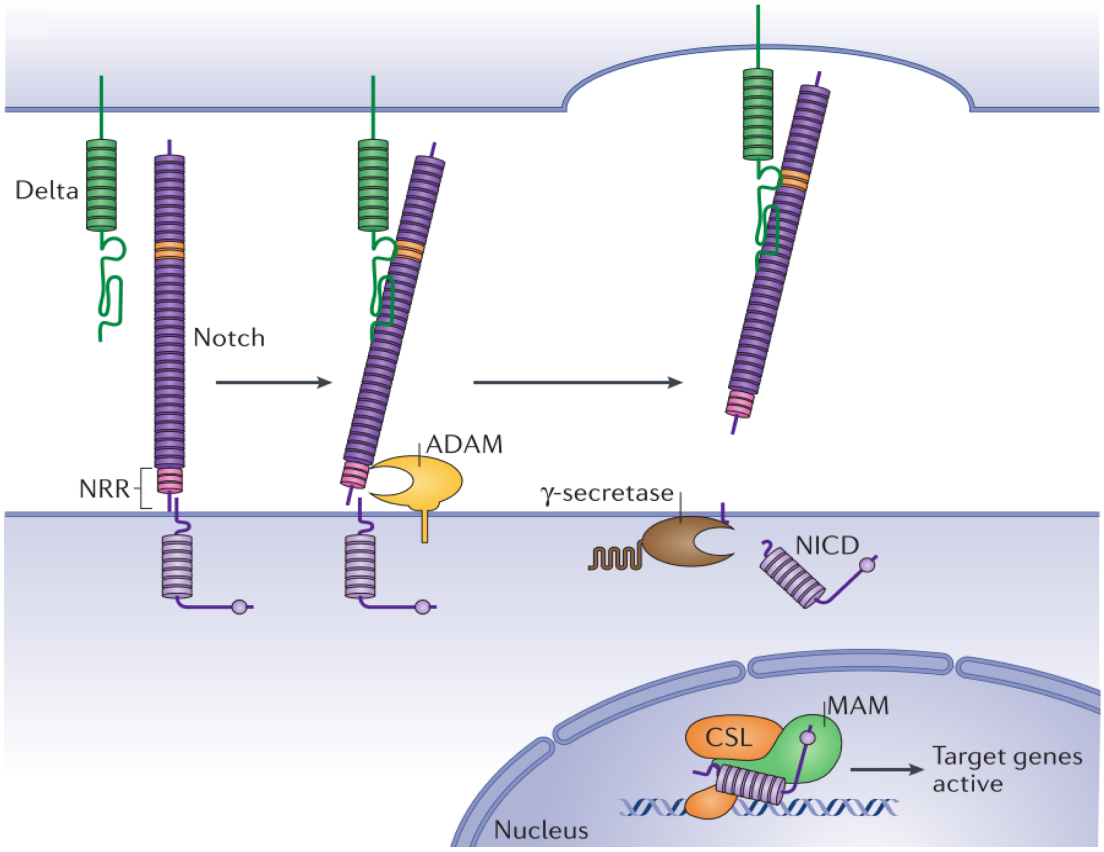

Figure 1.6. Notch signaling pathway. The Notch signaling pathways is composed by transmembrane ligands (Dll1,34 and Jag1,2) and receptors (Notch 1-4). Binding of Dll4/Jagged ligands to Notch receptors triggers two proteolytic reactions in the receptor, the first one mediated by ADAM and the second by γ-secretase, that release the NICD portion of the receptor. NICD interacts with the transcriptional regulators CSL/RBPJk and MAM to control the expression of its target genes (Adapted from Bray, 2016).

In the vasculature all four receptors are expressed, as well as the ligands Dll1, Dll4 and Jagged1 (Gridley, 2010), and many studies have revealed an indispensable function of this pathways during blood vessel development and homeostasis. Similar to the loss of VEGFR2 or VEGF, mouse

embryos with endothelial specific deletion of Notch1 (Limbourg *et al*., 2005) or heterozygous for Dll4 (Duarte *et al.,* 2004 and Krebs *et al.,* 2004) die during development with severe vascular defects. Mutants for Dll1 (Sörensen, Adams, and Gossler, 2009), Notch4 (Krebs *et al.,* 2000) and Jagged1 (Xue *et al.,* 1999) also showed varied defects during vascular development. Notch receptors and ligands are highly expressed by arterial endothelial cells, and some of the Notch receptor or ligand mutants lack arterial differentiation, which is one of the main processes controlled by Notch in developing vessels (Lawson *et al.,* 2001; Quillien *et al.,* 2014; Limbourg *et al.,* 2007; Duarte *et al.,* 2004; Krebs *et al.,* 2000; Krebs *et al.,* 2004).

1.5.3 Regulation sprouting angiogenesis by Notch and VEGF

Multiple studies in mice and zebrafish have explored in more detail how these two pathways control different aspects of endothelial sprouting during angiogenesis. Particularly VEGF and Notch has been placed as central regulators in the process of tip-stalk cell specification and a basic model for this process has been proposed to explain the phenotypes observed after genetic or pharmacological alterations of these pathways (Siekmann, Affolter, and Belting, 2013).

Angiogenesis is initiated by the expression of proangiogenic factors in avascular tissues. VEGFA is the most important factor that promotes angiogenesis. Hypoxia and lack of nutrients (Krock, Skuli, and Simon, 2011) are the main situations that induce VEGFA expression in cells from avascular tissues, like the astrocyte network in the retina (Stone *et al.,* 1995) or somites in zebrafish ISV sprouting (Liang *et al.,* 1998). Pharmacological or genetic alterations of VEGF levels during angiogenesis have been show to significantly alter angiogenic dynamics (Scott *et al.,* 2010; Okabe *et al.,* 2014) demonstrating its role as one of the main pro-angiogenic factors. Several isoforms of VEGFA can be secreted, with different affinities for the extracellular matrix *(Zhao et al.,* 2012) . Studies in animals expressing only one of the possible isoforms have shown that proper balance between soluble and matrix bound VEGFA forms is also required for normal angiogenesis (Ruhrberg *et al.,* 2002; Gerhardt *et al.,* 2003).

Vascular endothelial cells express VEGFR2, that it is activated upon VEGFA binding. VEGFR2 activation is essential for the specification of tip cells in the vessels closest to the avascular tissue (Blanco and Gerhardt, 2013) (Fig. 1.7). Deletion of VEGFR2 in ECs during angiogenesis lead to a highly underdeveloped vasculature (Benedito *et al.,* 2012; Zarkada *et al,.* 2015), similar to the ones formed under VEGFA inhibition. This has been mainly attributed to the insufficient specification of tip-cells and sprout formation. However, during normal angiogenesis not all cells at the angiogenic front are activated by VEGF, only a few endothelial cells are selected as tip cells.

Notch signaling has been placed as a central player in inhibiting tip cell specification, as inhibition of this pathway in ECs during angiogenesis leads to hypersprouting phenotypes with increased tip cell specification (Hellström *et al.,* 2007; Leslie *et al.*, 2007; Lobov *et al.*, 2007; Siekmann and Lawson, 2007; Suchting *et al.,* 2007). These studies proposed that high Dll4 expression in tip cells, mediated in part by high VEGF signaling through VEGFR2, activate notch receptors in adjacent ECs, denominated stalk cells. This constitutes a mechanism of lateral inhibition to specify two functionally different population of ECs, tip and stalk cells. The effect of Notch in blocking tip cell selection was initially attributed to the differential regulation of VEGF signaling responsiveness in tip versus stalk cells. Several mechanisms were proposed that would suppress VEGF signaling, involving the regulation of the expression levels of VEGF receptors and VEGF availability.

Initial studies based on *In vitro* experiments in HUVECs (Shawber *et al., 2007*; Harrington *et al.,* 2008; Taylor, Henderson, and Hughes, 2002; Ridgway *et al.*, 2006; Williams *et al*., 2006) and *In vivo* analyses of retinal vasculature from heterozygous mice (Suchting *et al.*, 2007) suggested that Notch could be inhibiting tip cell formation by repressing VEGFR2 expression. However this type of regulation was not found in other studies blocking Dll4/Notch signaling either pharmacologically or genetically (Lobov *et al.*, 2007; Benedito *et al.*, 2012). Furthermore, two studies that performed microarray transcriptional comparison between micro dissected tip or stalk cells (Strasser, Kaminker, and Tessier-Lavigne, 2010) or between endothelial cells from Wt or Dll4 heterozygous animals (del Toro *et al.*, 2010) also failed to see any enrichment of VEGFR2 in tip cells or in Dll4 heterozygous endothelial cells.

VEGFR3 levels have been found to be regulated by Notch in different studies (Benedito *et al.,* 2012; Tammela *et al.*, 2008) but not specifically enriched in tip cells (Strasser, Kaminker, and Tessier-Lavigne, 2010). This suggested that the hypersprouting phenotype after Notch inhibition could be due to VEGFR3 upregulation and overactivation of the VEGF signaling pathway, however elimination of VEGFR3 was not able to revert the hypersprouting phenotypes in mice retinal vasculature after Notch inhibition (Zarkada *et al.,* 2015).

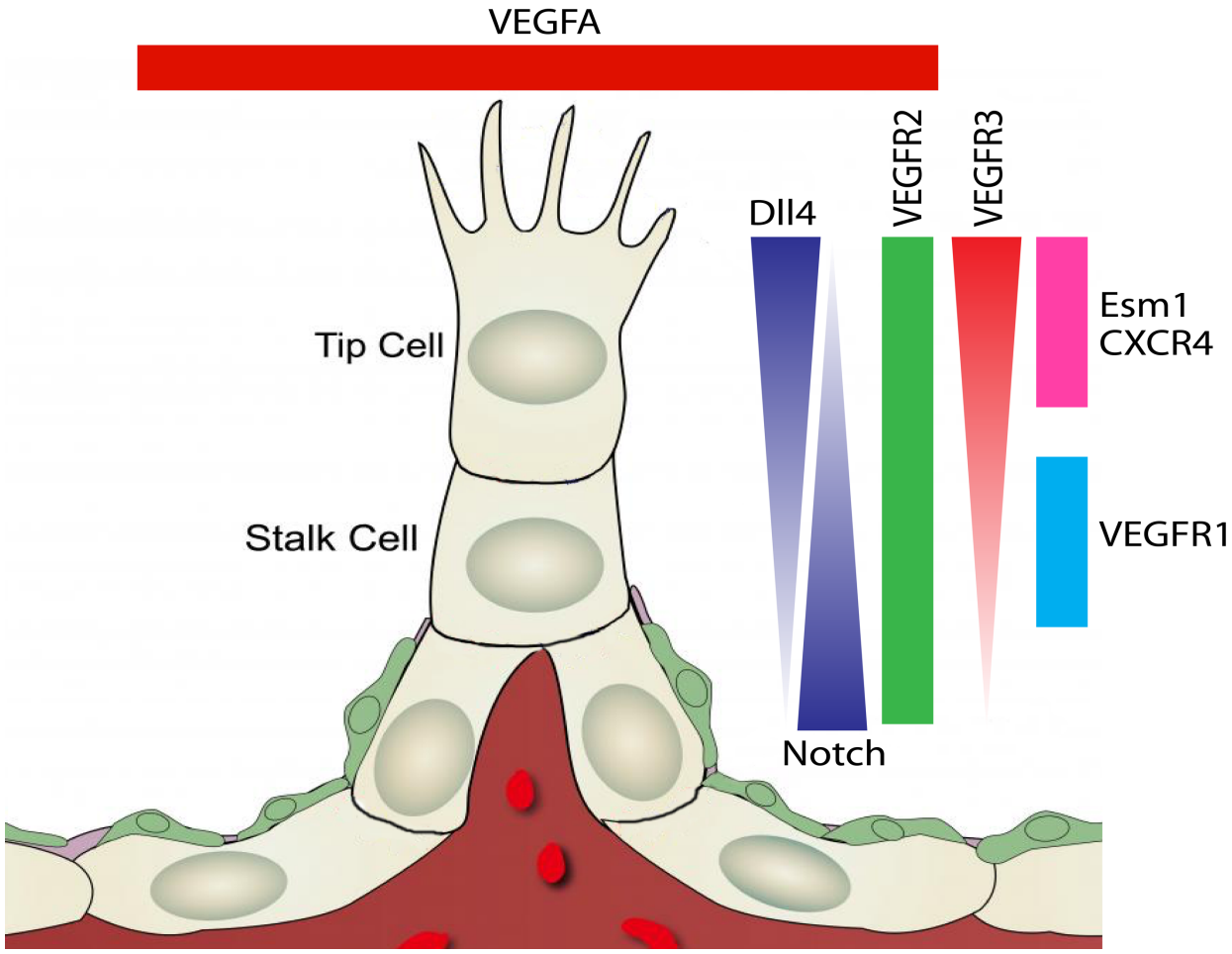

Figure 1.7. Molecular regulators of tip-stalk cell selection. VEGF expressed by hypoxic tissues binds to VEGFR2 in the endothelium. VEGFR2 downstream signaling promotes tip-cell differentiation and increases Dll4 expression which activates Notch in adjacent cells. Notch activity controls VEGFR3 expression and blocks the tip cell fate. VEGFR1 is expressed in stalk cells reducing their response to VEGFA from the tissue. Tip cells express other characteristic markers as Esm1 or CXCR4.

As previously mentioned VEGFR1 can acts as a VEGF sink, reducing VEGFR2 signaling. As stalk cells express both membrane and soluble isoforms of the receptor VEGF signaling is reduced in stalk cells at the base of sprouts (Chappell *et al.,* 2009; Krueger *et al.*, 2011). However VEGFR1

has been found to be upregulated by Notch signaling activation only in vitro (Harrington *et al.,* 2008; Funahashi *et al.*, 2010).

Additional genes have been found to be differentially expressed and enriched in tip cells that could be either modulators or being modulated by the VEGF and Notch signaling pathways. Tip cells express PDGFb, Angpt2, CXCR4 and Esm1 while stalks cells express the Notch ligands Jagged1 and 2 as well as other Notch target genes like Hes and Hey proteins (Strasser, Kaminker, and Tessier-Lavigne, 2010) (Fig. 1.7).

To permit the recurrent sprouting and branching necessary for the proper expansion of the vasculature, tip cell specification has been found to be transient. During angiogenesis endothelial cells at the tip cell position are switching depending of their response levels to VEGF and other pro-angiogenic stimuli (Jakobsson *et al.*, 2010). Hence this competition is controlled by the dynamic activation of VEGF and Notch pathways and It is generally assumed that the endothelial cells with the combination of High VEGF signaling and Low Notch activation preferentially occupy the tip cell position (Hellström *et al.*, 2007; Benedito *et al.*, 2009). However a recent study in zebrafish has shown that the effects of Notch in sprouting and tip cell selection depended on the specific sprouting mode of different kind vasculatures.(Hasan *et al.*, 2017)

1.5.4 Regulation of endothelial cell proliferation during angiogenesis

Endothelial cell proliferation is one of the most important processes of angiogenesis and has to be very tightly controlled, as the formation a proper vascular network require the precise generation of just the right amount of endothelial cells. Previous studies have associated different proliferative capacities to tip and stalk cells (Gerhardt *et al.*, 2003), and to cells with different VEGF and Notch signaling levels, which demonstrates their requirement for the regulation of endothelial proliferation.

VEGF and Notch mutant phenotypes showed that, similarly to tip-stalk cell selection, they have opposing effects on endothelial cell proliferation. VEGF suppression by blockade of VEGFA or VEGFR2 signaling leads to a less dense vascular network (Benedito *et al.*, 2012; Zarkada *et al.*,

2015)., while genetic deletion or inhibition of different members of the Notch signaling pathway cause an increase in vascular density (Hellström *et al.*, 2007; Lobov *et al.*, 2007; Suchting *et al.* ,2007; Benedito *et al.*, 2012). Thus, according to the model, tip cells should be more proliferative, as higher tip cell specification after Notch inhibition leads to increased endothelial cell number, and lower tip cell specification after VEGF inhibition generate vascular networks with less endothelial cells.

This effects would correspond to the pro-angiogenic and pro-mitogenic activity of VEGF while Notch would act as an anti-angiogenic signal. However studies of retinal angiogenesis have shown that proliferation of tip cells is very limited and is actually high in stalk cell *(*Gerhardt *et al.*, 2003; Lobov *et al.*, 2007; Benedito *et al.*, 2009). In contrast, live imaging in Zebrafish have shown that tip cells can divide at least as well as stalk cell while also sprouting and migrating (Siekmann and Lawson, 2007).

1.6. Cell cycle regulation

The cell cycle is defined as the ordered sequence of events a cell undergoes to replicate its DNA and divide, giving rise to two daughter cells. The two main events during cell cycle, DNA replication and cell division, constitute two separated phases: interphase and mitosis/cytokinesis respectively. Interphase can be further divided into G1 (Gap1), S and G2 (Gap2) phases.(Harashima, Dissmeyer, and Schnittger, 2013)

When an actively proliferating new cell is produced, it enters G1 phase. During this phase the cell integrates internal and external cues, like cell size, protein levels and mitogenic signaling. Once the cell reaches the minimal conditions to divide it commits to cell division. After the cell is committed to divide it enters S-phase and starts the process of DNA synthesis and replication.

After all chromosomes are properly replicated the cell transverse another Gap phase, G2, before entering mitosis. During mitosis condensed chromosomes separate and the cytoplasm is physically divided during cytokinesis producing the two daughter cells. This process is highly regulated at several stages of the cycle denominated checkpoints. Progression through these

checkpoints depends on the expression and activation of Cyclin-CDK (Cyclin Dependent Kinase) complexes. These complexes phosphorylate and regulate the activity of a multitude of effector proteins required for cell cycle progression.

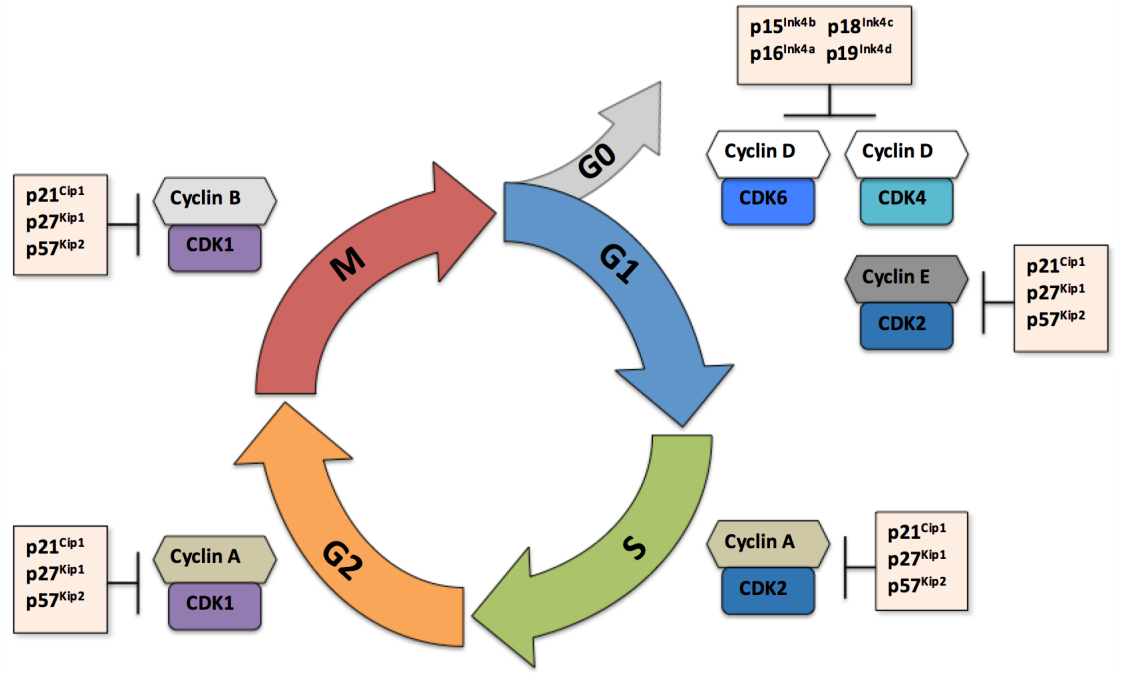

Figure 1.8. Cell cycle regulation by CKIs. The cell cycle is divided in 4 main phases, G1, S, G2 and M. Progression through these phases is controlled through the phosphorylation of effector proteins by different CDK/Cyclin complexes. The activity of this complexes is regulated by several CDK inhibitory proteins (CKIs) belonging to two families (Cip/Kip and Ink). Members of the ink family control progression through G1 while members of the Cip/Kip family have been shown to have a wider inhibitory capacity.

Regulation of their activity mainly depends on the oscillatory expression of Cyclins during cell cycle and on the expression of several cell cycle inhibitors belonging to two main families: the Cip/Kip family comprising p21Cip1, p27Kip1 and p57Kip2; and the Ink4 family including p16Ink4a, p15Ink4b, p18Ink4c and p19Ink4d (Besson, Dowdy, and Roberts, 2008). These proteins block the activity of different Cyclin-CDK complexes during different cell cycle checkpoints halting cell cycle progression until the cell is in the optimal condition for going through the checkpoints (Fig. 1.8).

Although the cell cycle has been widely studied in pathological process of deregulated proliferation like in cancer, one of its most important function is to control the number of cells generated in a multicellular organism during development. In this context is where a new level

of complexity arises, as any cell not only has to ensure that it replicates and divide properly, but also that it does it only when is required for the correct formation of the tissue it belongs and in a coordinated fashion with the surrounding cells. Moreover, cell cycle progression during development has to be tightly coupled with other cellular processes like differentiation and migration further increasing the regulatory burden on this process.

Cyclin-CDK complexes, as the main drivers of cell cycle progression, constitute central regulatory hubs in which both internal and external information about DNA replication, metabolic needs, morphogenetic trajectories or cellular differentiation converge to induce division only when it is needed (Rhind and Russell, 2012).Coupling of cellular differentiation to changes on cell cycle dynamics have been shown in different developmental processes like neurogenesis (Ohnuma and Harris, 2003) or cardiogenesis (Kaldis and Richardson, 2012). Alterations in the length of cell cycle phases, particularly of G1 (Boward, Wu, and Dalton, 2016), is essential and can drive differentiation processes. In this context the cell cycle inhibitors p21 and p27 have been shown to play a role in coordinating cell cycle dynamics with differentiation signals (Ruijtenberg and van den Heuvel, 2016; Tarui *et al.,* 2005).

1.7 Clonal analysis of genetic mosaics *in vivo*

Clonal analysis refers to the ability to track and follow the progeny of a single cell in time and space. It constitutes a very powerful tool to study the proliferation and differentiation of single cells during development (Blanpain and Simons, 2013).

Different approaches have been used to perform clonal analysis in various biological systems. Chemical dyes or radioactive tracers constitute the first attempts at labelling cells to perform clonal analysis (Buckingham and Meilhac, 2011). However, it was the use of genetic markers that unraveled its true potential, as they offered a permanent heritable reporter of the whole progeny of the labeled cell. These genetic mosaics can be generated in several ways like cell transplantation, viral transduction or in situ genetic recombination. (Kretzschmar and Watt, 2012). Currently the most used markers to differentially label cells are genetically encoded fluorescent proteins and the preferred strategy to induce their expression is the use of genetic

recombination. The Cre-LoxP system is widely used in mice as it allows for cell or tissue specific, inducible and permanent expression of fluorescent reporters encoded downstream of a LoxP-STOP-LoxP (LSL) sequences (Srinivas *et al.,* 2001; Madisen *et al.,* 2010).

In mice it is generally not possible to follow clonal dynamics in real time in most tissues. However, it still possible to perform retrospective clonal analysis by inducing recombination in some cells within the tissue and analyzing the clonally labeled progeny at later time points. The most important parameter when performing retrospective clonal analysis is clonal resolution (Blanpain and Simons, 2013). As it is not possible to directly control how many cells recombine and where they recombine at a given induction point, a seemingly isolated clone could have been originated by the progeny of more than one independently labeled cell. To avoid this situation two main strategies have been used to increase clonal resolution.

By titrating down the tamoxifen induction it is possible to induce very few recombination events within a tissue thus increasing the confidence that detected clones arise from a single cell. However, this strategy requires the analysis of a high number of mice to analyze a large enough number of clones.

High clonal resolution can still be achieved at higher recombination regimes, by using systems where is possible to induce the expression of multiple fluorescent proteins in different cells (Weissman and Pan, 2015). One way this has been achieved is by taken advantage of the existence of mutually exclusive lox pairs that recombine independently and after enable the permanent expression of different fluorescent proteins in distinct cells of the same animal, as in the Brainbow or Confetti (Brainbow 2.1) mosaic labeling strategies (Livet *et al.*, 2007; Snippert *et al.,* 2010), (Fig. 1.9).

Clonal analysis can also be performed in cells that constitute a functional genetic mosaic. Functional mosaics combine the genetic alteration of a gene of interest with the expression of the fluorescent reporter (Srinivas *et al.*, 2001). They are a particularly powerful research tool because they allow the study of cell-autonomous effects when distinct mutant and wild type cells confront the same environment in the same tissue or organism. The analysis of functional

mosaics can be more precise and informative than the use of classical genetics, in which the comparison is made between distinct wild type and mutant animals that may develop secondary and non-cell-autonomous phenotypes over time, distorting interpretation of the process under study. However, the generation of functional genetic mosaics in mice was so far technically challenging. Two different approaches have been used to induce functional genetic mosaics in mice, each with their own caveats.

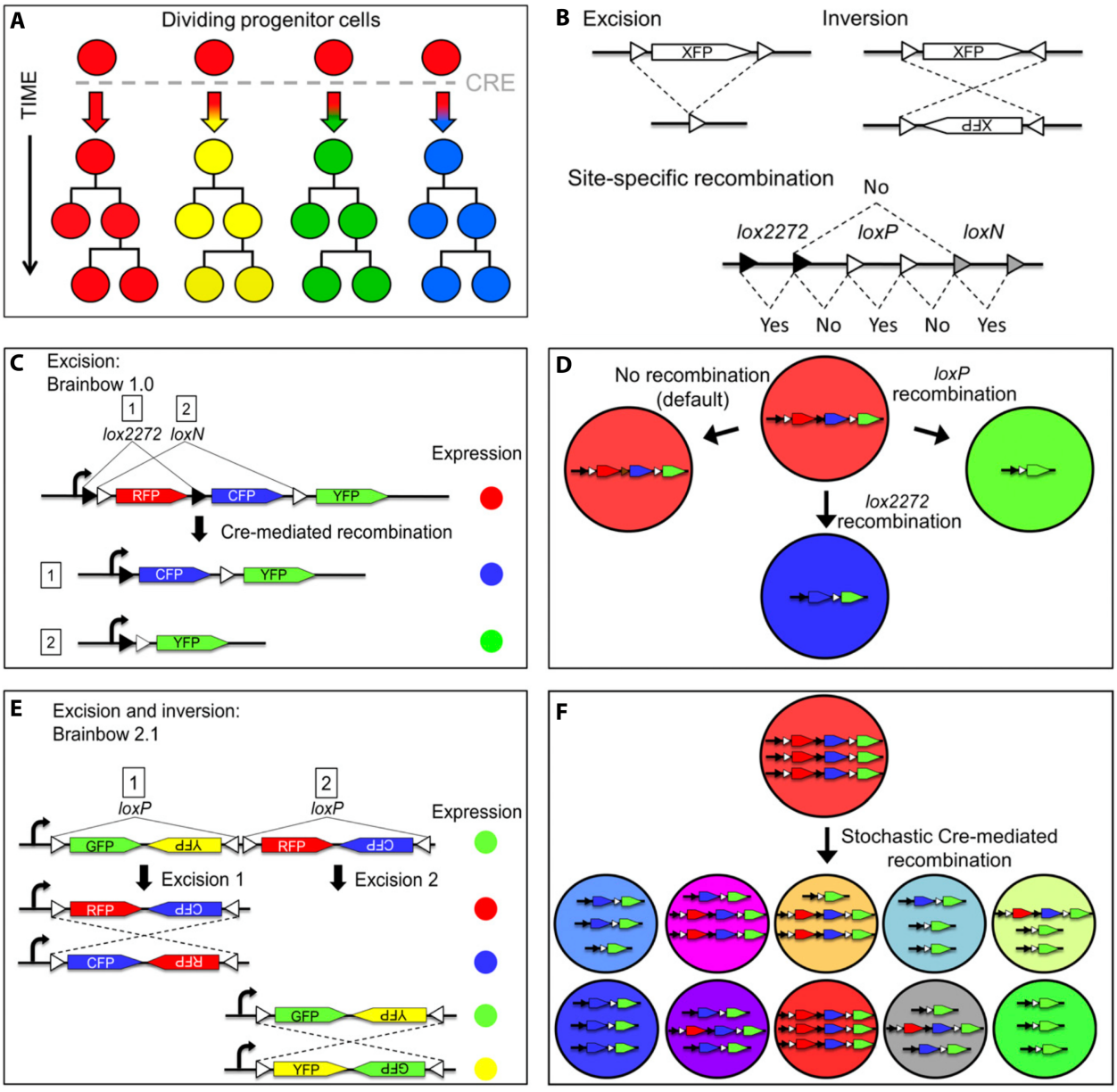

Figure 1.9. Multicolor genetic strategies for clonal analysis. A, Labelling progenitors cells with genetically encoded fluorescent proteins is used to perform clonal analysis and study cell cycle dynamics. **B**, Basic mechanism of Cre-induced recombination between Lox sites (Triangles) that are in the same orientation (Excision) or in opposite orientation (Inversion). Sequence diversity of Lox site sequence permits mutually exclusive recombination events. **C**,**D,F** Brainbow1.0 strategy combines mutually exclusive Lox sites to generate a random mosaic of cells expressing three different fluorescent proteins. In **F**, additional independent recombination outcomes can be generated by introduction of several copies of the Brainbow transgene. **E**, Brainbow 2.1 strategy based on the combination of inversion and excision events to generate a mosaic of four different cells. (Modified from Weissman and Pan, 2015).

The more widely used method to generate functional genetic mosaics in the mouse involves controlled mosaic induction of Cre-*LoxP* recombination, resulting in deletion of floxed genes and the expression of a genetically independent fluorescent reporter. However, several studies have shown that these cannot be used to reliably report another given gene deletion or activation (J. Liu *et al.,* 2013; Long and Rossi, 2009). This lack of correlation between recombination of a reporter allele, and alteration of the gene of interest, means that the majority of current conditional and mosaic genetic modifications and function analysis in the mouse are conducted without a reliable readout.

An alternative method that ensures total correspondence between functional genetic loss-of-function and fluorescent mosaics in mice is MADM (mosaic analysis with double markers) (Zong *et al.*, 2005). However, this system relies on very rare inter-chromosomal recombination events, leading to the generation of only a few clones of labeled control and mutant cells in the tissue. The generation of these genetic mosaics also cannot be accurately controlled in time, since these rare events can only occur with constitutively active Cre lines and not tamoxifen-inducible CreERT2 lines, which are weaker and only transiently active. In addition, the requirement for genetic linkage between the engineered MADM elements and another gene mutation means that currently this method can only be performed with genes located on 4 of the 20 mouse chromosomes (Zong, 2014).

OBJECTIVES

2 OBJECTIVES

The Notch signaling pathway has been shown to be fundamental in regulating endothelial cell behavior and generally in vascular biology. Alterations in the function of several of the proteins that are part of the pathway lead to imbalances in endothelial cell number during angiogenesis. This imbalance has been attributed to changes in the proliferative capacity of endothelial cells. Current models also couple proliferative changes to the process of tip-stalk cell differentiation through interactions with the VEGF signaling pathway. However, a detailed description of endothelial cell cycle dynamics and its regulation by these pathways is still lacking.

The objectives of this thesis were:

- To develop new genetic strategies to conditionally induce functional genetic mosaicism for genes of the Notch and VEGF pathway, follow their clonal dynamics and analyze at single-cell level the possible interaction of Notch and VEGF pathways in regulating endothelial cell proliferation.

- To evaluate with cellular and temporal resolution the effects of Notch alterations on endothelial cell cycle dynamic during angiogenesis.

- To discover, through next generation transcriptomics of angiogenic endothelial cells, new Notch target genes possibly involved in endothelial cell cycle regulation and to functionally assess their roles during angiogenesis.

MATERIAL AND METHODS

3 MATERIAL AND METHODS

3.1 Culture of mouse embryonic stem cells

Mouse embryonic stem cells (mESCs) with the G4 background (George *et al,*. 2007) were cultured in standard mESC media (DMEM containing Glutamax (31966-047, Gibco), 15% FBS (tested for germline transmission), 1 x NEAA (Hyclone, SH3023801), 0.1% ß-mercaptoethanol (Sigma, M7522), 1 x Pen/Strep (Lonza, DE17-602E) and LIF) in dishes covered with a feeder layer of mouse embryonic fibroblasts (MEFs). For induction of recombination mESCs harboring the iChr-Notch-Mosaic or iMb-Vegfr2-Mosaic were transfected with a Cre expressing plasmid with lipofetamine (Thermo Fisher, 11668030).

3.2 Embryoid bodies and endothelial differentiation

To generate embryoid bodies (EBs) from mESCs we used the standard hanging drop method. Briefly recombined mESCs were for 2 days on gelatinized plates and after, tripsinized and ressuspended at a density of 60.000 cells per ml in embryoid bodies media (DMEM Glutamax (Gibco, 31966-047), 15% FBS, HEPES (Biowhittaker EE17-737) and Monotyoglycerol (Sigma, M6145). For each EB, 20ul drops of this solution were pipetted onto the lid of a petri dish. This lid was inverted, to form the hanging drops, and the dish further filled with PBS to prevent evaporation. Four days after differentiation the embryoid bodies were plated on an OP9 cells monolayer and differentiated in basal media (MEM alpha (Gibco, 11900-016), supplemented with 20% FBS and 7.5% Sodium bicarbonate (Gibco, 25080-060) containing 30ng/ml of VEGF to further induce endothelial differentiation and proliferation for 5 days.

3.3 Mouse lines

Experiments involving animals were conducted in accordance with institutional guidelines and laws, following protocols approved by local animal ethics committees and authorities. Male and female mice were used for the analysis and maintained under specific pathogen-free conditions.

To express Cre for recombination of Mosaic, reporter or floxed alleles in endothelial cells we used either Tie2-Cre line (Kisanuki *et al.*, 2001) for constitutive recombination, or the *Cdh5(PAC)-CreERT2* mouse line (Wang *et al.*, 2010) for inducible recombination. For recombination during neurogenesis we used the *Polr2a-CreERT2* mouse line (Guerra *et al.,* 2003). For specific recombination in tip cells we generated the *Esm1*$^{\text{tm(HA-H2B-Cerulean-2A-iCreERT2)}}$ mouse line. By using CRISPR/Cas9-assisted homologous-dependent recombination in mESCs, we inserted the HA-H2B-Cerulean-2A-iCreERT2 cassette in-frame with the endogenous *Esm1* gene ATG initiation codon. These gene-targeted mESCs were validated by Southern blot and later used to produce mice as in (Pontes-Quero *et al.*, 2017).

The transgenic ifgMosaic lines (Pontes-Quero *et al.*, 2017) used to generate functional mosaics were: *iChr-Notch-Mosaic:(Gt(Rosa)*$^{26Sortm1(iChr\text{-}Notch\ \ Mosaic)}$*), iChr-Notch-V2-Mosaic: (Tg(BAC Rosa26)*$^{(iChr\text{-}Notch\_Mosaic\text{-}v2)}$*) or iMb-Vegfr2-Mosaic: (Tg(BAC Rosa26)*$^{(iMb\text{-}Vegfr2\ Mosaic)}$*).* Control mosaic lines used in clonal analysis experiments and for labelling of endothelial cells were: *iMb-Control-Mosaic: (Gt(Rosa)*$^{26Sortm1(iMb\text{-}Control\text{-}Mosaic)}$) or the *iChr-Control-Mosaic: (Gt(Rosa)*$^{26Sortm1(iChr\text{-}Control\text{-}Mosaic)}$) and *Cerulean/Gfp Mosaic: (Gt(Rosa)26Sor*$^{tm1(iChr\text{-}Cerulean/GFP/Kate2\ Mosaic}$ mouse lines (Pontes-Quero *et al.,* 2017)

To perform clonal analysis of tip cell progeny we used the *Gt(Rosa)*$^{26Sortm14(CAG\text{-}LSL\text{-}tdTomato)Hze}$ (Madisen *et al.,* 2010) reporter mouse line (abbreviated as *Rosa26-LSL- TdTomato).*To evaluate the role of p21 during angiogenesis we used Cdkn1a (p21) knockout mice (Brugarolas *et al.,* 1995).

To moderately activate Notch signaling in the endothelium, we generated the *Gt(Rosa)26Sor*$^{tm(LSL\text{-}MbTomato\text{-}2A\text{-}H2B\text{-}GFP\text{-}NICD\text{-}PEST)}$ mouse line, abbreviated here as *NICD-PEST*^{GOF}*.* To reduce Odc1 function with single-cell resolution, we generated the *Tg(BAC Rosa26)*$^{(LSL\text{-}HA\text{-}H2B\text{-}Cerulean\text{-}2A\text{-}Oaz1\text{-}Ac.)}$ mouse line, abbreviated here as *Oaz1*^{GOF}*.* Oaz1 is the endogenous negative regulator of Odc1, targeting it for degradation. *Oaz1-Ac* is the point mutated and constitutively active form of Oaz1 that is not sensitive to the translational frameshift induced by the cell polyamines levels.

To monitor the expression of Odc1 *in vivo* we used the *Odc1-lacZ* mouse line (*Odc1*$^{tm1a(EUCOMM)Hmgu/J}$ - Jax Stock No: 024246, unpublished). To conditionally delete Odc1, we interbred the Odc1-lacZ mouse line with the FlpO (Kranz *et al.*, 2010) mice. This generated the *Odc1*^{floxed} mice. To conditionally delete Myc we used the Myc^{floxed} mice (de Alboran *et al*., 2001).

A summary of the lines and genotyping primers is provided in Table 1.

Table 1: Mouse strains and genotyping primers

NAME	OFFICIAL STRAIN SYMBOL	OLIGONUCLEOTIDES
iChr-Notch-v2-Mosaic	TgBAC(Rosa)26Sor$^{(iChr\text{-}Notch\text{-}v2\text{-}Mosaic)}$	5' ACGTGAAGCTGAGCAAGGAT 3' 5' CTTAGTCACCGCCTTCTTGG 3'
iMb-Vegfr2-Mosaic	TgBAC(Rosa)26Sor$^{(iMb\text{-}Vegfr2\text{-}Mosaic)}$	5' GCGGCACGAAATATCCTCT 3' 5' ATTTCCCACAGCAAAACACC 3'
Polr2a-CreERT2	Polr2a$^{tm1(cre/ERT2)Bbd}$	5' GTCAGTACACATACAGACTT 3' 5' TGAGCGAACAGGGCGAA 3'
Cdh5(PAC)-CreERT2	Tg(Cdh5-cre/ERT2)1Rha	5' GGAGGCTGGAAAGTAGAGCA 3' 5' TCCCTGAACATGTCCATCAG 3'
Tie2-Cre	Tg(Tek-cre)1Ywa	5' GGGAAGTCGCAAAGTTGTGAGTT 3' 5' CTAGAGCCTGTTTTGCACGTTC 3'
Oaz1^{GOF}	TgBAC(Rosa26)$^{(LSL\text{-}HA\text{-}H2B\text{-}Cerulean\text{-}2A\text{-}Oaz1\text{-}Ac.)}$	5' CGACCACTACCAGCAGAACA 3' 5' CTTCTCTCTGGCGAAGCAGT 3'
p21 KO	Cdkn1a^{tm1Tyj}	5' ACCCAGCAAAGCCTTGATTCT 3' 5' CCTTCTATCGCCTTCTTGACGA 3' 5' CAGGTCGGACATCACCAGGAT 3'
Odc1-LacZ **Odc1$^{flox/flox}$**	Odc1$^{tm1a(EUCOMM)Hmgu/J}$	5' ATCCGGGGGTACCGCGTCGAG 3' 5' GCAATCCCATTGACTGGTGT 3' 5' TTCCCCTCTCAATTGTTCCA 3'
Myc$^{flox/flox}$	Myc^{tm2Fwa}	5' TTTTCTTTCCGATTGCTGAC 3' 5' TAAGAAGTTGCTATTTTTGGC 3'
Esm1-Cerulean-CreERT2	Esm1$^{tm(HA\text{-}H2B\text{-}Cerulean\text{-}2A\text{-}iCreERT2)}$	5' CTCCGTGCTAAGGGACTCTG 3' 5' CCTTAGTCACCGCCTTCTTG 3' 5' AACAAGAGAGGCTGGCAAGA 3' 5' TCCATGCCTGAGACTGTACG 3'
R26-LSL-Tomato	Gt(ROSA)26Sor$^{tm14(CAG\text{-}tdTomato)Hze}$	5' CGGGGTCATTAGTTCATAGCC 3' 5' CACCTCGACCATGGTAATAGC 3'
iMb-Control-Mosaic	Gt(Rosa)26Sor$^{tm1(iMb\text{-}Control\text{-}Mosaic)}$	5' CGGGGTCATTAGTTCATAGCC 3'
iChr-Control-Mosaic	Gt(Rosa)26Sor$^{tm1(iChr\text{-}Control\text{-}Mosaic)}$	5' CACCTCGACCATGGTAATAGC 3'
iChr-Notch-Mosaic	Gt(Rosa)26Sor$^{tm1(iChr\text{-}Notch\text{-}Mosaic)}$	
Cerulean/Gfp Mosaic	Gt(Rosa)26Sor$^{tm1(iChr\text{-}Cerulean/GFP/Kate2}$ Mosaic	
NICD-PEST^{GOF}	Gt(Rosa)26Sor$^{tm(LSL\text{-}MbTomato\text{-}2A\text{-}H2B\text{-}GFP\text{-}NICD\text{-}PEST)}$	

3.4 In vivo genetic recombination

To activate recombination during neurogenesis, tamoxifen diluted in EtOH:corn oil 1:7 was injected in combination with progesterone in pregnant adult females (2mg tamoxifen and 1mg progesterone per female at embryonic day (E)8.5).

To activate CreERT2 in pups we administered tamoxifen (Sigma-T5648) diluted in a 1:1:2 solution of EtOH:Cremophor:PBS (Chevalier, Nicolas, and Petit, 2014) To induce the recombination of iChr-Notch-Mosaic, *iMb-Vegfr2 Mosaic* and *Rosa26-LSL-TdTomato* in the neonatal endothelium, we injected a single dose of 250 microgram Tamoxifen per pup at P3 and collected eyes at P6 or at P7(when combined with anti-Dll4 treatment). To induce recombination of the alleles *NICD-PEST*^{GOF}, *Oaz1*^{GOF}, *Odc1*^{floxed}, *Myc* ^{floxed} we injected tamoxifen at 50mg/kg at P1, P2 and P3 and eyes were collected at P6 or at P7 (when combined with anti-Dll4 treatment).

3.5 In vivo pharmacological inhibition

Inhibition of Dll4/Notch signaling in ECs was achieved by using the humanized phage antibody YW152F, developed by Genentech (Ridgway *et al.,* 2006). Human IgG (Sigma, I4506) was used in littermates as a control treatment. A single subcutaneous injection of 40ul of IgG or anti-Dll4 (0.5 mg/ml in PBS) was administered at P5. Eyes were collected 12, 24, 48 or 72h after blocking antibody administration.

To inhibit ERK phosphorylation we injected two doses of the MEK inhibitor SL3278 (Selleckchem, S1066) the first at 24h and the second at 8h before eye collection at P6. The inhibitor was prepared in 2% DMSO+30% PEG 300+5% Tween 80 in ddH2O and injected intraperitoneally at 450ug/pup.

3.6 EdU proliferation assay

To detect proliferating cells actively synthesizing DNA, we injected EdU (Invitrogen A10044) intraperitoneally 4h before sacrifice and developed the signal with the Click-it EdU Alexa Fluor 647 Imaging Kit.

3.7 Cell/Tissue processing and immunofluorescence

For immunostaining of mESCs or ECs derived from EBs, cells were fixed for 10 minutes in PBS containing PFA4% and Sucrose 4%. After a brief rinse in PBS, cells were permeabilized in 0.1% Triton for 10 minutes and then immersed in a blocking solution (10% Fetal bovine serum in PBS). Primary antibodies were diluted in blocking solution and incubated for 2 hours at room temperature or overnight, followed by three washes in PBS of 10 minutes each and incubation for 1 to 2 hours with conjugated secondary antibodies at room temperature. After three washes in PBS, cells were mounted with Fluoromount-G (SouthernBiotech).

For immunostainings of mouse retinas, eyes were collected at the indicated time points and fixed in PFA4% in PBS for 1h at RT. After two PBS washes, retinas were micro-dissected and stained with modifications of previously described methods (Benedito et al. 2009; Pitulescu et al. 2010). Briefly, retinas were blocked and permeabilized in PBS with 0,3% Triton, 3% FBS and 3% Donkey Serum; washed twice in PBLEC buffer (1 mM CaCl2, 1 mM MgCl2, 1 mM MnCl2 and 1% Triton X-100 in PBS). Biotinylated isolectinB4 (Vector Labs, B-1205, diluted 1:50) or primary antibodies (see below) were diluted in PBLEC buffer and tissues with this solution incubated for 2h room temperature or overnight at 4ºC. After five washes in blocking solution diluted 1:2, Alexa-conjugated secondary antibodies were incubated for 1h at RT. After two washes in PBS, retinas were mounted with Fluoromount-G (SouthernBiotech). For EdU DNA labeling detection, an additional step before mounting was performed following the Click-It EdU kit (Thermo Fisher, C10340) manufacturer instructions.

For immunostaining of organ sections, mouse organs were collected and fixed 1h in PFA4% on ice. Following a wash in PBS, organs were dehydrated in 30% sucrose for a minimum of 8h and embedded in O.C.T. (*Tissue-Tek*; Sakura Finetek USA) for cryosectioning. Sections were washed in PBS 0,025% Triton and blocked in PBS 0,025% Triton, 10% Donkey Serum, 0,5% BSA for 2h at RT. Primary antibodies were incubated overnight at 4ºC. After three washes, secondary antibodies were incubated for 2h at RT. After three additional washes in PBS sections were mounted in Fluoromount-G (SouthernBiotech). The list of used antibodies is included in Table 2.

Table 2: List of antibodies used for IF		
ANTICUERPO	**COMPANY**	**REFERENCE**
Rabbit Anti-GFP	Clontech	Cat# 632592; RRID: AB_2336883
Goat Anti-GFP	Acris Antibodies	Cat# R1091P; RRID: AB_1002036
Rabbit anti-Dsred	Clontech	Cat# 632496; RRID: AB_10013483
Rabbit Anti-tRFP-CF594	Biotium	Cat# 20422; RRID: AB_2686890
Mouse Anti-HA-594	Thermo Fisher	Cat# A-21288; RRID: AB_2535830
Mouse Anti-HA -647	Cell Signaling	Cat# 3444S; RRID: AB_10693329
Mouse Anti-V5 -488	AbDSerotec	Cat# MCA1360A488; RRID: AB_770155
Guinea Pig anti-mKate2	Dawen Cai - University Michigan	N/A
Rabbit anti tRFP/Kate2	Evrogen	Cat# AB233; RRID: AB_2571743
Biotinilated Isolectin B4	Vector	Cat# B-1205; RRID: AB_2314661
Rabbit anti-ERG	Abcam	Cat# ab110639; RRID: AB_10864794
Rat anti-mouse VE-cadherin	BD Biosciences	Cat# 555289; RRID: AB_395707
Rabbit Anti-PhiYFP	Evrogen	Cat# AB602
Rabbit anti-Phospho-p44/42 MAPK (ERK)	Cell Signaling	Cat# 4370; RRID: AB_2315112
Goat Anti-p21	Santa Cruz	Cat# sc-397-G RRID: AB_632127
Rabbit Anti-ERG-AF-647	Abcam	Cat# ab196149
Rabbit Anti-Ki67	Thermo Fisher	Cat# RM-9106-S0 RRID: AB_2341197
Rabbit Anti-pERK	Cell Signaling	Cat# 4370S RRID: AB_2315112
Rat-Anti CD31	BD Biosciences	Cat# 553370 RRID: AB_394816
Donkey Anti-Rabbit-AF488	Molecular Probes	Cat# A-21206, RRID:AB_141708
Donkey Anti-Rabbit-AF680	Thermo Fisher	Cat# A10043, RRID:AB_2534018
Donkey Anti-Rabbit Fab-Cy3	Jackson ImmunoResearch Labs	Cat# 711-167-003, RRID:AB_2340606
Donkey Anti-Rabbit Fab-AF647	Jackson ImmunoResearch Labs	Cat# 711-607-003, RRID:AB_2340626
Donkey Anti-Goat-AF-488	Thermo Fisher	Cat# A-11055, RRID:AB_2534102
Donkey Anti-Goat-AF-633	Molecular Probes	Cat# A-21082, RRID:AB_141493
Donkey Anti-Goat-AF-647	Molecular Probes	Cat# A-21447, RRID:AB_141844
Donkey Anti-Goat-AF-680	Molecular Probes	Cat# A-21084, RRID:AB_141494
Streptavidin 405		Cat# S-32351

3.8 Image acquisition

Depending on the complexity of the immunostainings and the combination of FPs to detect, we used different laser-scanning confocal microscopes. For up to 4 channels acquisition of large fields we used the ZEISS LSM700 inverted microscope with laser lines 405, 488, 546 and 633nm. For multi-color detection of up to 7 different signals we used the inverted Leica SP5 confocal (405, 488, 514, 546, 594, 633nm) or the Leica SP8 confocal with a 405nm laser and a white laser that allows excitation at any wavelength from 470nm to 670nm. Occasionally, a ZEISS LSM780 with a GaAsP spectral detector was used. Individual fields or tiles of large areas were acquired with a 10x, 20x or 40x lens. All of the representative images shown represent the average of the results obtained for each group and experiment. Littermate animals were dissected and processed with exactly the same conditions. Comparisons of phenotypes or signal intensity are made with pictures obtained using the same laser excitation and confocal scanner detection settings.

3.9 Quantitative image analysis

Image processing was done using Fiji/ ImageJ (Schindelin *et al.,* 2012), Photoshop (Adobe) and Adobe Illustrator (Adobe) software. All quantifications were performed in Fiji/ ImageJ.

For images of mESCs and EBs, signal thresholds were manually defined before quantification of the number of cells/nuclei having a specific color. In the case of mosaics of cells expressing only membrane localized FPs, relative areas were quantified and correlate with cell number, after quantifying the average cell number per area based on Hoechst staining or nuclei marker proteins.

For clonal analysis of neural progenitor clones were scored based on their nuclei color, number and distribution. Sections with too many clones having the same color were not quantified. Cells within clones were assigned as being progenitors or differentiated cells based on their location relative to the limit between the ventricular (VZ) and marginal (MZ) zone

For quantification of endothelial clonal dynamics in the retina, clones were identified on large 3D tile confocal scanning volumes (2-4 Z slices). For the selection of clones in these volumes different parameters were considered: the clone single or dual color-code, its relative intensity (which varies between clones derived from different cells), its size and dispersion, and its proximity to other clones. To calculate the average clone dispersion, relative to its size, we measured the shortest path linking the center of the identified clone nuclei. For the accurate quantification and delimitation of the most frequent dual clones, in areas with higher frequencies of recombination, the average clone dispersion value was used to define areas that are very likely to contain all cells of an individual clone and no cells from adjacent single-cell derived dual clones.

For quantification of vascular parameters 387.5 x 387.5 μm fields were selected at the angiogenic fronts or at the mature are and considered as individual samples. Fields from at least 4 different retinas from 2 or more different animals were analyzed. Vascular IsolectinB4+ area and Erg+ cells were quantified semi-automatically using custom Fiji macros. Endothelial cell density (EC number/100 μm^2) was measured as the number of Erg+ cells relative to the total vascular area included in each field. The frequencies of EdU+, Ki67+ and p21+ ECs were manually determined as the ratio of double-positive cells to the total number of Erg+ cells per field.

For the quantification of pERK signal in iMb-Vegfr2-Mosaic, Individual IsolectinB4+/MbTomato+ and adjacent IsolectinB4+/ MbTomato- ECs were manually scored and assigned a region-of-interest (ROI) area based on the anti-dsred immunofluorescent signal. Within the MbTomato- endothelial population, tip cells were manually selected according to their position at the edge of the angiogenic front, and stalk-cells were selected as non-tip cells adjacent to MbTomato+ cells. The average absolute pixel pERK signal intensity was quantified in each ROI. The average background level of P-ERK immunofluorescence signal per field was subtracted to the average intensity signal of each ROI defined in that specific field. For quantification of pERK signaling in tip and front areas, single fields at the angiogenic front were automatically divided in tip areas included within the first 150 μm from the tip of the longest sprout, while front areas were defined from that limit to the lowermost limit of the field. The average pERK intensity was

calculated over the IsolectinB4+ area while the average background intensity was measure in the IsolectinB4- negative area for each field. After background subtraction, average intensities were normalized to the total IsolectinB4+ area for each field part. Global pERK intensity quantification for the validation of MEK inhibition was performed similarly in randomly selected fields from the angiogenic front and mature areas.

3.10 Flow cytometry of mESCs or isolated ECs

For quantification of fluorescent protein ratios in mESCs, cells were collected 3 days after Cre transfection and analyzed FACSAria cell sorter. Endothelial cells from EBs were collected after trypsinization and also analyzed in a FACSAria.

Embryos or organs were collected in PBS, minced, and digested with 2.5 mg/ml type I collagenase (Thermo Fisher, 17100017), 2.5 mg/ml dispase II (Thermo Fisher, 17105041), and 50 ng/ml DNAseI (Roche) at 37C for 20 minutes to create a homogeneous cell suspension. Cell suspensions were passed through a 70 μm filter to remove any undigested tissue. To remove erythroid cells, cell suspensions and blood samples were incubated for 10 minutes on ice in blood lysis buffer (0.15 M NH4Cl, 0.01M KHCO3 and 0.01 M EDTA in ddH20). Before analysis, cell suspensions were incubated at 4ºC for 30 minutes with APC rat anti-mouse CD31 (BD Pharmigen) The flow cytometry analyses were performed either with a FACS Aria Cell Sorter (BD Biosciences) or a Synergy4L Sorter. Viable (DAPI-) endothelial cells (APC-CD31+) were sorted and analyzed according to their endogenous fluorescence (GFP, Cherry or Cerulean).

3.11 qRT-PCR

For quantitative real time PCR (qRT-PCR), ECs from E10.5 mouse embryos or postnatal day 20 mouse hearts were sorted directly to RNeasy Mini Kit RLT buffer (Qiagen). RNA was extracted according to the Qiagen protocol. RNA was retrotranscribed with a High Capacity cDNA Reverse Transcription Kit with RNase Inhibitor (Thermo fisher, 4368814). cDNA was preamplified with Taqman PreAmp Master Mix containing a Taqman Assay based pre- amplification pool which contained the following assays: Hey1, Hey2, EphrinB2, PECAM-1, Cdh5, Odc1 (Thermo Fisher).

Preamplified cDNA was used to perform a standard qRT-PCR with gene-specific Taqman Assays (Thermo fisher) in a AB7900 machine (Applied Biosystems).

3.12 RNAseq

To isolate endothelial cells specifically from the newborn mouse retina angiogenic front, we first used a stereomicroscope to visualize and microdissect/separate the mature from the angiogenic front vascular area. Tissues from these two distinct areas were cut and processed for dissociation with the Neural Tissue Dissociation Kit (Mylteny 130-092-628). The resulting cell suspension was incubated with conjugated APC-anti-CD31 antibody (BD Pharmingen, 551262), followed by DAPI to exclude dead cells. Viable (DAPI-) endothelial cells (APC-CD31+) were FACS sorted and processed for total RNA extraction with RNAeasy Micro kit (Qiagen). A total of 200 to 800 ECs per sample was collected. Four retinas of two animals per group and litter were processed independently. In total, three independent litters, and 12 retinas per group were dissected for this analysis

RNA library was prepared using the Ovation RNA-seq system (NuGEN) and sequenced in a HiSeq2500 Illumina sequencer using a 60 bp single end elongation protocol. Sequenced reads were QC and pre-processed using cutadapt v1.6 and fastx-trimmer to remove adaptor contaminants. Quality control at each step was performed with FastQC. Resulting reads were aligned and gene expression quantified using RSEM v1.17 over mouse reference GRCm38. Differential gene expression was analyzed using the EdgeR package and ComBat. Gene Expression Heatmaps were performed using Genesis software.

3.13 Cell culture and luciferase assays

HEK293 cells were cultured in DMEM (Thermo Fisher, 41965039) 10% FBS 2mM and 1 x Pen/Strep (Lonza, DE17-602E) in gelatinized plates. For Dual Luciferase experiments the Dual-Luciferase® Reporter Assay System (Promega, Cat.# E1910) was used. Briefly cells were transfected with lipofetamine (Thermo Fisher, 11668030) following manufacturer instructions with 150 ng of pGL3 or pGL3-Odc1-promoter luciferase plasmid and 50 ng of the control pGL4

plasmid. For analysis of Hey1/Hey2 modulation of Odc1-promoter luciferase activity, 200 ng of a mix of pCS2-Hey1 and pCS2-Hey2 plasmids (a gift from Manfred Gessler) were co-transfected. Control experiments were performed by co-transfecting 200 ng of empty plasmids. 24h after transfection, cells were lysed and Firefly/Renilla Luciferase activity measured according to manufacturer instructions in a Promega GloMax® Luminometer. Firefly activity was normalized to Renilla activity for each well, and pGL3-Odc1-Promoter-luciferase normalized to control pGL3-only luciferase activity. Data shown is the average of three independent experiments with internal triplicates

3.14 Statistical Analysis

Statistical analyses were performed in Graph Pad (Prism 7.0). For comparisons of two samples with a Normal distribution we used the unpaired two-tailed Student *t*-test or the Welch unequal variances *t*-test unless otherwise specified. For non-Normal two sample comparisons, the non-parametric Mann–Whitney test was used. Comparisons among more than two groups were performed by ANOVA followed by the Turkey pairwise comparison for Normally distributed groups and by the Kruskal–Wallis test followed by the Dunn pairwise comparisons test for non-Normal groups. Data is presented as means ± SEM., unless otherwise indicated. Differences were considered statistically significant at $P < 0.05$. No randomization or blinding was used, and animals/tissues were selected for analysis based on their genotype, the detected Cre-dependent recombination frequency, and quality of multiplex immunostaining. The sample size was chosen according to the observed statistical variation and published protocols.

RESULTS

4 RESULTS

4.1 Dual ifgMosaic strategy to induce high resolution functional genetic mosaics in mice

Of the current methods outlined in the introduction section to induce Cre-dependent, fluorescent and cellular mosaicism in mice, the Brainbow strategy (Weissman and Pan, 2015) is the one that provides higher number of possible outcomes, and thus, the higher clonal resolution. MADM can induce only two different types of fluorescent proteins and cells (control and mutant), whereas the Brainbow can generate dozens or up to 90 different cell types in the same tissue. However, the Brainbow strategy requires the stochastic recombination and expression of several copies of the Brainbow transgene, to generate distinct combinations of fluorescent protein (FP) expression and in this way increase clonal resolution (Livet *et al.,* 2007). This stochastic recombination events and combinatorial FP expression cannot be combined with functional genetic modifications, as the relative expression levels of the gene of interest would be too complex and unknown. Hans Clever and colleagues generated the unicopy Confetti system, by targeting one of the Brainbow constructs to the Rosa26 locus (Snippert *et al.*, 2010). This system can be used to induce 4 distinct cells in a tissue expressing Cre, however, it relies on reversible genetic inversions, which are harder to induce than genetic deletions, and cannot be used for direct functional genetic alterations mediated by Cre.

For these reasons, my lab co-workers adapted and modified the Brainbow strategy to associate to each FP expression a given gene expression, and generate in this way multispectral functional genetic mosaics. To ensure full equimolecular expression of the fluorescent reporter and the gene of interest they used the viral 2A peptide *(*Trichas, Begbie, and Srinivas*,* 2008; Sharma *et al.*, 2012). They first developed iMb-Mosaic constructs, where is possible to induce three distinct cells expressing three different membrane localized FPs, and after inserted them into the Rosa26 locus or Rosa26 Bacterial Artificial Chromosomes (BACs) (Fig. 4.1 A). However, in order to perform statistically robust retrospective clonal analysis or lineage tracing and be able to faithfully resolve clonal identity in the induced mosaic, three possible outcomes are not enough,

unless used in very low recombination regimes. Consequently, they also developed Rosa26-targeted or Rosa26 BACs containing iChr-Mosaic constructs that enable the expression in distinct cells of three different chromatin/nuclei localized FPs (Fig. 4.1 B).

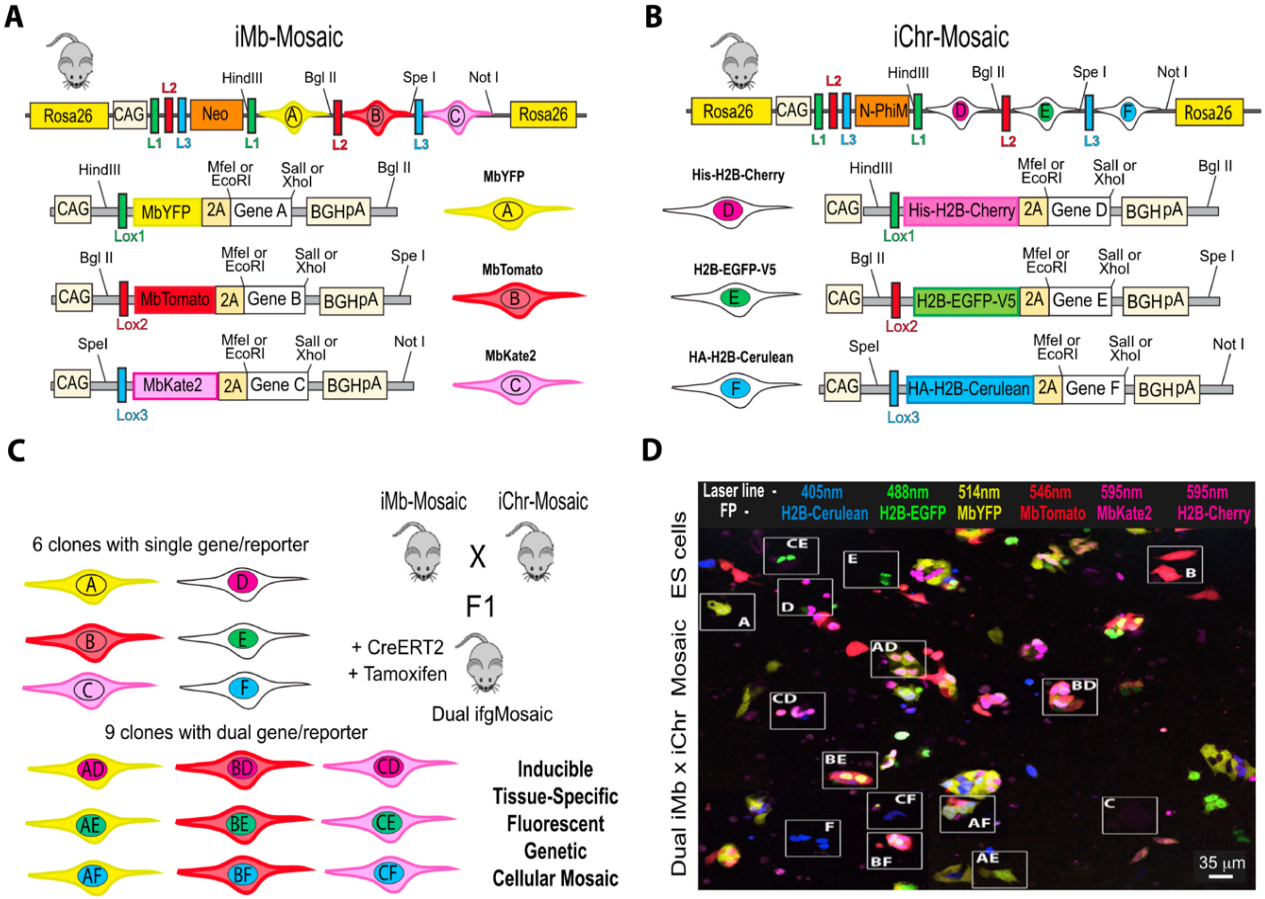

Figure 4.1. Dual Inducible Fluorescent Genetic Mosaic (ifgMosaic) strategy. A, B Diagrams showing the basic structure of iMb-Mosaic (**A**) and iChr-Mosaic (**B**) constructs. Cre activity induces random recombination between pairs of identical Lox (L) sites (L1, L2, L3) generating one out of three possible outcomes (A, B, C or D, E, F) in a single-cell. The DNA elements are as follows: Rosa26, flanking regions of the Rosa26 locus in which the construct are integrated. CAG, Strong and ubiquitous promoter; Neo, resistance marker for ES cell selection; L1, LoxN; L2, Lox2272; L3, LoxP; 2A, viral peptide allowing equimolar expression of multiple independent proteins from a single ORF; Mb, membrane tag; HA, V5 and His (small epitopes that can be used for specific antibody detection); H2B, histone tag that targets proteins to the chromatin/nucleus; BghpA, bovine growth hormone polyadenylation signal to stop transcription; N-PhiM, non-fluorescent protein that is used as a reporter of promoter expression. Restrictions sites are indicated. **C** When one mouse or cell line contains the two inducible mosaic alleles (iMb-Mosaic and iChr-Mosaic), up to 15 different cell clones can be induced by tamoxifen in a tissue expressing the CreRT2 recombinase, allowing combinatorial epistasis analysis at single-cell resolution. A–F indicate the single or dual color code for each clone. **D** Live imaging snapshot of mESCs cells expressing the Dual ifgMosaic. Indicated are the laser lines used to detect each fluorescent protein.

Thus by combining in the same mouse the expression of these two mosaic alleles (the Mb and Chr) we are able to generate Dual ifgMosaic mice. In these mice, is possible to induce after Cre recombination, a cellular mosaic of up to fifteen distinguishable clones of cells, of which nine result from a dual recombination event. Six of these fifteen will express a single fluorescent protein (and gene), while the other nine will have expression of a combination of two FPs, one localized in the membrane and one in the chromatin, with the correspondent equimolar expression of the proteins coded by the genes inserted downstream (Fig. 4.1 C, D)

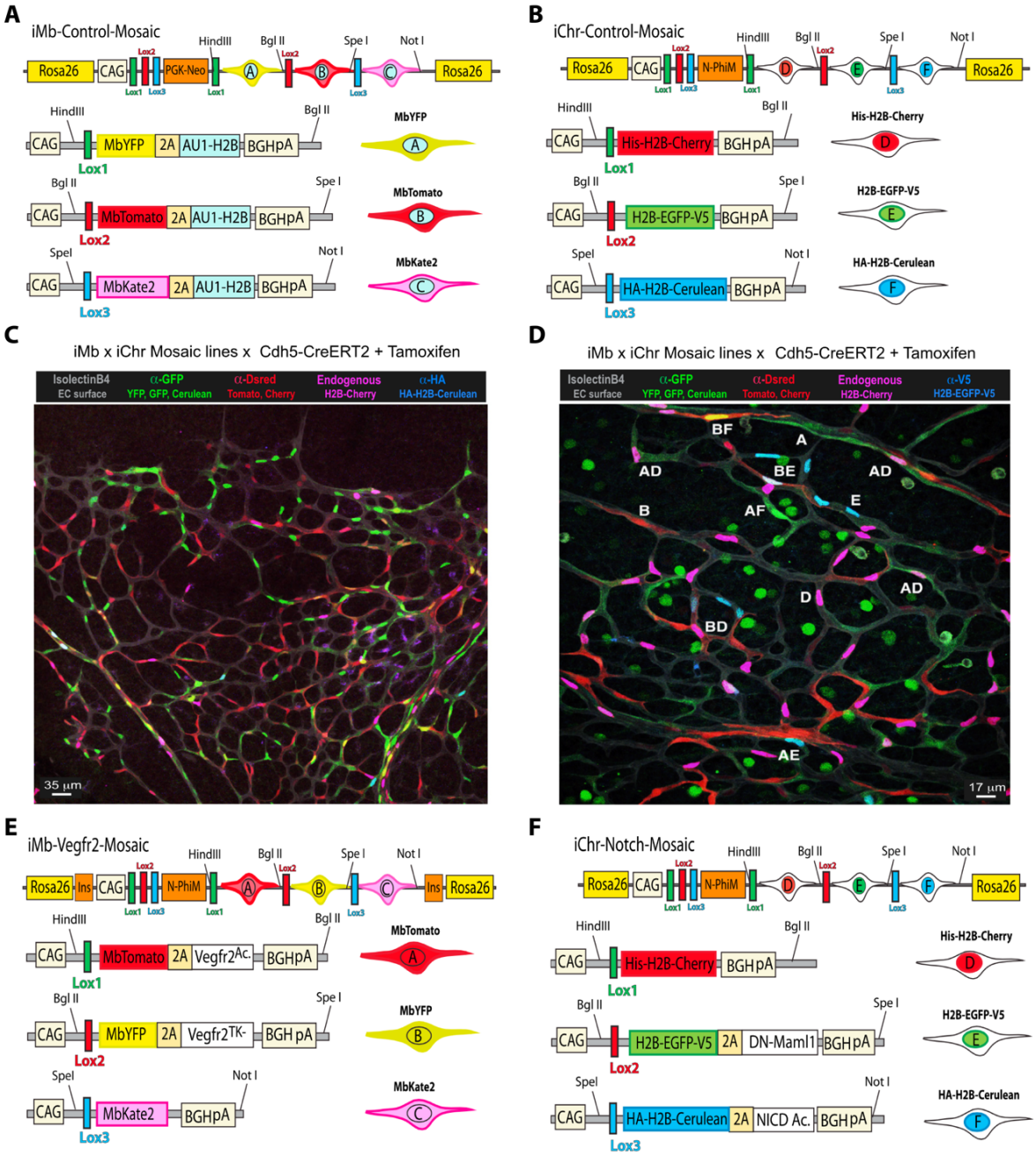

Figure 4.2. Inducible membrane and chromatin mosaic constructs and mice. A, B Diagrams showing the specific control constructs of iMb-Control-Mosaic (**A**) and iChr-Control-Mosaic (**B**). To facilitate detection and quantification, we associated a nuclear localized tag to the expression of membrane fluorescent proteins in the iMb-Control-Mosaic in A. **C, D** Retinal vasculature of P6 mouse containing the *iMb-Mosaic*, *iChr-Mosaic*, and *Cdh5(PAC)-CreERT2* alleles, 3 days after induction of recombination with tamoxifen. The genetic mosaic is detected within the IsolectinB4+ vascular tissue by confocal scanning of a combination of endogenous fluorescence (Cherry) and immunostainings (a-GFP to detect GFP, YFP and Cerulean; a-dsRed to detect Cherry and Tomato; a-HA for HA-Cerulean) Single- and dual-labeled clones are visible at low **(C)** and higher **(D)** magnification. **E, F** Diagrams showing the functional mosaic constructs of iMb-VEGFR2-Mosaic (**E**) and iChr-Notch-Mosaic (**F**). DN-MAML1 is dominant-negative protein that sequester the endogenous NICD and reduce Notch receptor signaling in a cell-autonomous manner. NICD Ac. is the active form of NICD, containing the native PEST domain that results in a relatively moderate increase of ligand independent Notch activity. $VEGFR2^{AC.}$ is the constitutively active form of VEGFR2 without the extracellular domain. $VEGFR2^{TK-}$ a tyrosine kinase-domain mutant version of murine VEGFR2 that strongly reduces VEGF signaling in a cell-autonomous manner.

To facilitate the correct identification of each clone my lab coworkers selected proteins that have easily distinguishable fluorescent spectra and included short tags in the nuclear proteins that are easily detectable by immunostaining. They also coupled this genetic design to a modular DNA engineering strategy that allows for the rapid generation of several different transgenic and gene-targeted mESC and mouse lines. Thus, they were able to generate a variety of mosaic mouse lines that I screened and used in my studies. The iChr- and iMb-Control-Mosaics only express fluorescent proteins and can be used as experimental controls or to combine with the functional mosaics to increase clonal resolution (Fig. 4.2 A-D).

In the iChr-Notch-Mosaic allele (Fig. 4.2 F) there is the expression of a Dominant Negative (DN)-Maml1 sequence to block Notch function (Maillard *et al.*, 2004) and a NICD-PEST to activate it (Kopan and Ilagan, 2009) In the iMb-Vegfr2-Mosaic allele (Fig. 4.2 E) we used the expression of a constitutively active VEGFR2 (Dosch and Ballmer-Hofer, 2010) to activate VEGFR2 signaling ($VEGFR2^{Ac.}$) and a tyrosine kinase mutant (Y1173) form of VEGFR2 (Sakurai *et al.,* 2005) that can sequester VEGF and dimerize with the endogenous VEGFR2, thus decreasing VEGFR2 signaling ($VEGFR2^{TK-}$) in a cell autonomous manner. In each of these functional genetic mosaics, one of the three fluorescent proteins is expressed alone and will label the “normal/control” cells. The activation or inhibition of the Notch and VEGFR2 signaling pathways by these genetic sequences was determined by measuring the expression or activity of Notch or VEGF signaling targets (Pontes-Quero *et al.,* 2017).

4.2 Functional characterization of iChr-Notch- and iMb-Vegfr2-Mosaics

In order to test the function of these new constructs, we analyzed their effects on different cellular aspects during biological processes known to be regulated by the Notch and VEGF signaling pathways.

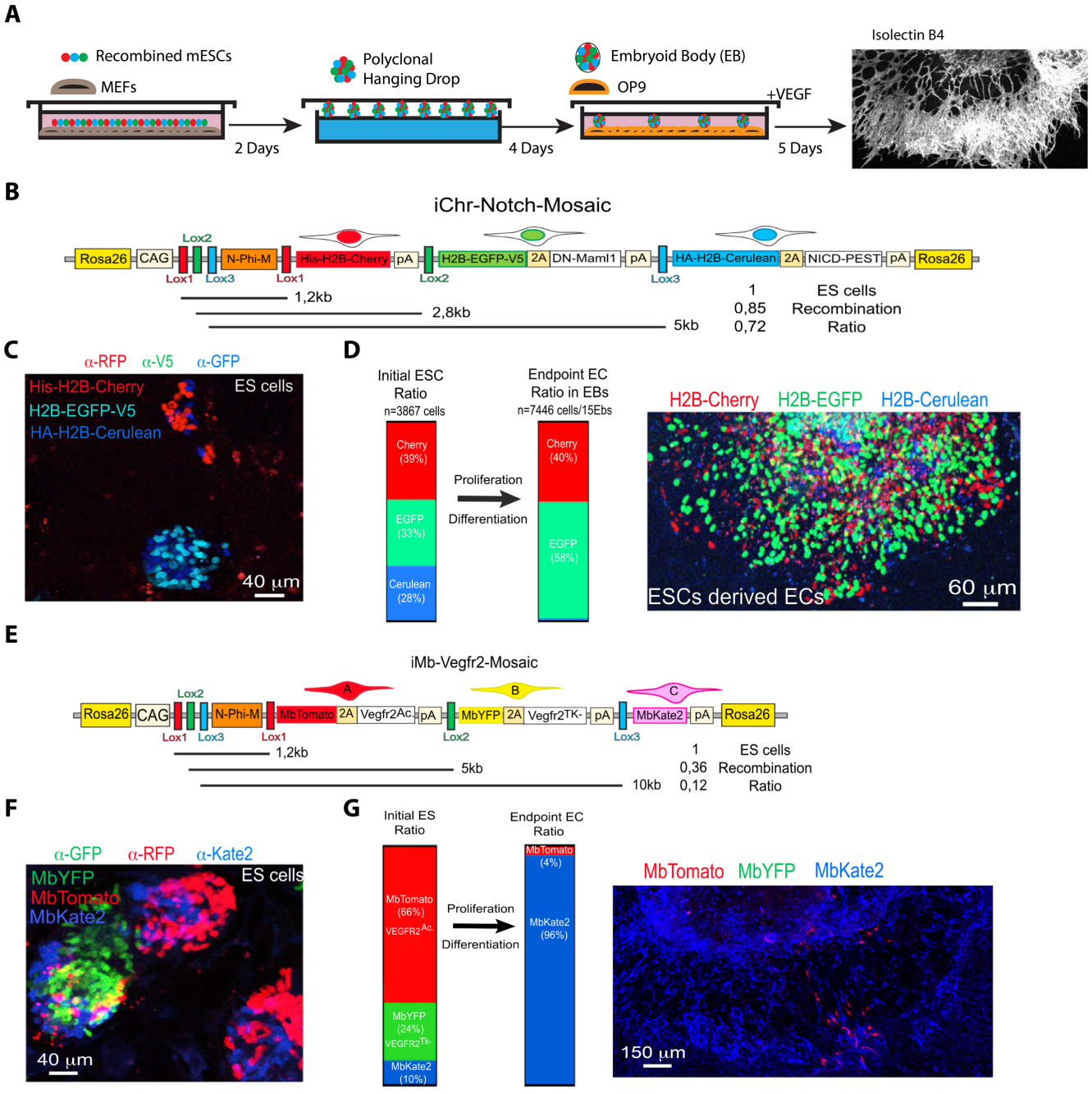

Figure 4.3. Characterization of Notch and VEGFR2 mosaics in embryoid bodies *In vitro*. A, Experimental protocol for in vitro differentiation of ECs from EBs. Embryoid bodies derived from mESCs were plated on a OP9 monolayer to induce EC differentiation and sprouting. An example of a typical endothelial cell network is shown. **B,** *iChr-Notch-Mosaic* DNA construct inserted in the *Rosa26* locus. Below the genetic distance (kb) between different *LoxP* sites and the relative recombination ratios obtained after Cre-expressing plasmid transfection in mESCs. **C,** Representative picture of iChr-Notch-Mosaic mESCs expressing the different fluorescent proteins immunostained with a-GFP, a-dsRed and a-HA antibodies. **D**, Ratios of the recombined cells observed in mESCs and after differentiation to ECs. Right shows a representative picture of an EB-derived endothelial monolayer expressing the iChr-Notch-Mosaic. **E**, iMb-Vegfr2-Mosaic DNA construct. Below the genetic distance (kb) between different *LoxP* sites and the relative recombination ratios obtained after Cre transfection. **F**, Representative picture of iMb-Vegfr2-Mosaic ES cells expressing the different fluorescent proteins immunostained with a-GFP, a-dsRed and a-Kate antibodies. **G**, Ratios of the recombined cells observed in mESCs and after differentiation to ECs. Right shows a representative picture of an EB-derived endothelial monolayer expressing the *iMb-Vegfr2-Mosaic*.

As an initial approach, we studied *In vitro* how the induction of the two mosaics in mouse Embryonic Stem Cells (mESCs) influence their capacity to differentiate to ECs and their subsequent expansion using and embryoid body (EB) differentiation assay on OP9 cells (Hirashima *et al.*, 1999; Feraud, Cao, and Vittet, 2001) (Fig. 4.3 A).

mESCs expressing the iChr-Notch-Mosaic and transfected with Cre-expressing plasmids displayed relatively balanced recombination rates for each of the three cassettes, with some bias for the recombination of closer Lox sites (Fig. 4.3 B, C). However, after differentiation to ECs, these proportions were considerably altered. ECs expressing DN-MAML1 *In vitro* were more frequent compared with ECs only expressing the reporter protein (control), while very few ECs expressing the NICD-PEST gene were detected (Fig. 4.3 D), suggesting that Notch activation blocks EC differentiation, proliferation or survival. In the case of mESCs expressing the iMb-Vegfr2-Mosaic, initial recombination biases were more apparent, probably due to the bigger distance between Lox sites (Fig. 4.3 E, F). Moreover, VEGF alterations produced a much more striking effect on EC mosaic frequencies. Not a single EC expressing the $VEGFR2^{TK-}$ was detected, probably due to its essential requirement during EC differentiation (Marcelo, Goldie, and Hirschi, 2013). Furthermore, very few endothelial cells expressing $VEGFR2^{Ac.}$ were found and most differentiated EC were the ones expressing the fluorescent protein only (Fig. 4.3 G), which could also indicate that excessive VEGFR2 signaling might also be detrimental for mESC differentiation to EC, or their proliferation, as it will be mentioned later.

To evaluate their performance *In vivo,* we examined how they influence cellular differentiation and proliferation during embryonic neurogenesis in the neural tube (iChr-Notch-Mosaic) or during retinal angiogenesis (iMb-Vegfr2-Mosaic).

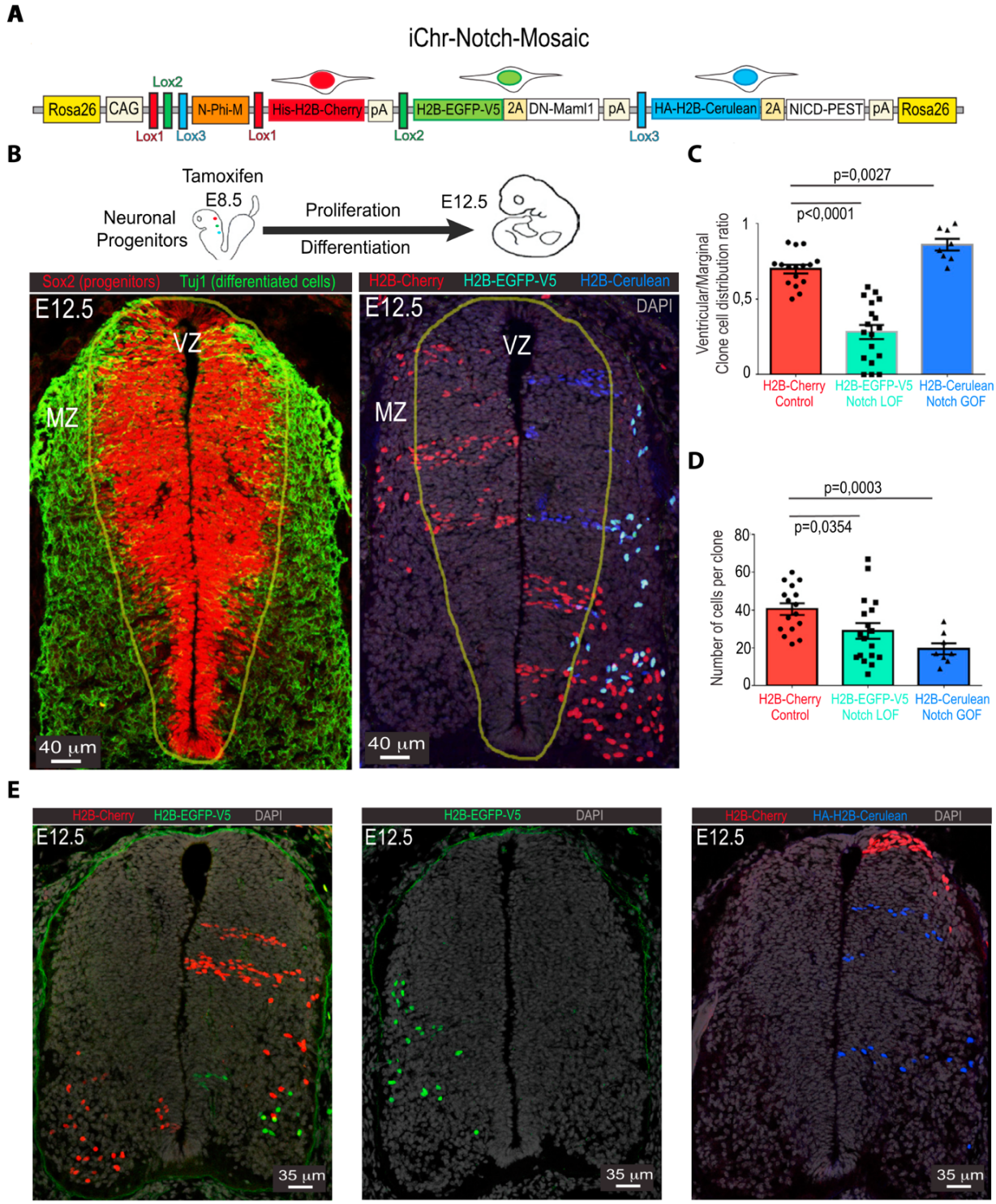

Figure 4.4. Characterization of iChr-Notch-Mosaic during embryonic neurogenesis. A, iChr-Notch-Mosaic DNA construct inserted in the Rosa26 locus. **B,** Confocal micrographs of 20-micron thick cryosections of E12.5 embryos immunostained for the indicated markers. The border between the marginal (MZ) and ventricular (VZ) zones is indicated by a yellow line. **C,** Quantification of the ratio of Ventricular to Marginal localization of the cells for each clone analyzed. **D,** Quantification of clone size for each of the three possible fluorescent clones. **E**, Additional confocal micrographs of 20-micron thick cryosections of E12.5 embryos immunostained for the indicated markers showing the isolated clones analyzed. Error bars indicate SEM. Statistical analysis was performed by ANOVA with $P<0.05$ considered statistically significant.

During neurogenesis, progenitor cells located in the Ventricular Zone (VZ) of the neural tube proliferate and progressively differentiate to neurons that migrate to the Mantle Zone (MZ) (Briscoe and Small, 2015) (Fig. 4.4 B). During this process Notch activity regulates the balance between proliferation and differentiation for optimal production of neurons (Louvi and Artavanis-Tsakonas, 2006).

We crossed the iChr-Notch-Mosaic with the ubiquitously expressed *Polr2a-CreERT2* mouse line (Guerra *et al.,* 2003) and induced recombination with a single injection of Tamoxifen at embryonic day E8.5. Embryos collected at E12.5 were immunostained for the three fluorescent proteins (Fig. 4.4 A, B).

Within this time period, neural progenitors (Tuj1-, Sox2+) with normal Notch activity (H2B-Cherry+) formed clones that preferentially located in the VZ and only partially differentiated to Tuj1+, Sox2- neurons that migrated to the MZ. In contrast, progenitor cell expressing the NICD-PEST (H2B-Cerulean+) mostly remained as undifferentiated cells in the VZ, while the ones expressing DN-MAML1 (H2B-GFP-V5+) seemed to preferentially commit to terminal differentiation, and their progeny was mainly located in the MZ (Fig. 4.4 B, C, E).

Moreover, both of these populations showed reduced clone size (Fig. 4.4 B, D, E). indicating that, although Notch has opposing effects on their differentiation, it similarly reduced their proliferative capacity, impairing neurogenesis.

During retinal angiogenesis VEGF signaling is involved in endothelial cell proliferation and tip-cell selection (Blanco and Gerhardt, 2013). We crossed the iMb-Vegfr2-Mosaic line with the endothelial specific inducible Cre driver line Cdh5-(PAC)-CreERT2 and analyzed immunostained retinas at P6, three days after a single tamoxifen injection.

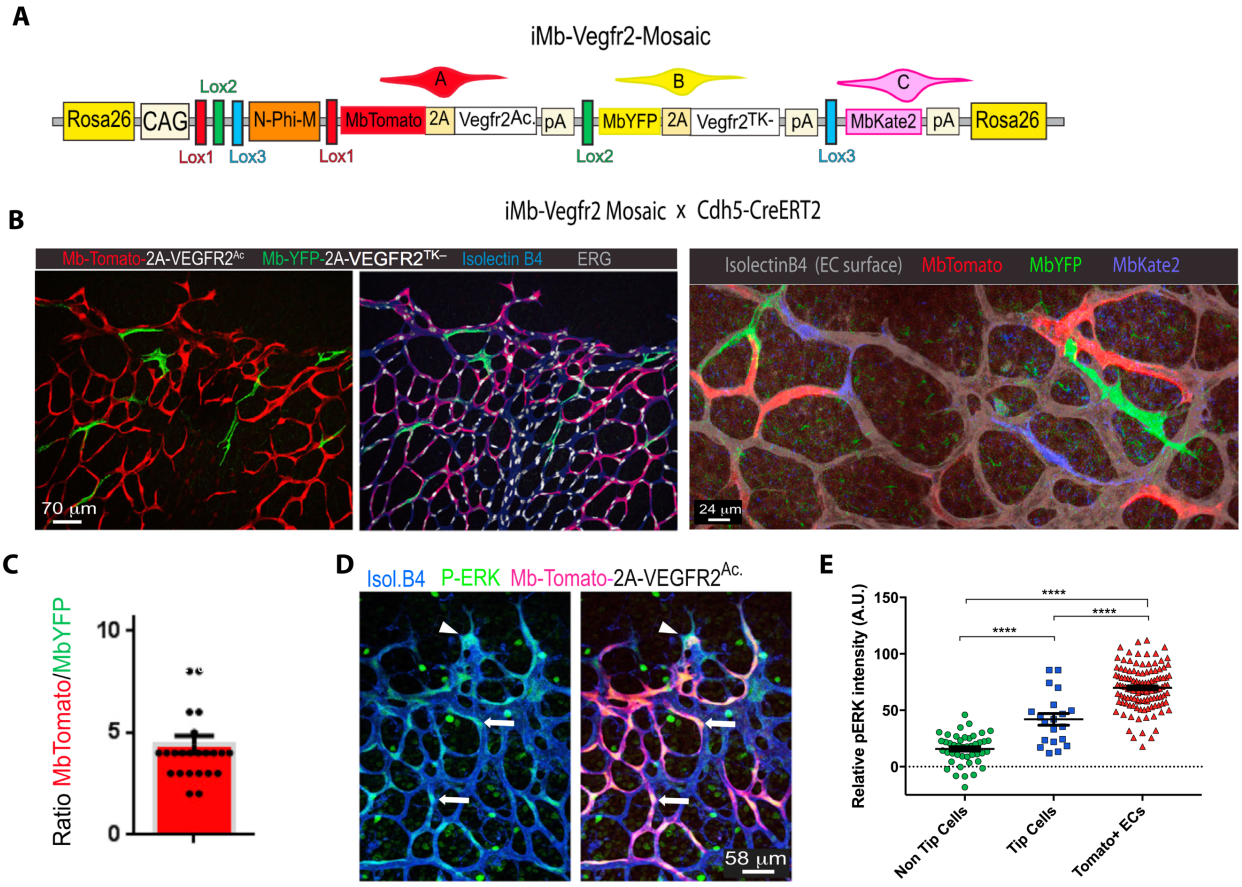

Figure 4.5. Characterization of iMb-Vegfr2-Mosaic during retinal angiogenesis. A, iMb-Vegfr2-Mosaic DNA construct. **B,** Confocal micrographs of the retinal vasculature from a P6 animal carrying the iMb-Vegfr2-Mosaic and Cdh5-CreERT2 transgenes, 3 days after tamoxifen injection, immunostained to detect the different mosaic markers, MbYFP in green, MbTomato in red and MbKate in blue(right). IsolectinB4 labels the surface and ERG the nuclei of all ECs. **C**, Quantification of the relative proportion of MbTomato to MbYFP occupied vascular surface per field. **D,** Retinal vessels from P6 animals carrying the iMb-Vegfr2-Mosaic and Cdh5-CreERT2 transgenes, 3 days after tamoxifen injection, immunostained of MbTomato(Red), pERK(Green) and IsolectinB4 (Blue). Arrowhead indicates a tip cell; arrows indicate MbTomato+ cells. **E,** Quantification of relative intensity of pERK immunostaining in three different EC population of these retinas: stalk cell, tip cells and MbTomato+ cells. Error bars indicate SEM. Statistical analysis was performed by ANOVA. **** P<0.0001.

These retinas showed a strong disparity in the proportions of each fluorescent cell; cells expressing VEGFR2$^{Ac.}$ (MbTomato+) were much more frequent than the ones expressing VEGFR2^{TK-} (MbYFP+) (Fig. 4.5 A-C), and control cell (Kate2+) were practically absent, maybe reflecting similar recombination biases to the ones found in mESC in this short time experiment. Further analysis of cells expressing VEGFR2$^{Ac.}$ (MbTomato+) showed an increase in the levels of ERK phosphorylation, a downstream target of VEGFR2 activation (Gille *et al.,* 2001). These levels were even higher than in tip cells, which are the cells that have higher physiological activation of VEGFR2 during angiogenesis (Fig. 4.5 D, E). We also found these MbTomato+ cells frequently at the angiogenic front, as tip cells, and the MbYFP+ cells more in the stalk region, but we could not safely distinguish it from the strong initial recombination bias. A higher clonal resolution and stronger quantitative analysis is required to determine precisely the effect of these single-cell VEGFR2 signaling genetic manipulations on sprouting behavior.

4.3 Single-cell clonal analysis of loss and gain of Notch signaling during angiogenesis

By using the Dual ifgMosaic strategy we were able to perform a detailed clonal analysis of endothelial cells during retinal angiogenesis and determine how Notch signaling alterations affect the proliferation of single-cells in a short time interval. To maximize the number of analyzed clones while maintaining enough resolution to identify them, we combined in the same mouse the iChr-Notch-Mosaic and iMb-Control-Mosaic alleles (Dual-ifgMosaic) with the Cdh5-(PAC)-CreERT2 allele and induced recombination with a single Tamoxifen dose at P3 (Fig. 4.6 A, B).

After three days of clonal expansion we analyzed only clones with expression of both nuclear and membrane fluorescent proteins. The low frequency of double recombination events enables a more precise discrimination of clonal identity. To further improve clone discrimination, especially in areas with higher frequency of double recombined clones, we defined a size-dependent, average clone dispersion area in highly isolated clones (Fig. 4.6 C). We then identified as individual clones the ones enclosed within the defined dispersion area (Fig. 4.6 E).

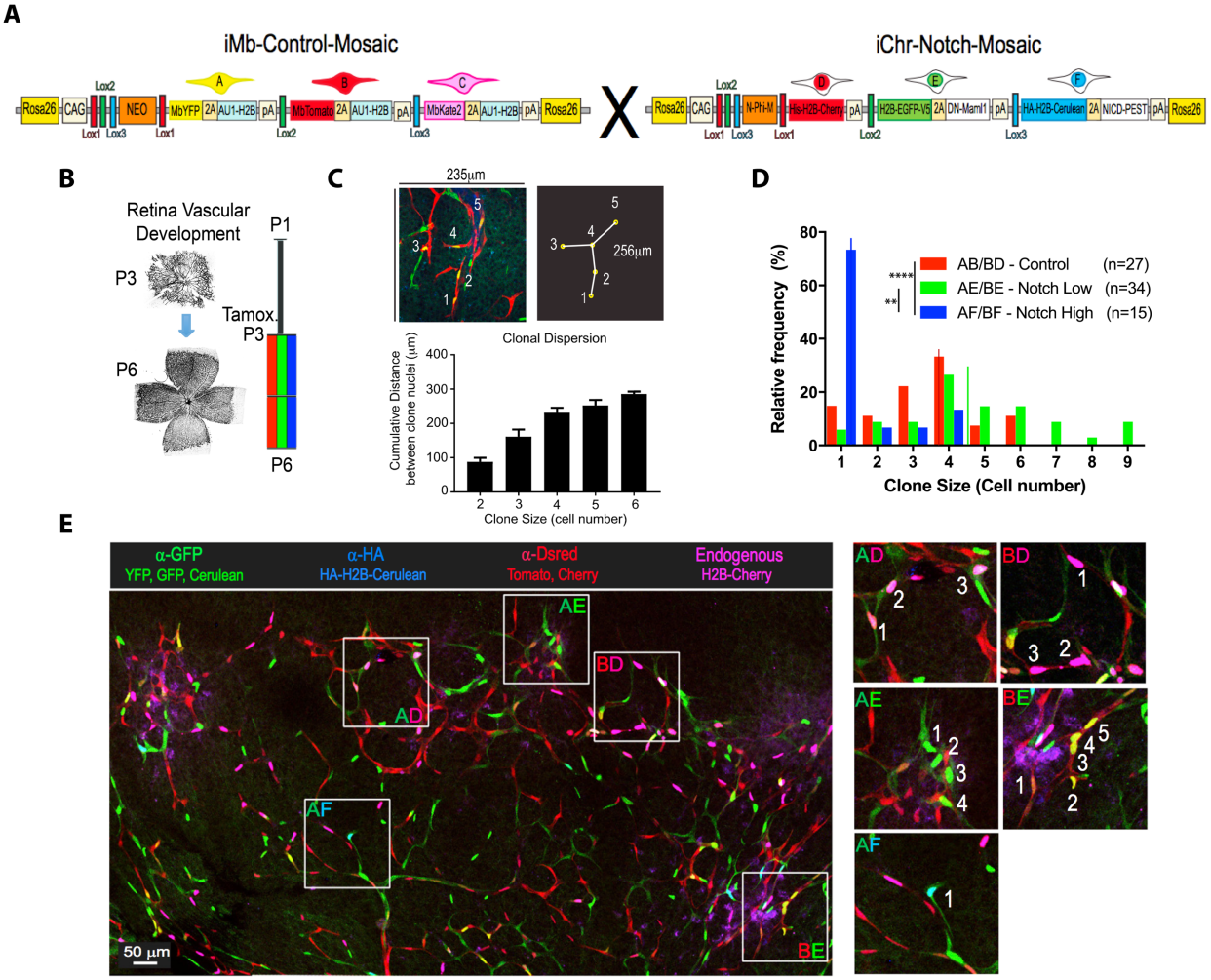

Figure 4.6. Short-term clonal expansion of endothelial iChr-Notch-Mosaic during angiogenesis. A, iMb-Control-Mosaic and iChr-Notch-Mosaic were intercrossed in animals carrying the *Cdh5*-CreERT2 transgene. **B**, Diagram of the experimental setting. Tamoxifen was injected at P3, labelled endothelial clones were allowed to expand in the for 3 days and were analyzed at P6. **C**, Representative picture of a dual clone with 5 cells and a cumulative distance between all nuclei of 256 µm. Quantification of the average cumulative cell distance within clones of different sized used to define the clone dispersion area. Error bars indicate SEM. **D**, Histogram showing the frequency distribution of clone size for dual clones only, grouped according to their nuclear marker (Notch-signaling level). Vertical lines indicate median values. Statistical analysis was performed with a Kruskal-Wallis test. *p < 0.05 ***p<0.001. **E, Left,** Representative confocal micrograph of a retina 3 days after tamoxifen induction, showing the four different acquisition channels used, Green for the immunostaining of three GFP related proteins, Blue for HA-Cerulean, Red for the dsred related proteins and pink for endogenous Cherry fluorescence. White boxed areas delimitate some double fluorescent clones. **E, Right**, Higher magnification pictures of the boxed areas allow visualization of the cell shape and nuclei for quantification of clone size and distribution. Letter codes were assigned to double recombined clones according to their membrane (A–C) or nuclear (D–F) color.

We found that endothelial cells without modifications in Notch activity present a Gaussian distribution of clone sizes centered around a size of four cells and with a maximum of six cells (Fig. 4.6 E, Red). This indicates that EC cycling dynamics greatly vary in normal conditions, with some cell not dividing at all and others undergoing more than two rounds of division within a three-day period, with a median of two rounds of divisions per labeled cell.

We also found that cells expressing the DN-MAML1 gene had a similar distribution of clone sized, but displaced towards slightly bigger clones with a maximum of seven cells and a median clone size of four and a half (Fig. 4.6 E, Green). This could indicate that blocking Notch could be promoting or accelerating endothelial cell cycle progression during this short time window. In contrast, cell expressing the NICD-PEST showed a clear impairment in proliferation as most of the clones were formed by a single cell (Fig. 4.6 E, Blue). The few that showed endothelial cell division were limited to a maximum of three cells per clone indicating either an earlier cell cycle exit or a very slow cell cycle progression.

4.4 Excessive or insufficient VEGFR2 activity impairs EC clonal expansion

We similarly evaluated the effects that VEGFR2 signaling alterations on short term endothelial single cell clonal expansion during angiogenesis. We combined in the same mouse the iMb-Vegfr2-Mosaic and iChr-Control-Mosaic alleles (Dual ifgMosaic) with the Cdh5-(PAC)-CreERT2 allele, and induced recombination with a single Tamoxifen dose at P3, and analyzed the clone size after three days of clonal expansion (Fig. 4.7 A, B).

As in this line the recombination is strongly biased to the first cassette, and the generation of Kate+ control cells is rare, we were not able to quantify clone size of control cells with normal VEGFR2 signaling in the same retinas. We restricted the quantifications in these mice to only to double fluorescent clones expressing either membrane YFP or membrane tomato in combination with GFP or Cerulean only, excluding clones with expression of the more frequently recombined nuclear Cherry, to ensure clonality

We show that, in contrast to Notch mosaics, for VEGFR2, both increased and decreased activity lead to a reduction clone size (Fig. 4.7 C, D) with VEGFR2$^{Ac.}$ clones having a median size of 1 cell and a maximum of 3 and VEGFR2^{TK-} also a median size of 1 and a maximum of 2 indicating that VEGFR2 activity must be within strictly regulated levels to allow ECs to undergo normal cell cycle progression.

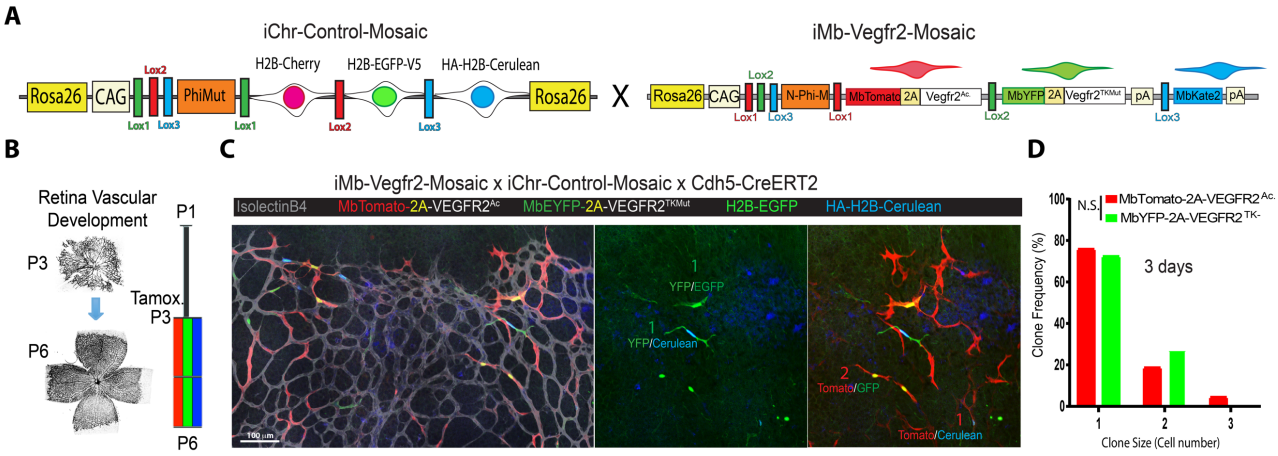

Figure 4.7. Short-term clonal expansion of endothelial iMb-Vegfr2-Mosaic during angiogenesis. A, iChr-Control-Mosaic and iMb-Vegfr2-Mosaic were intercrossed in animals carrying the *Cdh5*-CreERT2 transgene. **B**, Diagram of the experimental setting. Tamoxifen was injected at P3, labelled endothelial clones were allowed to expand in the for 3 days and were analyzed at P6. **C,** Representative confocal micrograph of a retina 3 days after tamoxifen induction, showing the three different acquisition channels used, Green for the immunostaining of three GFP related proteins, Blue for HA-Cerulean, Red for the dsred related proteins. Individual double fluorescent clones are indicated, as well as their size. **D,** Histogram showing the frequency distribution of clone size for dual clones only, grouped according to their membrane marker (Vegfr2-signaling level). Statistical analysis was performed with a Mann–Whitney test. N.S, not significant.

4.5 VEGFR2 signaling partially modulates the effect of Notch on the proliferation of single ECs

The dual ifgMosaic strategy enabled us to study at the single cell level how the Notch and VEGF signaling pathways interact to control endothelial cell cycle dynamics. To this end we performed similar clonal analysis in mice carrying the iChr-Notch-Mosaic, iMb-Vegfr2-Mosaic and Cdh5-(PAC)-CreERT2 alleles. Retinas were analyzed at P6, three days after a single tamoxifen injection.

Unlike in previous analysis, here the dual recombined/labelled clones will have a combinatorial modification of both the Notch and VEGF signaling pathways in single cells, which enables epistasis analysis at single cell resolution. For technical reasons related with the very low frequency of Kate2+ clones and the need of using an additional Ab (channel) to detect it, we compared the data obtained with this Dual functional mosaic approach with the single functional mosaic analysis showed in Figs. 4.6 and 4.7 (Fig. 4.8 A, B).

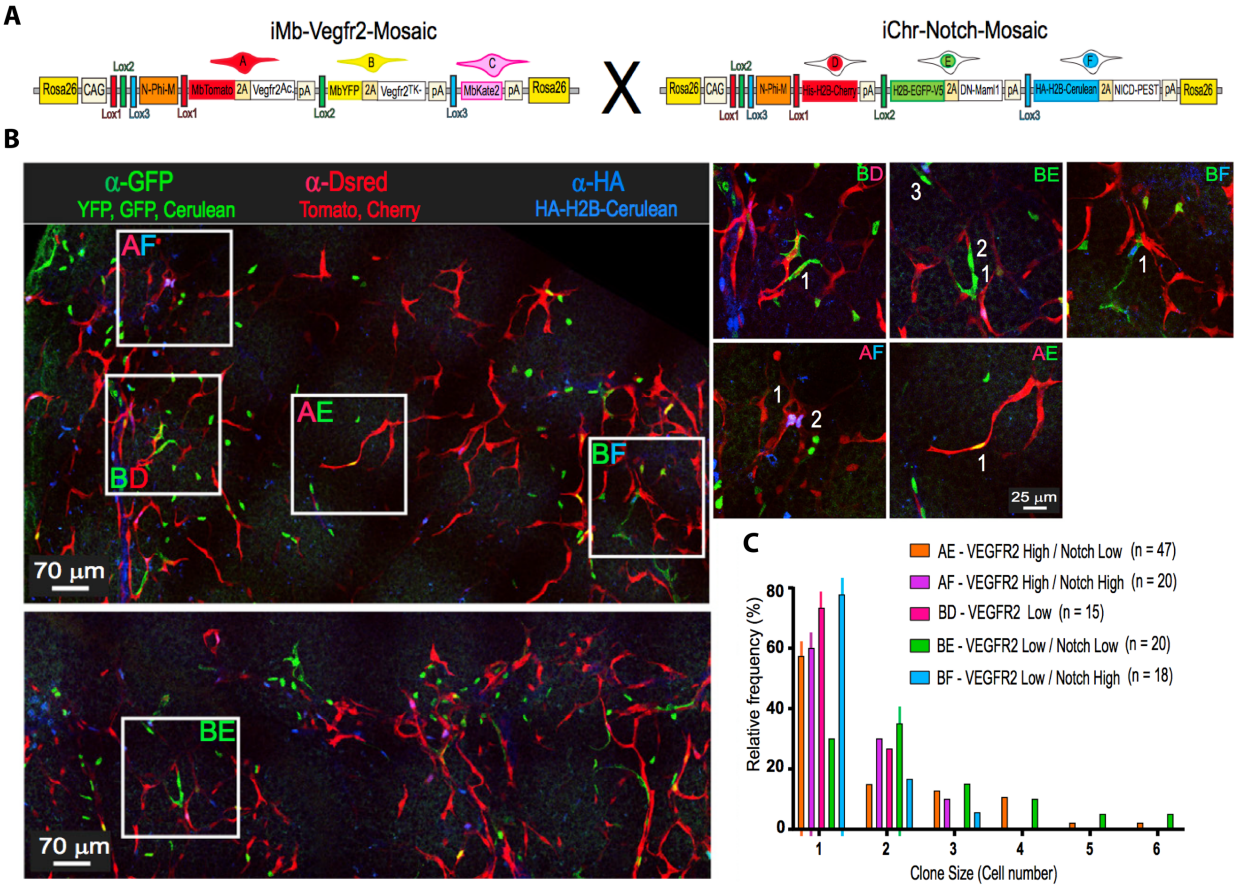

Figure 4.8. Single-cell, epistasis analysis of Notch and VEGFR2 signaling pathways with Dual ifgMosaic. A, iMb-Vegfr2-Mosaic and iChr-Notch-Mosaic were intercrossed in animals carrying the *Cdh5*-CreERT2 transgene and processed as before **B, Left** Representative confocal micrograph of a retina 3 days after tamoxifen induction, showing the three different acquisition channels used, Green for the immunostaining of three GFP related proteins, Blue for HA-Cerulean, Red for the dsred related proteins. White boxed areas delimitate some double fluorescent clones. **B, Right**, Higher magnification pictures of the boxed areas allow visualization of the cell shape and nuclei for quantification of clone size and distribution. Letter codes were assigned to double recombined clones according to their membrane (A–C) or nuclear (D–F) color. **C**, Histogram showing the frequency distribution of clone size for dual clones only, according to their nuclear (Notch-signaling level) and membrane (Vegfr2-signaling level) markers. Vertical lines indicate median values. No significant differences were found with a Kruskal-Wallis test.

In contrast with the previous analysis, single cells expressing DN-MAML1 produced smaller clones when VEGFR2 signaling was also altered. Both VEGFR2 activation or inhibition (Fig. 4.8 C). reduced the expansion of DN-MAMLl1 expressing clones, but these cells still proliferated more than cells with single activation or inhibition of VEGFR2 signaling (Compare with Fig. 4.6 F). The clone size of cells with High Notch was however small, regardless of the additional activation of inhibition of VEGFR2 signaling (Fig. 4.8 C).

Importantly, single cells expressing the VEGFR2TK- protein were able to expand more when DN-MAML1 was also expressed (Fig. 4.8, C), suggesting that inhibition of Notch can result in additional cell-cycle progression in cells with VEGFR2 signaling impairment. Although VEGFR2 function is still partially required for the effective proliferation of cells with lower Notch signaling (Dn-MAML1+).

4.6 Cells with a permanent increase or decrease in Notch or VEGF signaling expand less throughout embryonic development

The previous short-term experiments show that alterations in VEGFR2 and Notch activity in ECs during angiogenesis significantly alter their proliferative capacities. In the field it is assumed that ECs with lower Notch signaling or higher VEGF signaling always sprout and proliferate more (Benedito and Hellström, 2013; Siekmann, Affolter, and Belting, 2013), however this was mostly evaluated in relatively short-term angiogenesis assays due to the severity of classical full Notch and VEGF signaling mutants. We set out to evaluate the consequences that the induction of these mosaics in all ECs, early during development, could have in the development of vessels and formation of the postnatal vasculature. We separately bred iChr-Notch-Mosaic (Fig. 4.9) or iMb-Vegfr2-Mosaics (Fig. 4.10) mouse lines with animals carrying the Tie2-Cre allele *(Kisanuki et al.,* 2001), in which Cre is expressed from E8.5 in all ECs.

In iChr-Notch-Mosaic animals we analyzed the cellular mosaic distribution in vascular networks of several tissues at P20 (Fig. 4.9 A, B). We found that all vascular networks were normal and predominantly formed by control (Cherry+) cells, with very small contribution of cells with low

Notch signaling (DN-MAML1/GFP+) and no contribution by cells with high Notch signaling (NICD-PEST/Cerulean+) (Fig. 4.9 B).

In order to have an independent confirmation of this data with another mouse line, we performed similar experiments with a second Notch mosaic line, iChr-Notch-V2-Mosaic (Fig. 4.9 C-F). This line express DN-RBPJ instead of DN-MAML1 and the functional cassette order is inverted, with the control cassette in the last position, and the NICD in the first one. Analysis of ECs from dissociated tissues showed a similar situation, with a preferential contribution of control (Cerulean) ECs to the mature vasculature of different organs (Fig 4.9 C-F).

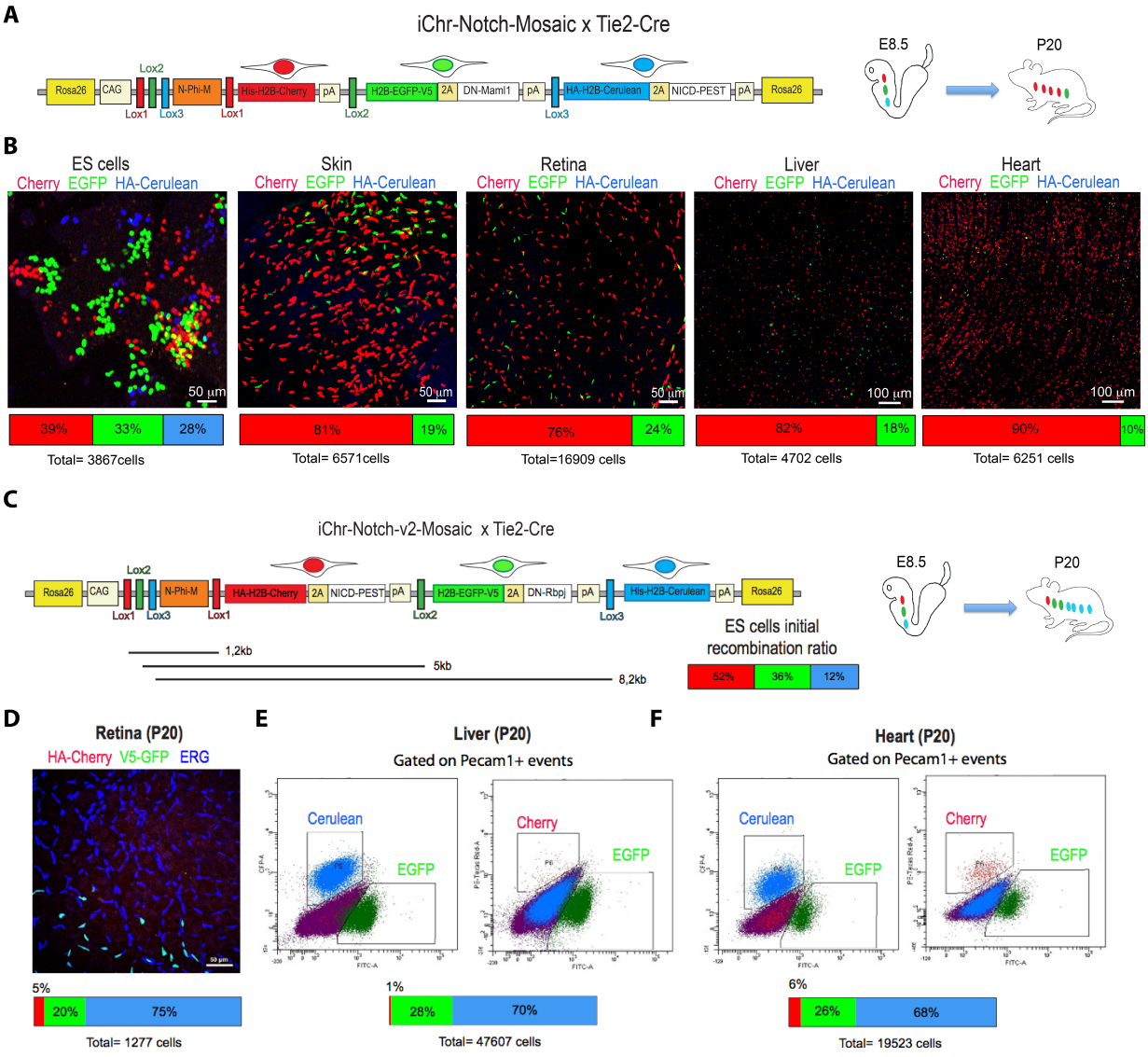

Figure 4.9. Long-term clonal expansion of endothelial iChr-Notch-Mosaic during vascular development. A, iChr-Notch-Mosaic mice were bred with Tie2-Cre animals, inducing the formation of mosaics around E8.5, and analyzed at P20. **B**, Micrographs of the vasculature from different tissues immunostained for the three fluorescent markers. Below is indicated the proportion of each fluorescent marker detected in the endothelial population. An image of the recombination frequencies in mESCs is also included for comparison. **C**, iChr-Notch-v2-Mosaic was similarly bred with Tie2-Cre animals, inducing the formation of mosaics around E8.5, and analyzed at P20. Indicated below the construct are the distances between LoxP sites and the recombination ration in mESCs. Note the reversed cassette orientation compared to A. **D,** Representative image of the retinal vasculature at P20 immunostained for the indicated proteins. ERG only cells were considered H2B-Cerulean. Indicated below are the frequencies of each population of ECs. **E, F**, Flow cytometry dot plots of cells from the indicated dissociated tissue, gated for the immunostained endothelial marker PECAM and analyzed for the endogenous fluorescence of the three proteins markers.

The results obtained for cells with higher Notch signaling are in agreement with previous results and suggest that these ECs, apart from not proliferating, may also die during vascular development, since they are found initially at E9.5/E10.5 but not at P20. However, the results obtained for the cells with a decrease in Notch signaling are surprising and indicate that the apparent short-term proliferative advantage of cells with low Notch (Fig. 4.6), is lost with time, during embryonic development.

In the case of VEGFR2 mosaics, defects in proliferation in both kinds of modified cells, and the low recombination of control Kate2 cells lead us to expect a patent defect in the vasculature. However retinal vasculature at P6 was normal. We found that this was due to a predominant expansion of a population of recombined cells with weaker expression of the Tomato+ VEGFR2$^{Ac.}$ gene (Fig. 4.10 B). This population, in combination with the expanded Kate2+ control cells, constituted the majority of the vasculature.

We detected few cells with normal , strong expression of the Tomato-VEGFR2$^{Ac.}$ cassette and even fewer expressing the MbYFP-2A-VEGFR2^{TK-} cassette, indicating once again that cells with high or low VEGF signaling do not expand well during vascular development, even though ECs with weaker, but constitutive, VEGFR2 signaling activation proliferate well and form apparently normal and mature vessels.

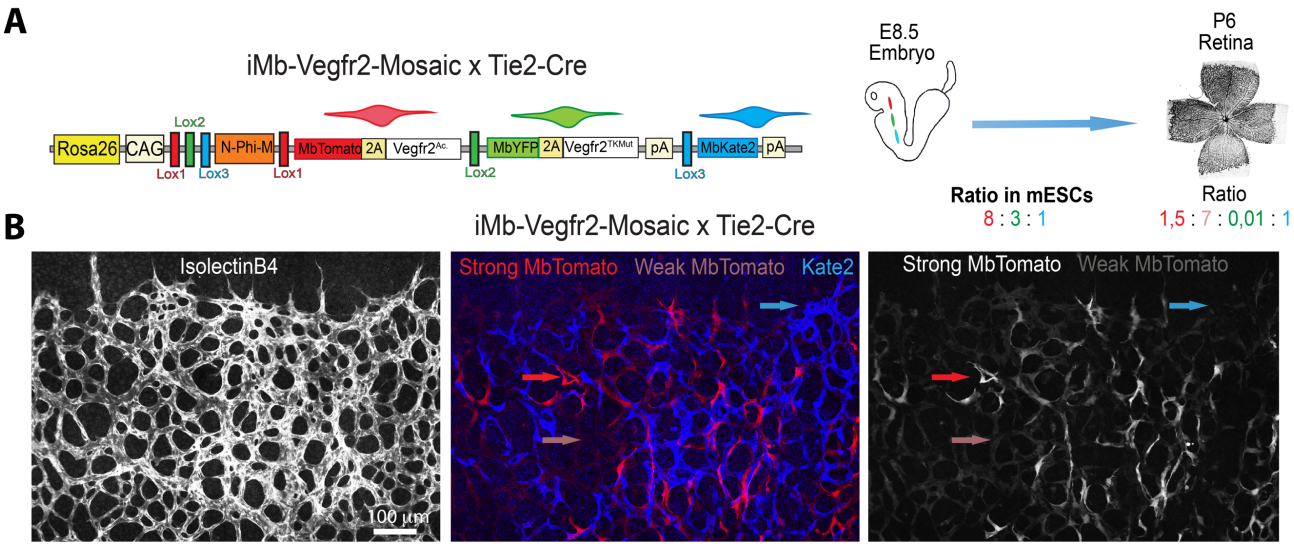

Figure 4.10. Long-term clonal expansion of endothelial iMb-Vegfr2-Mosaic during vascular development. **A,** iMb-Vegfr2-Mosaic mice were bred with Tie2-Cre animals, inducing the formation of mosaics around E8.5, and retinas were analyzed at P6. Indicated below the diagrams are the ratios of recombined mESCs and retinal ECs. **B**, Micrographs of a retinal vasculature immunostained for Isolectin B4 (left), Tomato and Kate2 (center). Right, Single channel image of the tomato signal showing the two differentiated populations based on fluorescence intensity.

4.7 Inhibition of Dll4-mediated Notch signaling during retinal angiogenesis increases EC number but decreases expression of cell cycle markers

As mentioned in the introduction, several studies have shown before that Notch inhibition increases EC proliferation. Our own *In vitro* results and *In vivo* short-term single cell clonal expansion data also support this (Fig. 4.6). However, the long term clonal analysis suggests the opposite (Fig. 4.9). To further understand these discrepancies, we decided to perform a global and detailed analysis of endothelial cell proliferation during retinal angiogenesis in conditions of low Notch signaling.

However classical genetic experiments mediated by the Cre/Lox system, previously used to understand the Notch function during angiogenesis (deletions of Dll4, Notch1 or RBPJ), do not allow for time-controlled loss-of-function studies, since the turnover of these proteins may vary after the gene deletion is induced, some of these proteins cannot be immunostained, and 3 days of genetic deletion induction are required to achieve a significant gene loss-of-function. For this reasons, and because we wanted to study what happens at 12h to 72h after endothelial Notch signaling is compromised, we used a specific and potent Dll4 blocking antibody (a-Dll4) to block endothelial Notch signaling, as Notch is mainly activated by the ligand Dll4 during retinal angiogenesis (Ridgway *et al.,* 2006). The proliferative status of ECs was analyzed by immunofluorescent detection of several cell-cycle markers in combination with the endothelial specific nuclear protein ERG at different time points after a single injection of a-Dll4.

Retinas from animals treated with a-Dll4 showed the expected hyperplasic phenotype already after 24h of a-Dll4 (Fig. 4.11 A, B). This effect was much more prominent at 48h, expanding towards mature areas, and with a much denser angiogenic front (Fig .4.11 C, D).

Hyperplasic phenotypes were associated with an almost two-fold increase in endothelial cell number at the angiogenic front (Fig 4.12 A-E).

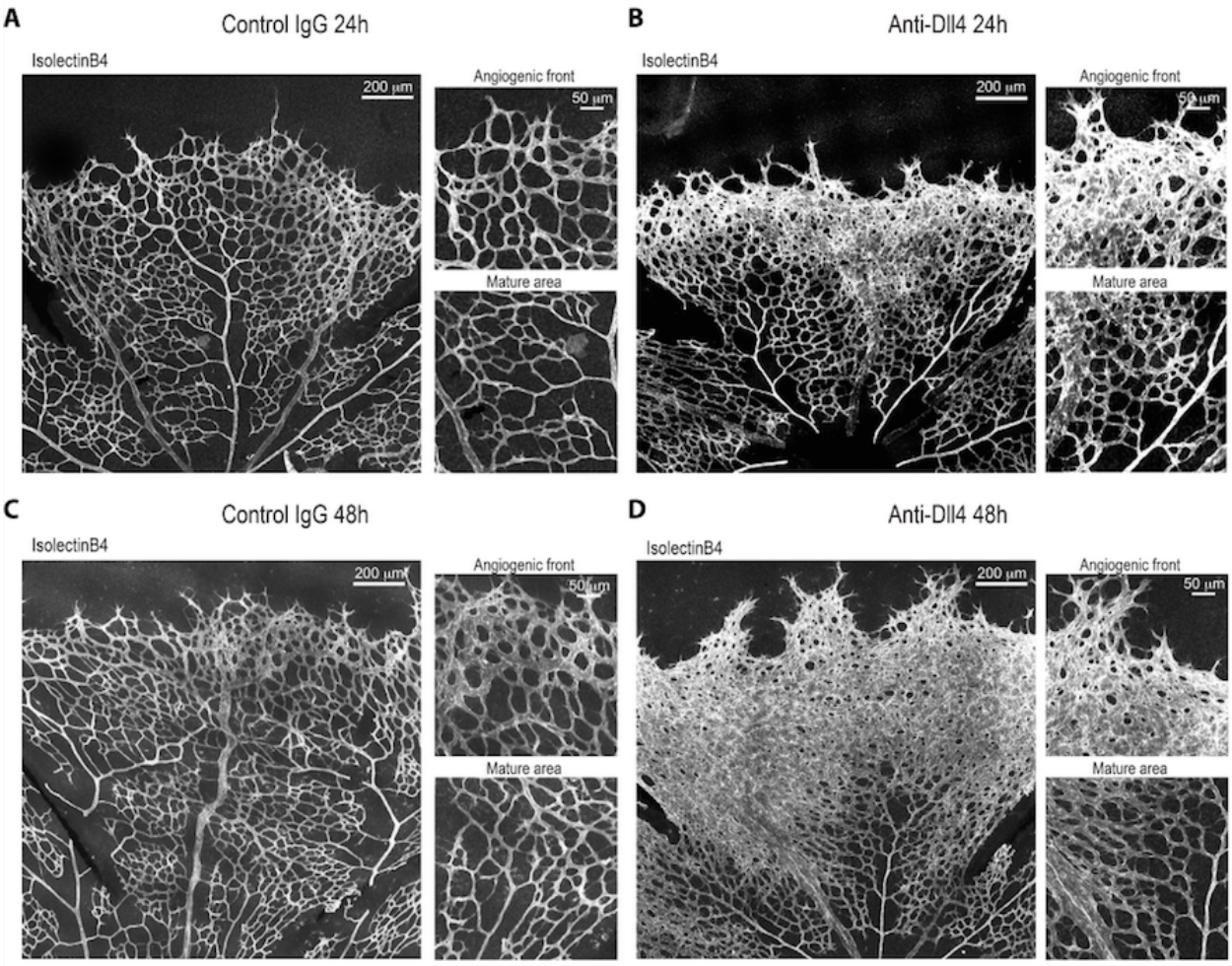

Figure 4.11. Pharmacological inhibition of Dll4-induced Notch signaling causes retinal vascular hyperplasia. A-D, Immunofluorescent detection of the vascular glycoprotein Isolectin B4 in the postnatal retinal vasculature of animals treated at P5 with control IgG or anti-Dll4 and imaged after 24h (**A, B**) or 48h (**C, D**). Global retinal vasculature (left) as well as higher magnification images from angiogenic front and mature areas (right) are shown

S-phase labelling with EdU is generally used as a marker of the number of proliferating cells, increasing when more cells are undergoing DNA synthesis. However, we did not see an increase in the S-phase ratio of ECs at the angiogenic front after 24h of Notch inhibition (Fig. 4.12 A-B, F). More interestingly, we saw that almost no ECs was labeled by EdU after 48h of Dll4/Notch LOF (Fig. 4.12 C-D, F). Mature vascular areas also showed an increase in EC number, although more modest and only after 48h (Fig 4.12 G). However, these areas did show an increase in the frequency of endothelial cells in S-phase (Fig. 4.12 H).

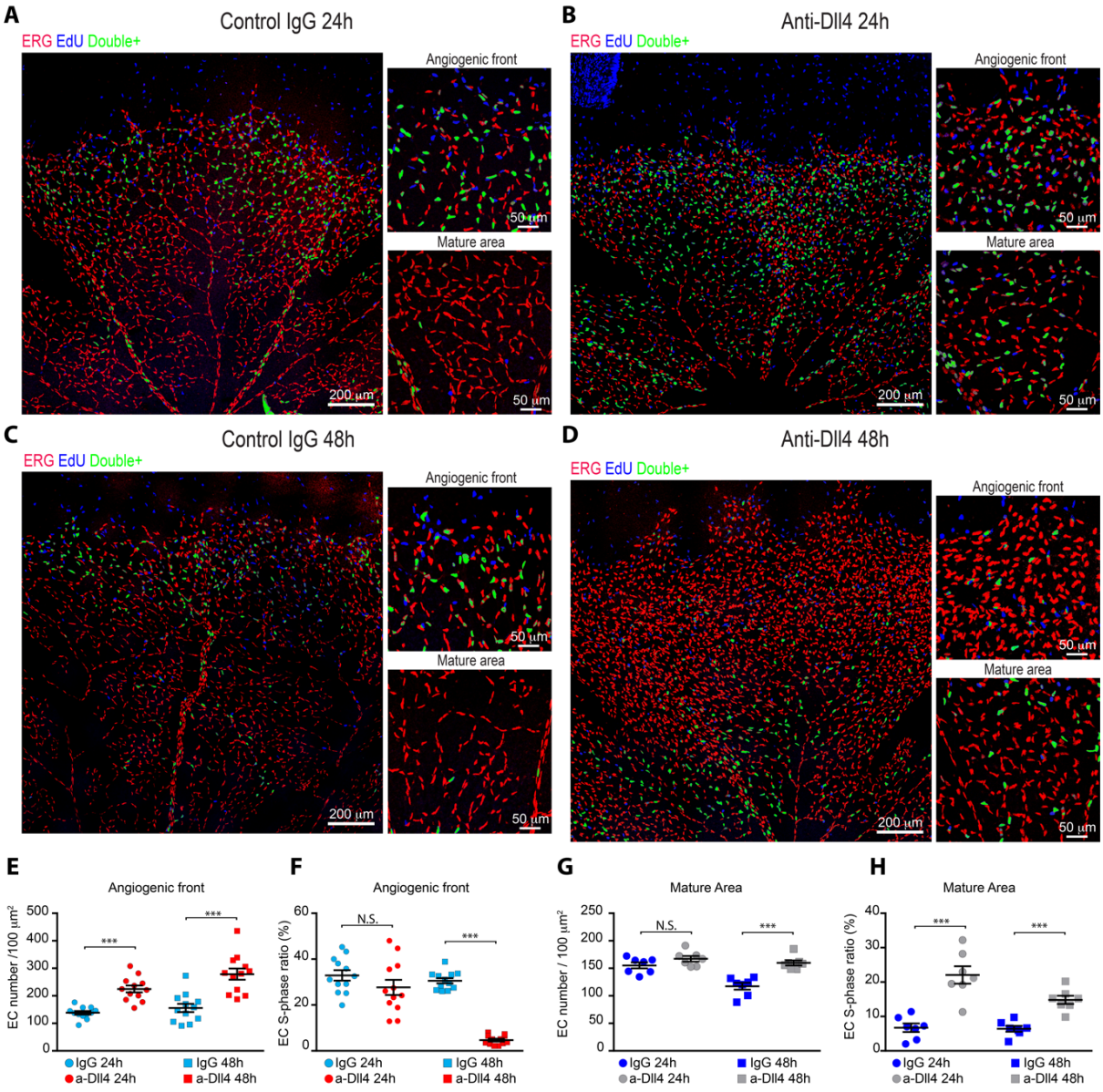

Figure 4.12. Context-dependent alterations in EC number and proliferation in retinal vasculature after Notch inhibition. A-D, Confocal micrographs of the postnatal retinal vasculature from animals treated at P5 with Control IgG or anti-Dll4 for 24h (**A-B)** or 48h (**C-D**). Anti-Erg (red) labels EC nuclei. EdU (blue or green) labels nuclei of all cells that underwent DNA synthesis in the 4 hours previous to sacrifice. Blue nuclei mark non-endothelial replicating cells, and double positive (Erg+/EdU+) cell nuclei are pseudocolored green to better highlight ECs in S-phase. Global retinal vasculature (left) as well as higher magnification images from angiogenic front and mature areas (right) are shown. **E-H**, Quantification of endothelial nuclei density (ERG+ nuclei per vascular area) and S-phase ratio (% of EdU+ERG+ among all ERG+ EC nuclei per field) in angiogenic front (**E, F**) or mature areas (**G, H**) after 24h or 48h of Notch inhibition. Error bars indicate SEM; NS, non-significant; *** p<0.0005 with an unpaired t-test.

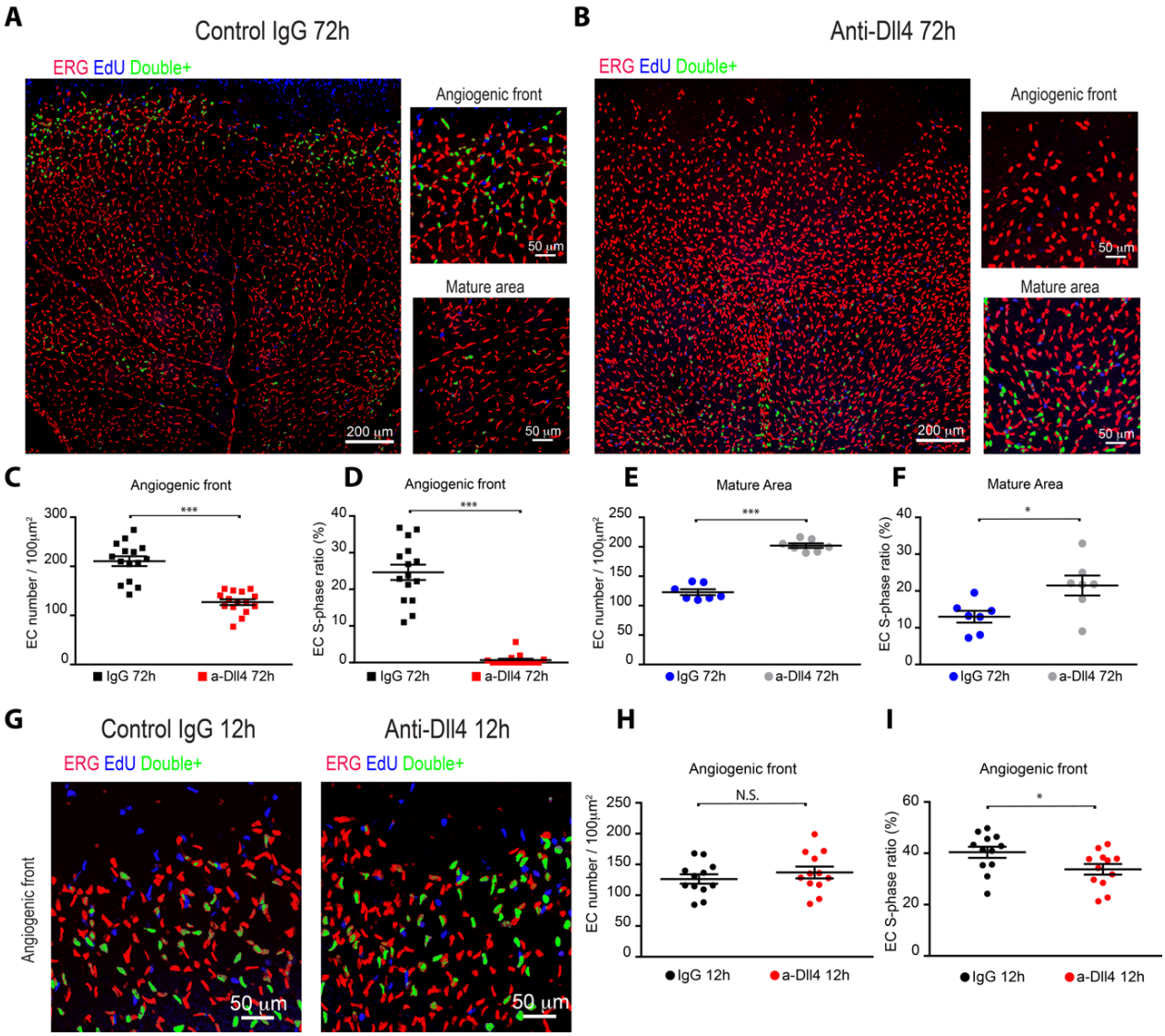

Figure 4.13. Expanded temporal analysis of retinal vascular phenotypes produced after Notch inhibition. **A, B**, Confocal micrographs of the postnatal retinal vasculature from animals treated at P5 with Control IgG or anti-Dll4 for 72h. Anti-Erg (red) labels EC nuclei. EdU (blue or green) labels nuclei of all cells that underwent DNA synthesis in the previous 4 hours. Blue nuclei mark non-endothelial replicating cells, and double positive (Erg+/EdU+) cell nuclei are pseudocolored green to better highlight ECs in S-phase. Global retinal vasculature (left) as well as higher magnification images from angiogenic front and mature areas (right) are shown. **C-F**, Quantification of endothelial nuclei density (ERG+ nuclei per vascular area) and S-phase ratio (% of EdU+ERG+ among all ERG+ EC nuclei per field) in angiogenic front (**C, D**) or mature areas (**E, F**) after 72h of Notch inhibition. Error bars indicate SEM; NS, non-significant; *** p<0.0005 with an unpaired t-test. **G**, Confocal micrographs of angiogenic fronts from the postnatal retinal vasculature of animals treated at P5 with control IgG or anti-Dll4 for 12h similarly immunostained for ERG and EdU. **H, I**, Quantification of endothelial nuclei density (ERG+ nuclei per vascular area) and S-phase ratio (% of EdU+ERG+ among all ERG+ EC nuclei per field) in angiogenic the front after 12h of Notch inhibition. Error bars indicate SEM; NS, non-significant; *** p<0.0005 with an unpaired t-test.

The increase in cell number after 24h of Dll4/Notch inhibition at the angiogenic front without an increase in the frequency of ECs in S-phase was not due to higher proliferation at earlier time points after Notch inhibition, as retinas analyzed 12h after a-Dll4 injection showed no clear differences in the frequency of ECs in s-phase (Fig. 4.13 G-I). Analysis at a later time point (72h) revealed that the absence of S-phase labelling at the angiogenic front was permanent, although the angiogenic front started to reorganize, and had less ECs (ERG+ nuclei) per vascular surface (Fig. 4.13 A-F). Moreover, the mature area still presented a higher number of EdU-labeled ECs, which indicate a sustained EC proliferation in this area.

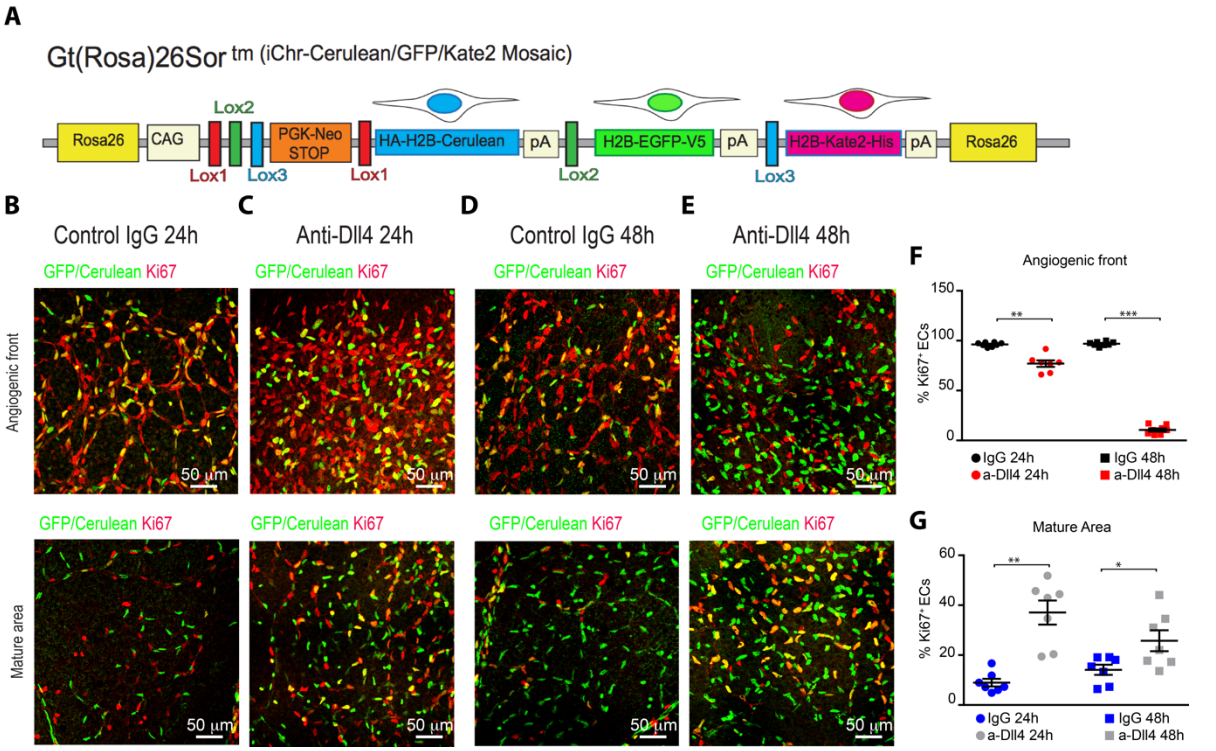

Figure 4.14. Alterations in endothelial cell expression of the cell cycle marker Ki67 after Notch inhibition. A, Diagram illustrating the mouse transgene used to specifically label the nuclei of the endothelium with GFP and Cerulean proteins, in order to perform GFP/cerulean and Ki67 immunostaining. (Rabbit anti-ERG and rabbit anti-Ki67 antibodies cannot be distinguished in double immunostainings) **B-E,** Confocal micrographs of retinal vessels from animals carrying the *Tie2-Cre* and *iChr-Cerulean/GFP* Mosaic reporter alleles, treated with aDll4 and immunostained for GFP/Cerulean (Green) and Ki67 (red) after 24 or 48 hours. Yellow nuclei correspond to Ki67-expressing ECs and green nuclei to ECs that don't express Ki67. **F, G,** Quantification of the proportion of EC expressing Ki67 per field in the angiogenic front (**F**) or mature (**G**) areas, after 24 or 48 hours of Notch inhibition. Error bars indicate SEM; NS, non-significant; * p< 0.05; ** p<0.005; *** p<0.0005. with an unpaired t-test.

As single-injection EdU labelling experiments cannot really identify the complete proliferative population in a tissue, we analyzed the expression of the protein Ki67. This protein is a generally accepted marker for cells undergoing cell cycle progression (Zambon, 2010). However, due to antibody species-specificity incompatibilities, we could not perform double ERG and Ki67 staining in the same samples. For this reason, we performed similar Notch inhibition experiments in mice carrying the *Tie2-Cre* driver and *iChr-Cerulean/GFP-Mosaic* reporter allele (Fig. 4.14 A). In these mice, most endothelial cells express either GFP or cerulean in their nuclei, allowing for their identification without using ERG.

We found that, at the angiogenic front, most ECs are Ki67+, probably indicating that all ECs are already actively undergoing cell cycle during normal angiogenesis (Fig. 4.14 B, D). Thus, the increase in EC numbers after Notch inhibition could not be due to more cells entering cell cycle. Ki67+ ECs were reduced at the angiogenic front after Notch inhibition (Fig. 4.14 C, E, F), similar to the results obtained with EdU labelling. However, Ki67 reduction was stronger both 24 and 48 hours after Notch inhibition. In mature areas we saw the opposite effect (Fig. 4.14 B-E, G), similar to our observations in EdU labelling experiments. During normal angiogenesis most of these ECs do not cycle and are considered quiescent. After Notch inhibition a higher proportion of EC are labeled with Ki67 indicating that they have entered cell cycle.

Altogether these results suggest that the effect of Dll4/Notch inhibition in vessels varies in time and space. In angiogenic ECs, it initially induces an increase in EC proliferation, followed by cell-cycle arrest whereas in more mature vessels it reactivates quiescent ECs, to enter the cell-cycle, and these remain in cycle for long periods of time.

4.8 Notch inhibition causes an increase in ERK phosphorylation

Previous studies have shown that Notch could control endothelial cell proliferation through modulation of the MAPK pathway among others (Sundaram, 2005). In the retina we could detect strong P-ERK signals in sprouting tip cells (Fig. 4.15 A-D) and weaker signals in stalk cells or mature vessels.

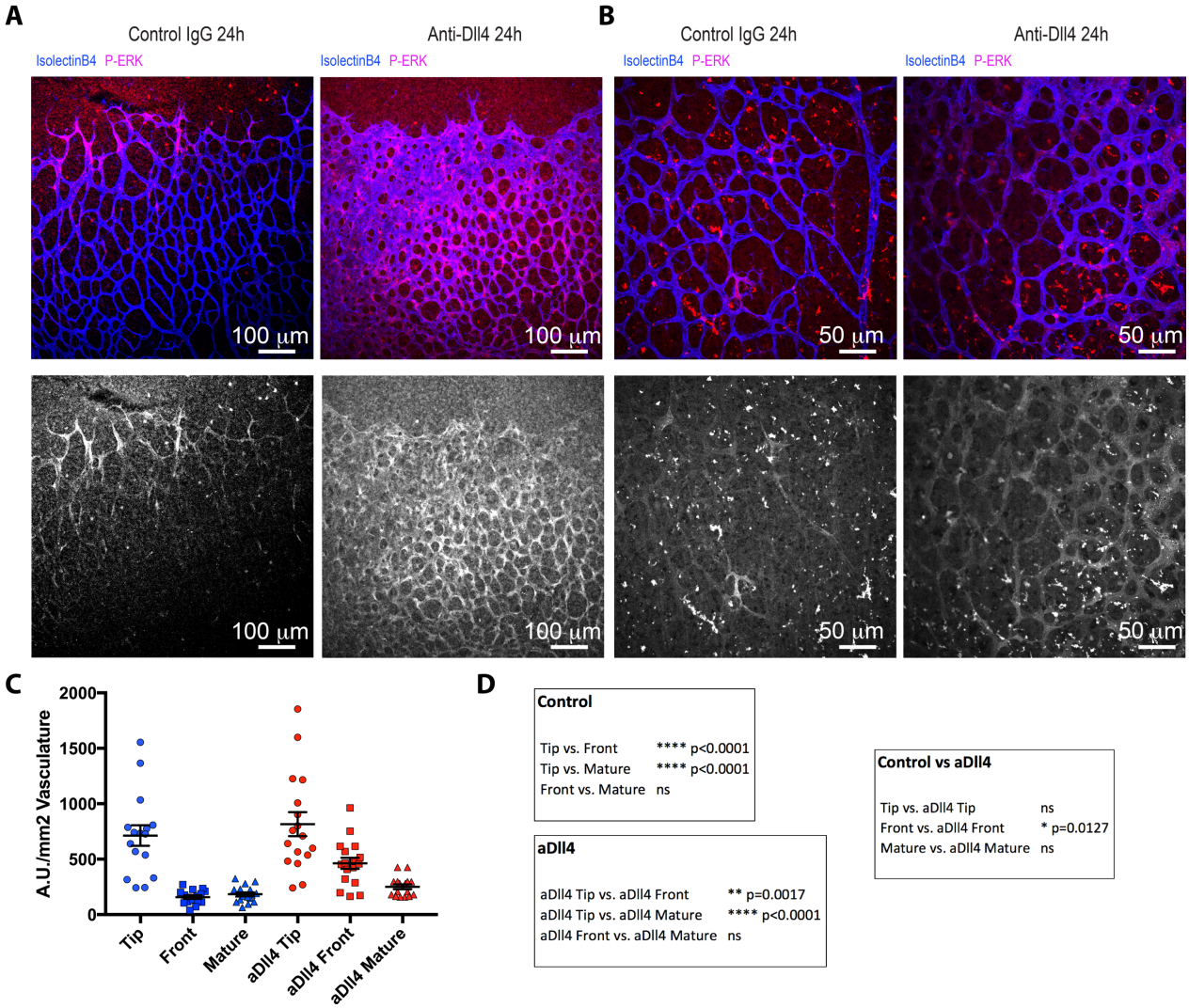

Figure 4.15. Effects of Notch on ERK phosphorylation during angiogenesis. A, **B**, Confocal micrographs of retinal vasculatures co-immunostained with IsolectinB4 (Blue) and anti-pERK (Red) in angiogenic fronts (**A**) and mature areas (**B**) 24h hours after control IgG or aDll4 injection. Single channel images for pERK are shown below. Note the higher levels of ERK phosphorylation in sprouting cells and the increased levels after Notch inhibition. **C,** Quantification of the relative intensity of pERK signal in different areas of the retina in control or aDll4-treated animals. Error bars indicate SEM. **D**, One-way ANOVA results for the comparison between vascular areas and anti-Dll4 treatment. ns, not significant.

Notch activity was previously proposed to be higher in stalk cells, the cells with low or undetectable P-ERK signals. To investigate if ERK activity was indeed modulated by Notch signaling *In vivo* we evaluated P-ERK signals in vessels treated with a-Dll4 for 24h. After Notch inhibition, we found the pERK levels increased throughout the angiogenic front and also noticeably increased in mature areas of the retina, however not as pronounced (Fig. 4.15 A-D).

These results suggest that the increase in MAPK signaling could be involved in the context-dependent proliferative responses observed after Notch inhibition, a topic that will be further analyzed in section 4.14.

4.9 VEGFR2 activation induces strong ERK phosphorylation and arrests angiogenesis

As shown before, phosphorylation of ERK is prominent in cells with high activation of VEGFR2, either forced (VEGFR2$^{Ac.}$ mosaic, Fig. 4.5) or physiological (Tip-cells, Figs. 4.5 and 4.15). In previous experiments we have shown that cells with high expression of VEFGR2 and ERK signaling are outcompeted, whereas cells with a weak increase in VEGFR2 signaling seem to proliferate better.

To address the short-term phenotype of ECs with strong VEGFR2 GOF, we crossed the iMb-Vegfr2-Mosaic line with the endothelial specific Cre driver line Cdh5-(PAC)-CreERT2 and analyzed retinas at postnatal day 6, three days after a single Tamoxifen injection.

As shown before, due to the recombination bias, the Mbtomato-2A-VEGFR2$^{Ac.}$ cells were the most abundant shortly after tamoxifen injection (Fig. 4.16 A, B). Only three days after recombination we already were able to detect the two tomato+ populations, weak and strong, although the weak population was still relatively minor (Fig. 4.16 C). Retinas in which a high percentage of EC expressed the VEGFR2$^{Ac.}$ showed decreased vascular density (Fig. 4.16 D), normally associated with decreased EC proliferation.

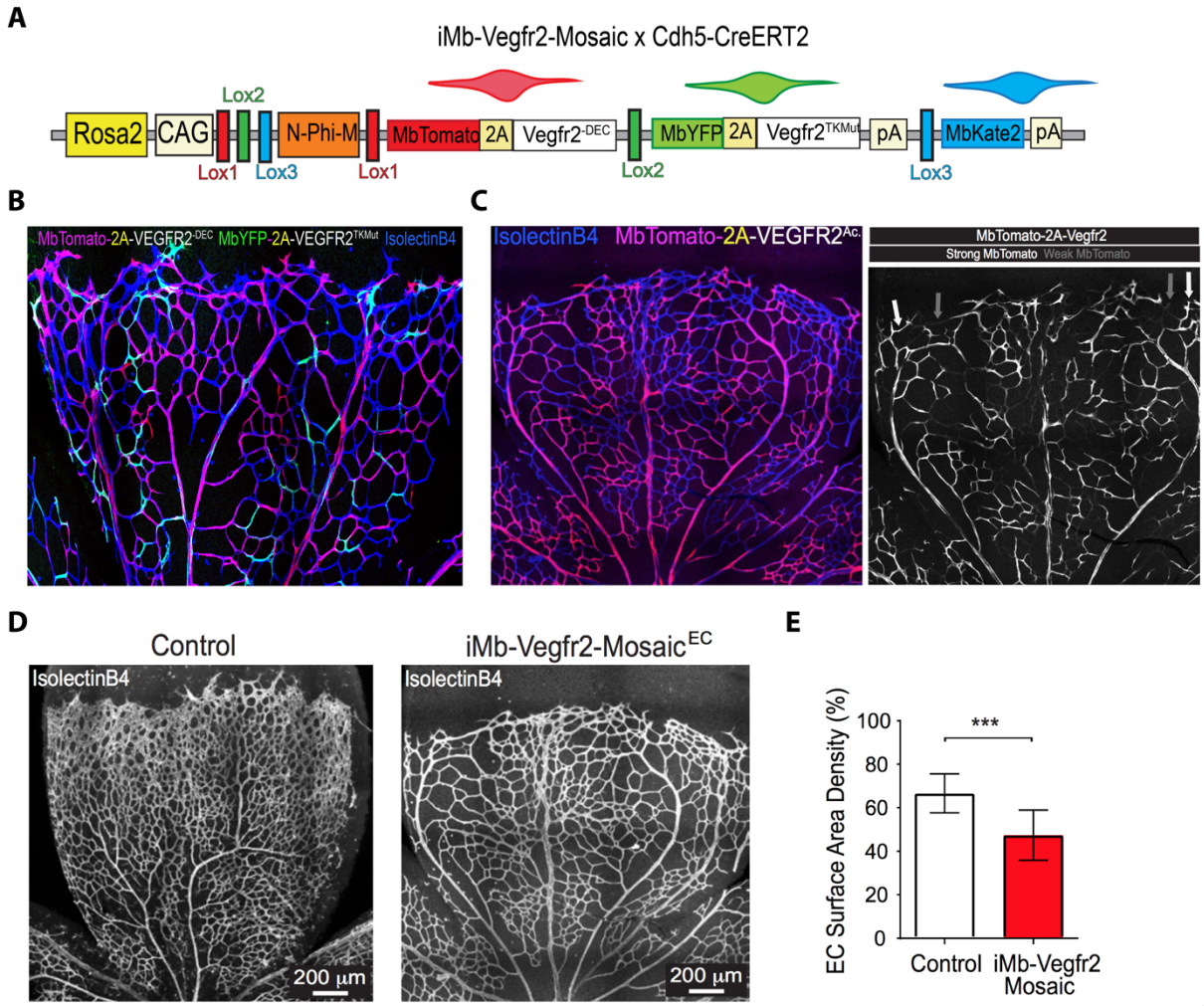

Figure 4.16. Mosaic VEGFR2^{Ac}-mediated increase in ERK phosphorylation is associated with defective angiogenesis. A, Diagram of the iMb-VEGFR2-mosaic **B**, Confocal micrograph of a P6 retina from iMb-Vegfr2-Mosaic animals in which recombination was induced with tamoxifen at P3. Immunostaining for tomato (Red) and YFP (Green) show cells expressing VEGFR2$^{Ac.}$ or VEGFR2^{TK-} respectively. Vascular area is shown in blue stained with IsolectinB4 **C**, Confocal micrograph of a P6 retina showing two different populations of Tomato expressing ECs, one with high and the other with low tomato expression. **D**, Confocal micrograph of P6 retinas from animals carrying either the iMb-Vegfr2-Mosaic only (left) or in combination with *Cdh5-CreERT2* (right) showing the vasculature labeled with IsolectinB4. **E**, Quantification of vascular density measured as the percentage of vascular area covered by IsolectinB4 per field at the angiogenic front. Error bars indicate SEM. *** p<0.0005 with an unpaired t-test.

Detection of incorporated EdU during the 4h prior to analysis showed that a smaller percentage of VEGFR2$^{Ac.}$-expressing ECs were synthesizing DNA compared to control cells (Fig. 4.17 A, C), further suggesting a reduction in the proliferative activity of cells with high VEGFR2 activity and high ERK phosphorylation. As expected, the reduction in proliferation was even stronger in cells

expressing VEGFR2^{TK-}, due to the cell-autonomous suppression of VEGFR2 signaling activation (Fig. 4.17 B,C).

Thus, these results support the hypothesis that balanced VEGFR2 and MAPK signaling is required for normal EC proliferation, while too high or too low levels negatively affects cell cycle progression.

4.10 VEGFR2 signaling is not required for the cell cycle entry of mature ECs after Notch signaling inhibition

Notch inhibition had a distinct proliferation effect on angiogenic and mature ECs. The mature vascular areas have less VEGF and ERK signaling and are quiescent, but enter cell cycle after Notch inhibition, associated with a more moderate increase in ERK phosphorylation (Figs. 4.12-14). Therefore, we wondered if ECs with low VEGFR2 signaling could also proliferate and enter cell-cycle in the absence of Notch signaling. To test this hypothesis, we injected control IgG or aDll4 at P5, in animals carrying the iMb-Vegfr2-Mosaic and Cdh5-(PAC)-CreERT2 alleles that were previously injected with tamoxifen at P3 to induce mosaic recombination, and analyzed retinas 48h later, at P7.

In animals treated with control IgG, mYFP-VEGFR2^{TK-} expressing cells were not very frequent, and were sparsely distributed throughout the vasculature. In contrast retinas from animals treated with aDll4 showed an expanded population of VEGFR2^{TK-} cells, most of them in very close proximity, forming clusters (Fig. 4.17 D). Analysis of Ki67 expression in these cells also showed that a higher percentage of VEGFR^{TK-} cells were undergoing active cell cycle (Fig. 4.17 E, F).

These results show that both mature and VEGFR2^{TK-} expressing cells, that normally have low levels of ERK phosphorylation and are out of cycle or arrested, can enter cell cycle in the absence of Notch signaling.

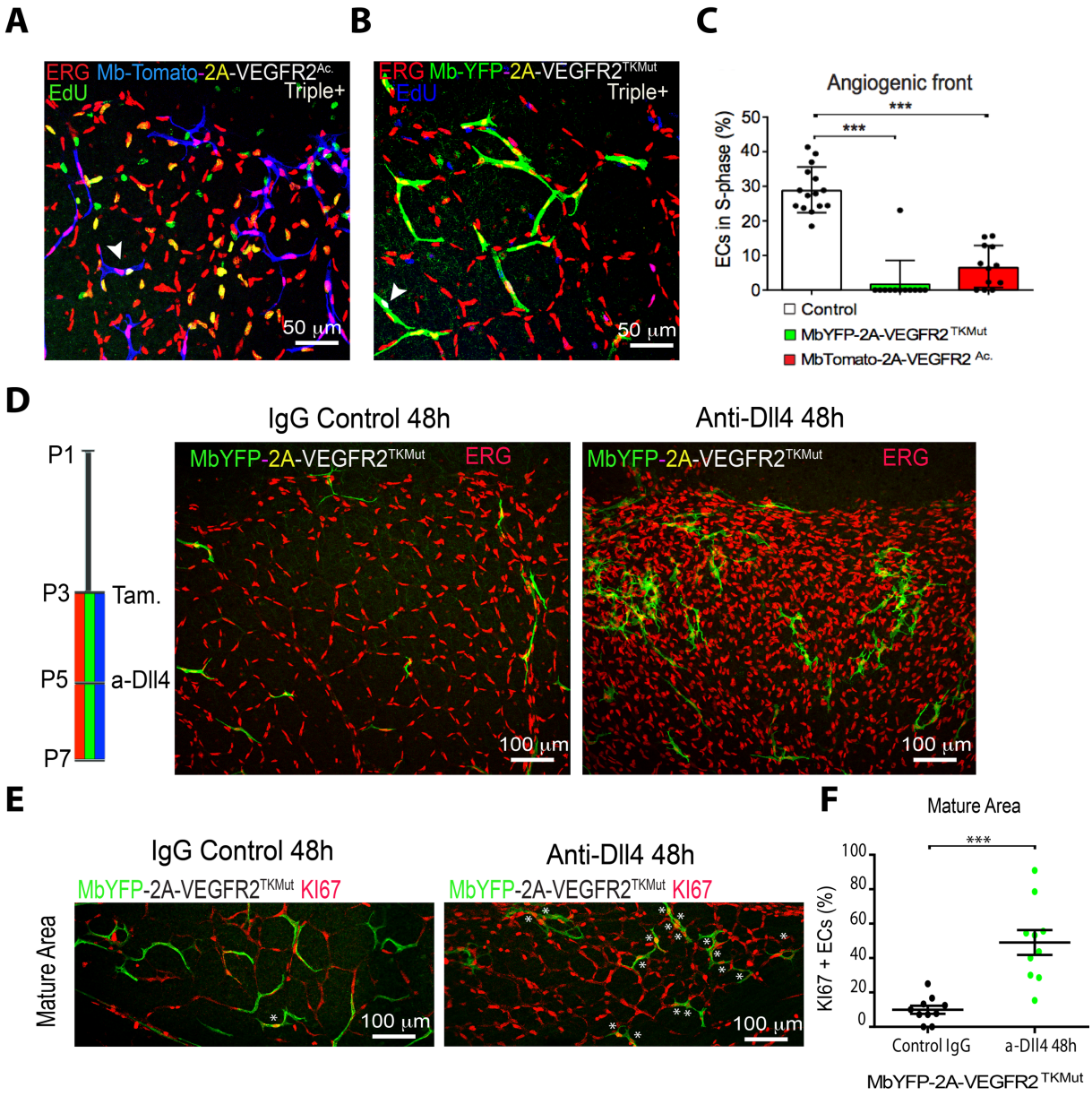

Figure 4.17. Changes in the expression of proliferation markers in iMb-Vegfr2-Mosaic retinas. A, B, Confocal micrographs of P6 retinas from iMb-Vegfr2-Mosaic animals in which recombination was induced with tamoxifen at P3 and co-stained for ERG(Red) and either Tomato (Blue, **A**) or YFP (Green, **B**). EdU positive cells are indicated in green (**A**) or blue (**B**). Indicated in white with arrowheads are triple positive ECs. **C**. Quantification of S-phase ratio in the angiogenic front for the three populations 3 days after recombination: non recombined, expressing Tomato or expressing YFP (% of EdU+ERG+ among all ERG+ nuclei of each population per field). Error bars indicate SEM; NS, non-significant; *** p<0.001 with ANOVA. **D**, Confocal micrographs of P7 retinas from iMb-VEGFR2-Mosaic animals in which recombination was induced with tamoxifen at P3 and injected at P5 with either control IgG (Left) or aDll4 (Right). Retinas were immunostained for ERG (red) and YFP (Green) 48h later at P7. **E,** Confocal micrographs of mature areas from retinas of the same animals immunostained for Ki67 (Red) and YFP(Green) **F**, Quantification of the proportion of YFP+ EC expressing Ki67 per field in the mature areas after 48 hours of Notch inhibition. Error bars indicate SEM; NS, non-significant; *** p<0.0005 with an unpaired t-test.

4.11 Tip cells with endogenous high VEGF signaling have reduced proliferative capacity

So far we analyzed how ECs with induced high amounts of VEGFR2/ERK signaling behave. To analyze how physiological MAPK activation could be affecting EC proliferation during normal angiogenesis we focused our analysis on tip cells, as we have seen that they have the highest levels of pERK and are thought to receive the highest combined mitogenic input, since they experience both high VEGFR2 activation and low Notch signaling (Fig. 4.15).

However, we could not detect tip cells experiencing high VEGF and low Notch signaling, just by looking at their location, since tip cell specification is a very dynamic process and tip cell position alone could not be reflecting the true VEGFR2 and Notch activation status of ECs at the angiogenic front.

To label with high resolution only those ECs that received a high VEGF signaling input (or have low Notch signaling) at the angiogenic front, and fate-map their progeny, we generated Esm1-Cerulen-CreERT2 mice that express HA-labelled nuclear cerulean and a CreERT2 only in cells highly expressing the Esm1 gene (Fig. 4.18 A).

Unlike most genes expressed by angiogenic vessels, *Esm1* is strongly and exclusively expressed in endothelial tip cells (Rocha *et al.*, 2014), probably reflecting a high threshold for transcriptional activation by VEGFR2 signaling.

Analysis of postnatal retinal vasculatures from these mice revealed that, at any given moment, only a subset of tip cells showed detectable HA-H2B-Cerulean expression (Fig. 4.18 B). Consistent with our previous results, a small percentage (31 %) of HA-H2B-Cerulean+ cells were also co-labeled with Ki67, indicating limited cycling of these tip cells, particularly compared with surrounding non tip cells (96%), (Fig. 4.18 B, compare to Fig. 4.14).

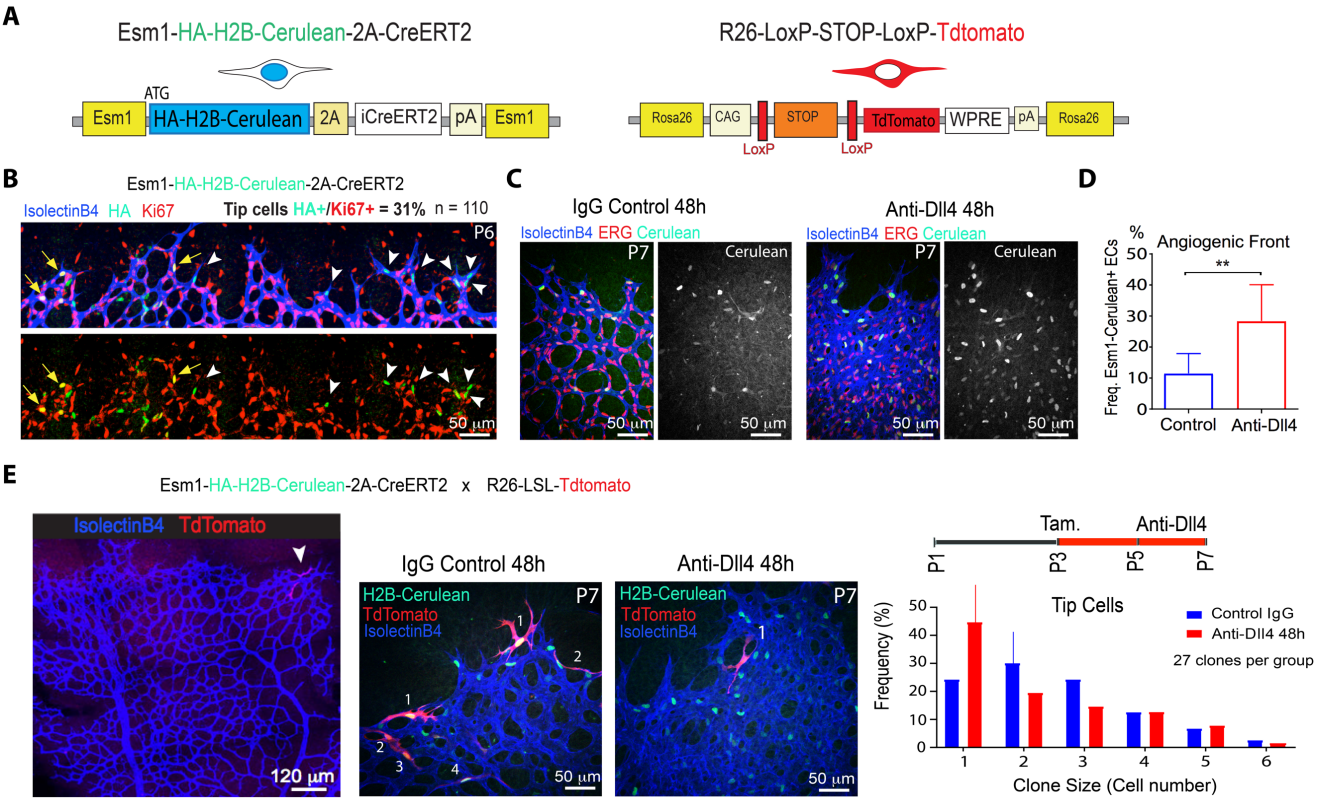

Figure 4.18. Analysis of cell cycle dynamics in tip cells. A Left, Diagram of the DNA construct inserted in the Esm1 locus, in which the nuclear expression of cerulean is associated with CreERT2 expression. **Right,** Diagram of the R26-LSL-TdTomato in which expression of the fluorescent protein tomato is induced after Cre recombination. **B**, Confocal micrographs of a Esm1-HA-H2B-Cerulean-2A-iCreERT2 mouse retinal vasculature at P6, immunostained for IsolectinB4 (Blue), HA (Green) and Ki67 (Red). Indicated on top is the fraction of HA positive cells that express Ki67. **C,** Micrographs of retinal vasculatures from these mice 48h after Control (Left) or aDll4 (Right) treatment, immunostained for IsolectinB4 (Blue), ERG (Red) and Cerulean (Green). **D,** Quantification of the frequency of Cerulean+ ECs after Notch inhibition. Error bars indicate SEM; NS, non-significant; ** $p<0.005$ with an unpaired t-test. **E,** Clonal analysis of the progeny of Esm1 expressing cells. Animals harboring both Esm1-HA-H2B-Cerulean-2A-iCreERT2 and LSL-Tomato transgenes were injected with tamoxifen at P3 and either control IgG or aDll4 at P5 and retinas were analyzed at P7. **Left,** Representative image of a control retina immunostained for IsolectinB4 and Tomato showing an isolated 2-cell tomato clone (arrowhead). **Center.** Micrographs of P7 retinas from control and aDll4 treated animals immunostained for Isolectin B4, Tomato and cerulean. **Right,** Histogram showing the frequency distribution of clone size for tomato clones in retinas from control or aDll4 treated animals. Vertical lines indicate median values.

As Esm1 expression is correlated with VEGFR2 activation, like ERK phosphorylation, we tested if its expression was also expanded after Notch inhibition. Injection of aDll4 in these animals induced a marked increase in the number of Esm1-expressing stalk cells (Fig. 4.18 C, D) similar to our findings with pERK.

To further characterize single tip-cell proliferation dynamics during normal angiogenesis we performed clonal analysis of the tip cells expressing high Esm1. We crossed Esm1-Cerulen-CreERT2 with Rosa26-LSL-TdTomato (Madisen *et al.*, 2010) reporter mice (Fig. 4.18 A, E) and induced recombination with tamoxifen at P3. To additionally characterize the effect of Notch signaling on their proliferation dynamics we also blocked Notch activity by injecting aDll4 two days after recombination at P5 and analyzed clone size 48h later, at P7.

We found very few recombined clones per retina arising from a few Esm1+ tip cells (Fig. 4.18 E Left), enabling us to score and assign single, tip-cell-derived clonal identity. Individual Esm1+ tip cells produced on average fewer progeny than non-tip cells as quantified before (Fig. 4.6). In most cases, Esm1+ tip cells generated 2-cell clones after 4 days (Fig. 4.18 E, blue), whereas non-tip cells tended to generate 4-cell clones after only 3 days (Fig. 4.6). Interestingly, when Dll4/Notch signaling was blocked, Esm1+ tip cells proliferated even less and most clones were formed by only one, instead of two cells (Fig. 4.18 E, Red). This shows that, similarly to mosaic cell expressing VEGFR2$^{Ac.}$, tip cells proliferate less and the progeny of these cells form smaller clones that those formed by angiogenic non-tip cells.

4.12 The cell cycle inhibitor p21 is expressed in cells with high ERK phosphorylation

Our results showed that high and sustained ERK phosphorylation were correlated with reduced proliferation and cell cycle exit. Strong ERK activation causes cell cycle arrest and upregulation of the cell cycle inhibitor p21 in established cell lines *In vitro* (Pumiglia and Decker, 1997; Sewing *et al.,* 1997). However, previous studies with EC lines suggested that p21 might positively regulate EC proliferation (Dou *et al.,* 2008; Noseda *et al.,* 2004). Therefore, we decided to evaluate the expression of p21 in cells with distinct levels of pERK, VEGFR2 and Notch signaling.

To evaluate if p21 is associated with high ERK phosphorylation in tip cells, during normal angiogenesis, and if its expression was changed after Notch inhibition, P6 retinas from animals treated with Control IgG or aDll4 for 24h (from P5 to P6), were co-immunostained for ERG and p21 (Fig. 4.19 A, B).

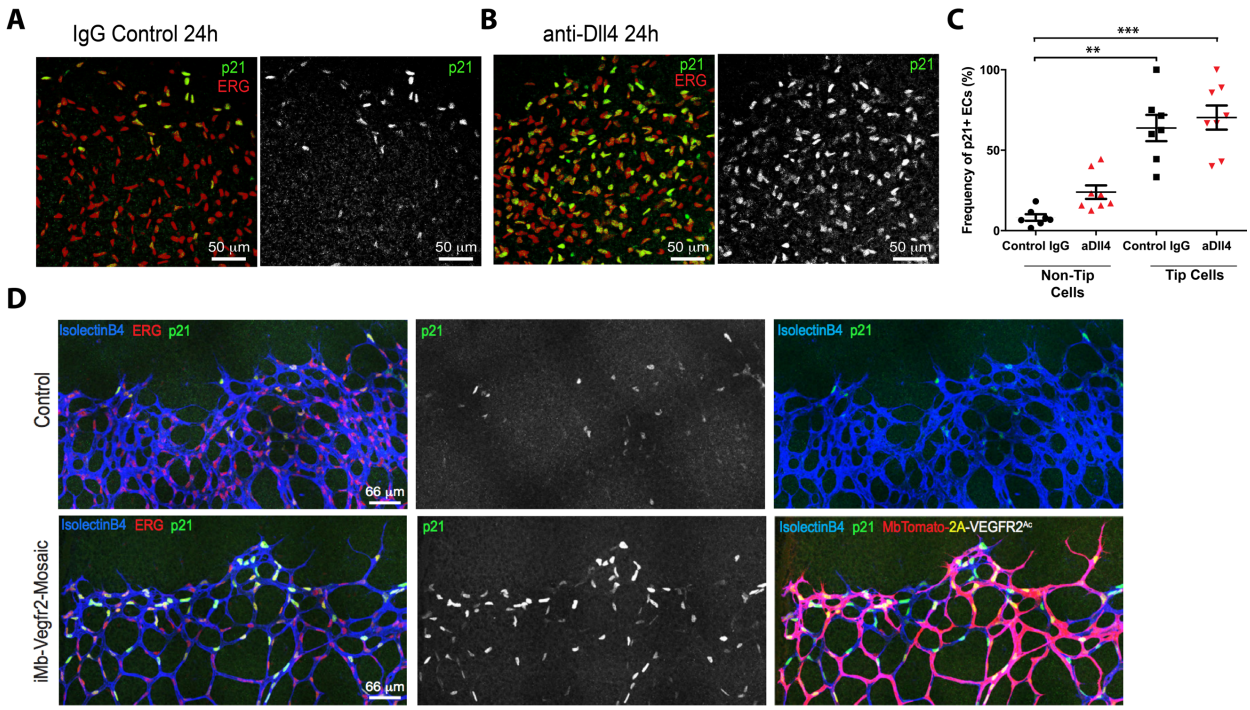

Figure 4.19. Alterations of p21 expression in ECs are associated to changes in ERK phosphorylation. A, B, Micrographs of P6 retinal vasculatures from Control or aDll4 treated mice immunostained for ERG and p21. Single channel image for the p21 signal is shown in the right. **C,** Quantification of the frequency of p21-expressing ECs in two different retinal populations: tip and non-tip cells, at the angiogenic front. Error bars indicate SEM; **p<0.001; *** p<0.001 with ANOVA. The comparisons not shown are all non-significant. **D,** Confocal micrograph of P6 retinas from animals carrying either the iMb-Vegfr2-Mosaic only (top) or in combination with *Cdh5-CreERT2* (bottom) injected with tamoxifen at P3 and immunostained for Isolectin(Blue) p21 (Green, single channel in the center) and ERG (Red, left) or tomato (Red, right).

We found that very high p21 protein levels were normally restricted to tip cells (Fig. 4.19 A, C) during normal angiogenesis, the cells with highest pERK levels. Moreover, only 24h after Notch inhibition, which as we have shown before induces an increase in pERK levels, p21 protein levels increased significantly in ECs throughout the angiogenic front (Fig. 4.19 B, C). As shown in Figure 4.14, 24h after Notch inhibition, most ECs were still expressing Ki67 and a large fraction was in S-phase (EdU+). This could indicate that the p21 upregulation precedes and might be one of the inducers of the cell cycle exit process seen 48h after Notch inhibition. To analyze if p21 was also expressed in VEGFR2$^{Ac.}$ cells we analyzed P6 retinas from animals carrying the iMb-Vegfr2-Mosaic and Cdh5-(PAC)-CreERT2 alleles that received a single tamoxifen injection at P3. Co-immunostaining for ERG, Tomato and p21 showed that most cells with activated VEGFR2 and high ERK phosphorylation also strongly upregulated p21 (Fig. 4.19 D).

Our results thus show that EC p21 expression *In vivo* is correlated with elevated pERK levels, that can be either induced by high VEGFR2 signaling or Notch inhibition, suggesting that p21 may mediate the cell cycle exit process observed in these cells.

4.13 Vessels of p21 knockout mice proliferate more after Notch inhibition

To evaluate if p21 might have a causal relationship with the observed cell cycle exit observed after Notch inhibition we analyzed postnatal retinal angiogenesis in p21 Knock Out mice. These animals develop normally but are more sensitive to tumor formation (Brugarolas *et al.,* 1995).

We injected p21 KO animals with control IgG or aDll4 at P5 and analyzed retinas 48h after injection. Analysis of EC number and DNA synthesis was performed as before.

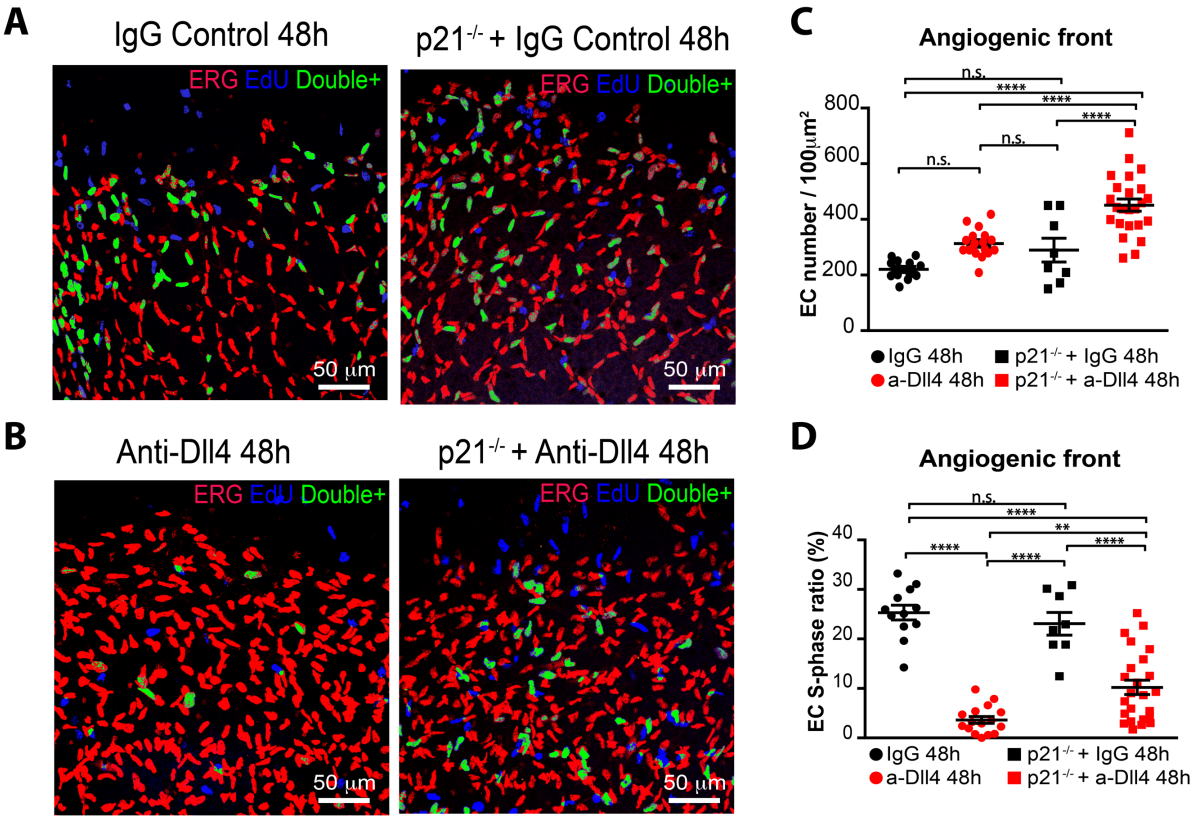

Figure 4.20. Effects of Notch inhibition in mice lacking p21. A, B, Confocal micrographs of P7 retinal vasculature fronts from WT or p21 homozygous knockout animals treated with Control IgG (A) or aDll4 (**B**) at P5, 48 hours before dissection. ERG in red, EdU in blue and Double positive cell in Green. **C, D**, Quantification of endothelial nuclei density (ERG+ nuclei per vascular area) and S-phase ratio (% of EdU+ERG+ among all ERG+ EC nuclei per field) in the angiogenic front of these animals. Error bars indicate SEM; NS, non-significant; **p<0.01 **** p<0.0001 with ANOVA.

Interestingly, the absence of p21 did not significantly affect retinal angiogenesis or the S-phase ratios in ECs at the angiogenic front with physiological Notch signaling (Fig. 4.20) presumably because p21 expression is low and undetectable in most of these cells as we have shown before. However, after inhibition of Notch signaling, p21 expression increases significantly, and in this context we observed that p21 loss leads to a greater increase in EC number compared to animals with normal p21 expression (Fig. 4.20 B-C). This was also associated with an increase in the frequency of ECs in S-phase after Notch inhibition (Fig. 4.20 D). These results indicate that p21 is partially responsible for the reduction in EC proliferation and cell cycle arrest of ECs after Notch inhibition.

4.14 Inhibition of ERK phosphorylation results in context-dependent effects in ECs

Our previous experiments suggest that ERK could be a fundamental regulator of endothelial cell cycle during angiogenesis and a central driver of endothelial cell expansion after Notch inhibition.

In order to evaluate this hypothesis, we performed similar Notch inhibition experiments during retinal angiogenesis in combination with inhibition of MEK, the main kinase that mediates ERK phosphorylation (Ussar and Voss, 2004). To this end we injected either the MEK inhibitor SL327 or control vehicle in combination with control IgG or aDll4 at P5 and analyzed retinas 24h later at P6. The MEK inhibitor was injected twice, at 24h (P5) and 8h time points to guarantee a pronounced MEK activity inhibition. Immunostaining of these retinas for pERK revealed that the treatment resulted in a complete loss of detectable ERK phosphorylation (Fig. 4.21 A, B). Retinas from animals treated with SL327 showed a slight increase in vascular surface density (IsolectinB4), although we could not detect a parallel increase in EC number (Fig. 4.22 A, B, D, E).

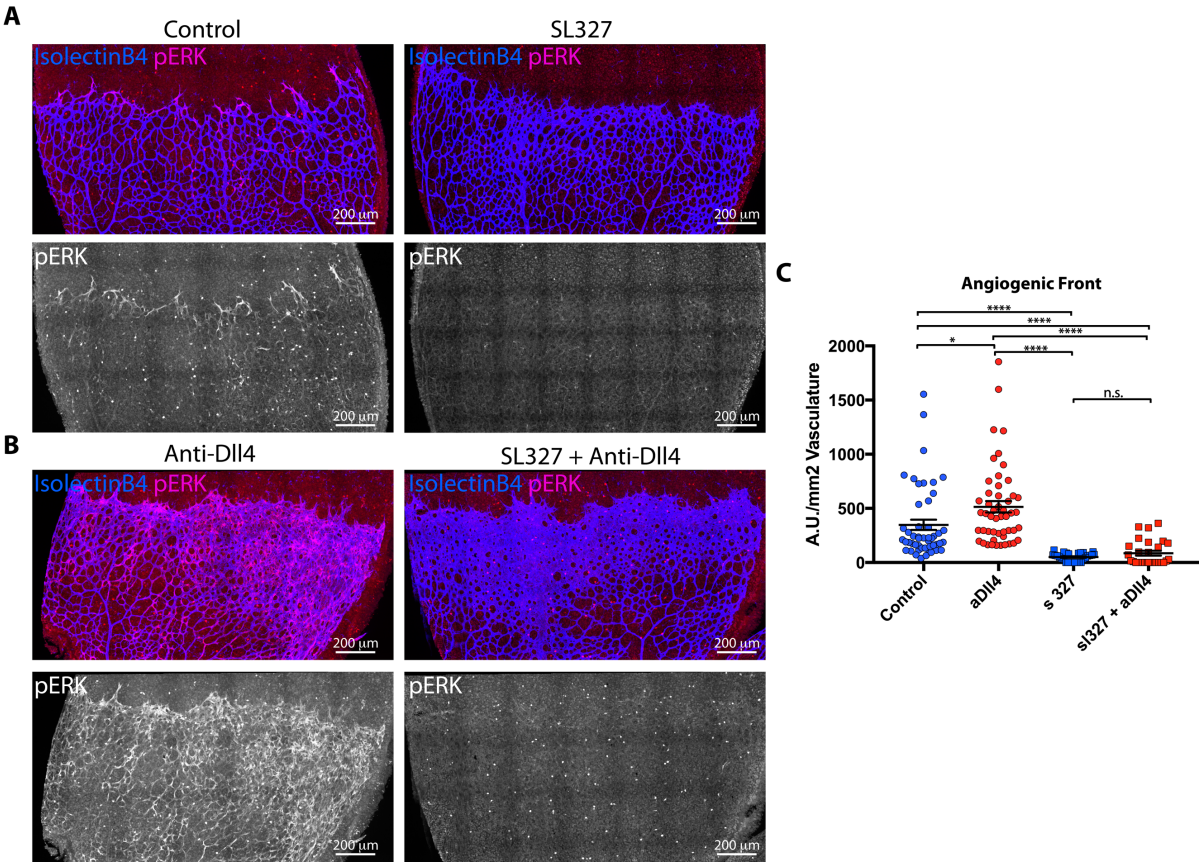

Figure 4.21. Effects of treatment with the MEK inhibitor SL327 in retinal endothelial ERK phosphorylation. A, B Micrographs of P6 retinas from animals treated with control, SL327, aDll4 or SL327 and aDll4 at P5, 24h before analysis. Retinas were immunostained for IsolectinB4 and pERK. The single channel images for the pERK signal is show at below. **C**, Quantification of relative pERK intensity per field in randomly selected fields over all the retinal vasculature. Error bars indicate SEM; NS, non-significant; *p<0.05 **** p<0.0001 with Kruskal-Wallis test.

However, the EC population at the AF of the animals treated for 24h with the MEK inhibitor, showed a considerable reduction in the frequency of stalk ECs in S-phase (EdU+). Regarding the expression of p21, we only detected a slight reduction in p21 immunostaining frequencies at the angiogenic front of these retinas (Fig. 4.22 C, G). This data suggests that p21 expression does not seem to be fully controlled by the MAPK pathway in tip cells, or alternatively, once p21 expression is induced in tip cells, it lasts for more than 24h, and its levels cannot be significantly reversed by the acute loss of ERK signaling. This data also suggests that inhibition of ERK activity for 24 hours only seem to decrease the frequency of EC proliferation at the 24h time point, but before ECs seem to proceed and complete their cycle normally, since the inhibitor treatment does not significantly change the number of ECs generated until the 24h time point.

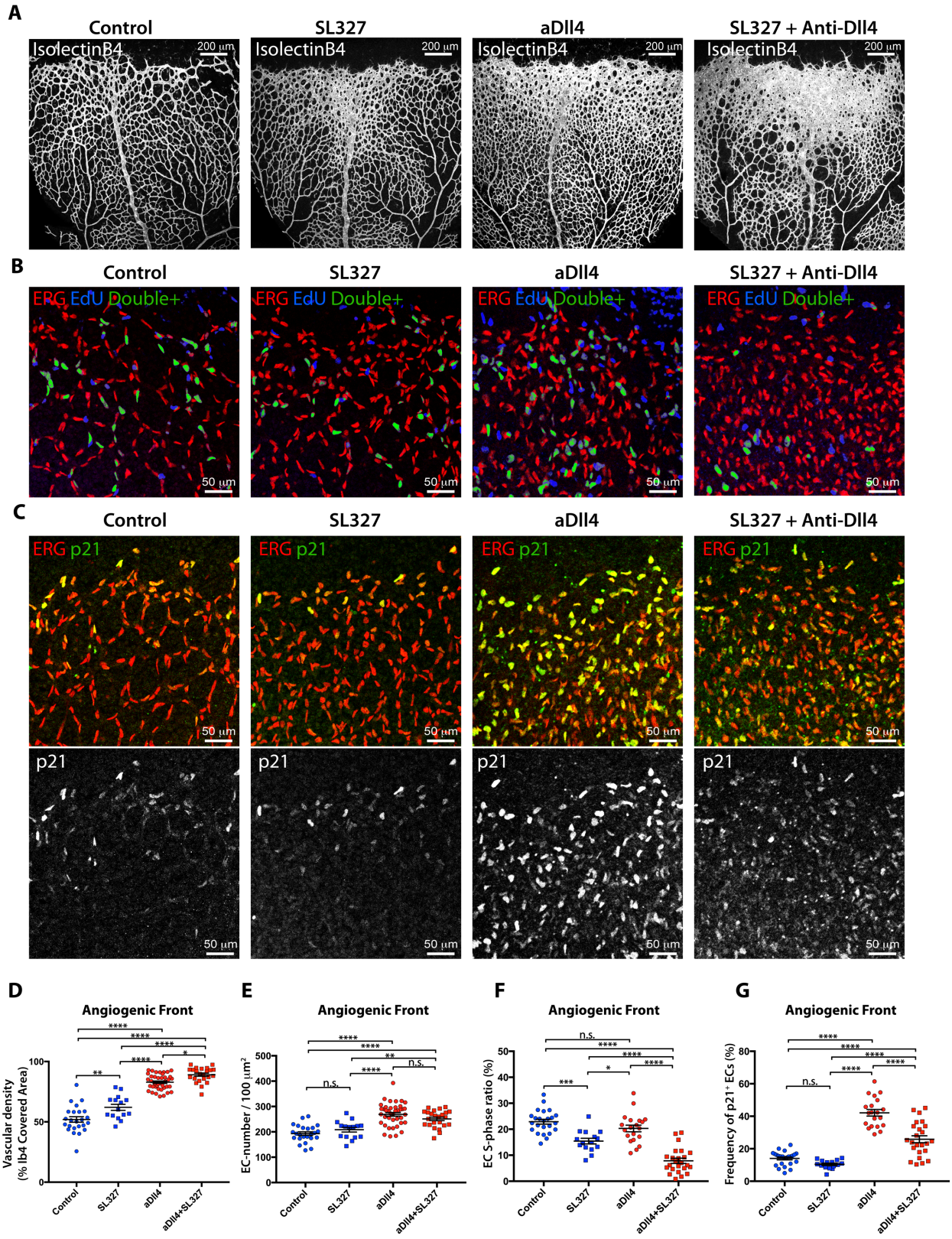
A
Control
SL327
aDll4
SL327 + Anti-Dll4
IsolectinB4
200 µm
B
ERG EdU Double+
50 µm
C
ERG p21
p21
D
Angiogenic Front
Vascular density (% Ib4 Covered Area)
E
EC-number / 100 µm²
F
EC S-phase ratio (%)
G
Frequency of p21⁺ ECs (%)
Control
SL327
aDll4
aDll4+SL327
n.s.

Figure 4.22. Vascular alterations after MEK inhibition alone or in combination with Notch inhibition during retinal angiogenesis. A, Micrographs of P6 retinas from animals treated with control, aDll4, SL327 or SL327 and aDll4 at P5, 24h before analysis. Retinas were immunostained for IsolectinB4. **B,** Confocal micrographs of the P6 retinal vasculatures from animals treated 24h before, at P5, with control, aDll4, SL327 or SL327 and aDll4 immunostained for ERG in red, EdU in blue and pseudocolored double positive cell in green. **C** Confocal micrographs of the P6 retinal vasculatures from animals treated 24h before, at P5, with control, aDll4, SL327 or SL327 and aDll4 immunostained for ERG in red and p21 in Green. Single channel image for p21 is shown below **D-G,** Quantification of vascular density, **D** (% of IsolectinB4 covered vascular area per field), endothelial nuclei density, **E** (ERG+ nuclei per vascular area), S-phase ratio, **F** (% of EdU+ERG+ among all ERG+ EC nuclei per field) and the frequency of p21-expressing ECs (**G**) at the angiogenic front in these retinas. Error bars indicate SEM; NS, non-significant; *p<0.05; ** p<0.01; *** p<0.001; **** p<0.0001 with ANOVA.

Retinas from animals treated with aDll4 and the MEK inhibitor also showed a slightly higher vascular surface density, but no significant changes in endothelial cell number when compared with animals treated with aDll4 alone (Fig. 4.22 A, D, B, E). However, these SL327+aDll4 treated vessels showed a considerably reduction in the frequency of ECs in S-phase (EdU+) and a strong decrease in the frequency of p21+ stalk cells 24h after the start of the inhibition (Fig. 4.22). These results suggest that after Notch LOF, the increase in ERK activation is required for the observed p21 upregulation and likely the associated cell cycle arrest process observed after Notch LOF. However, if ERK phosphorylation is inhibited completely, both EC S-phase entry and p21 expression are strongly reduced at 24h. This data also suggest that ERK activity is not required initially in AF ECs in order for these to accelerate their proliferation shortly after Notch inhibition, suggesting that other molecular mechanisms may be involved in this process.

Importantly, and in contrast to the results obtained in angiogenic vessels, we found that ERK activity is absolutely required for the cell cycle entry of more mature and previously quiescent ECs, that upon loss of Notch signaling become reactivated and EdU+ (Fig. 4.23). When these ECs are treated with the SL327 inhibitor, they cannot enter cell cycle. This data suggests that there is a context-dependent effect of ERK signaling on EC proliferation, that is more pronounced in vessels with low Notch signaling and increased ERK activity.

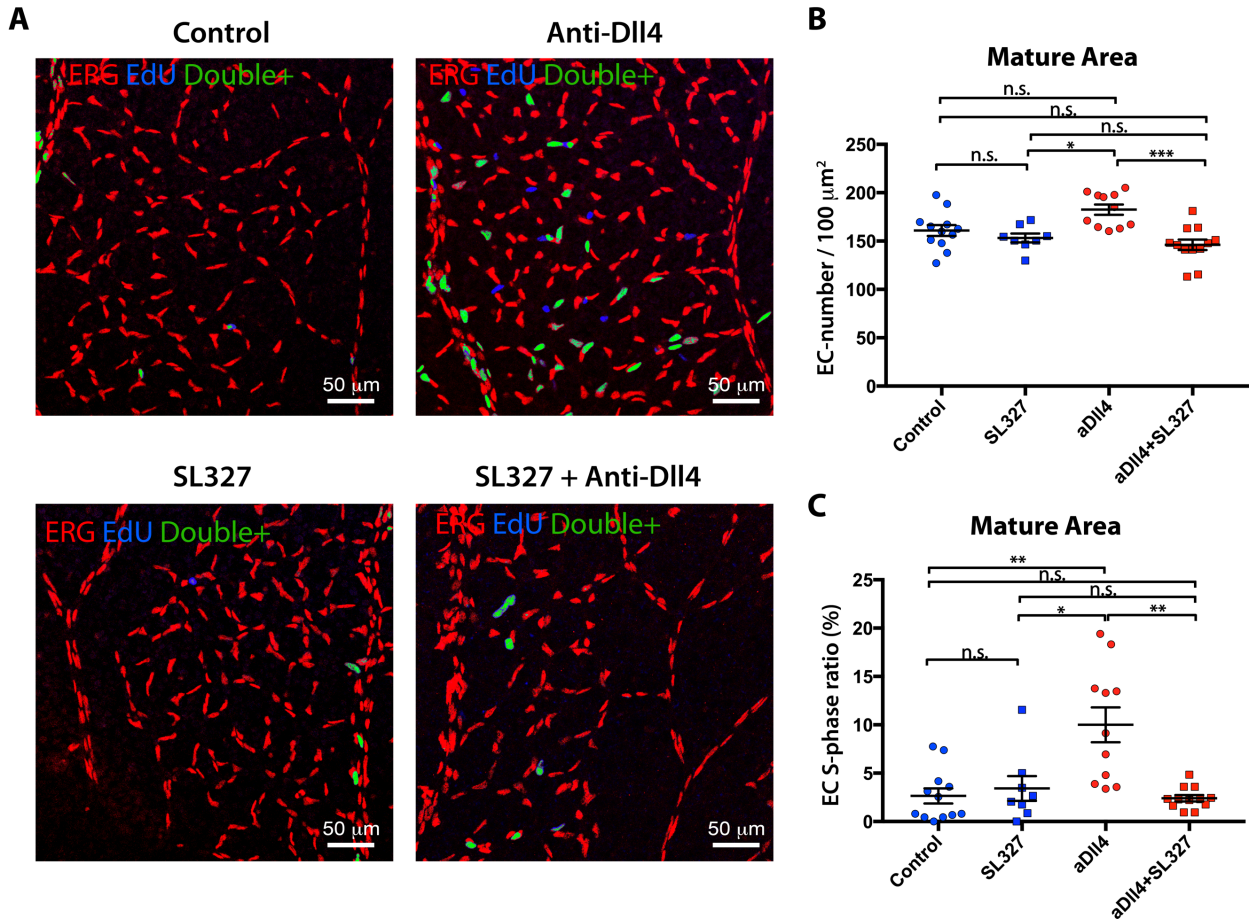

Figure 4.23. Effects of MEK inhibition in the proliferative status of quiescent ECs. A, Confocal micrographs of mature areas from P6 retinal vasculatures of animals treated 24h before, at P5, with control, aDll4, SL327 or SL327 and aDll4 immunostained for ERG in red, EdU in blue and pseudocolored double positive cell in green. **B, C,** Quantification of endothelial nuclei density, **B** (ERG+ nuclei per vascular area) and S-phase ratio, **C** (% of EdU+ERG+ among all ERG+ EC nuclei per field) in the mature areas from these retinas. Error bars indicate SEM; NS, non-significant; *p<0.05; ** p<0.01; *** p<0.001; with ANOVA.

4.15 Comparative transcriptomic analysis of angiogenic EC after Notch inhibition

Notch/RBPJ complexes directly regulate the transcription of a multitude of genes, including several Hey/Hes basic helix-loop-helix (bHLH) transcription factors, which in turn repress transcription of numerous genes, resulting in an altered cell status

To identify genes specifically regulated by Notch in proliferating ECs *In vivo*, and most likely responsible for its effect on EC proliferation, we dissected and FACS sorted proliferating ECs from the retinal angiogenic front (Fig 4.24 A) of animals receiving control IgG or Anti-Dll4 antibodies for 24 hours, and performed pre-amplification and RNAseq from a few hundreds of ECs collected per animal. This allowed us to identify genes strongly regulated by Notch, specifically in angiogenic vessels.

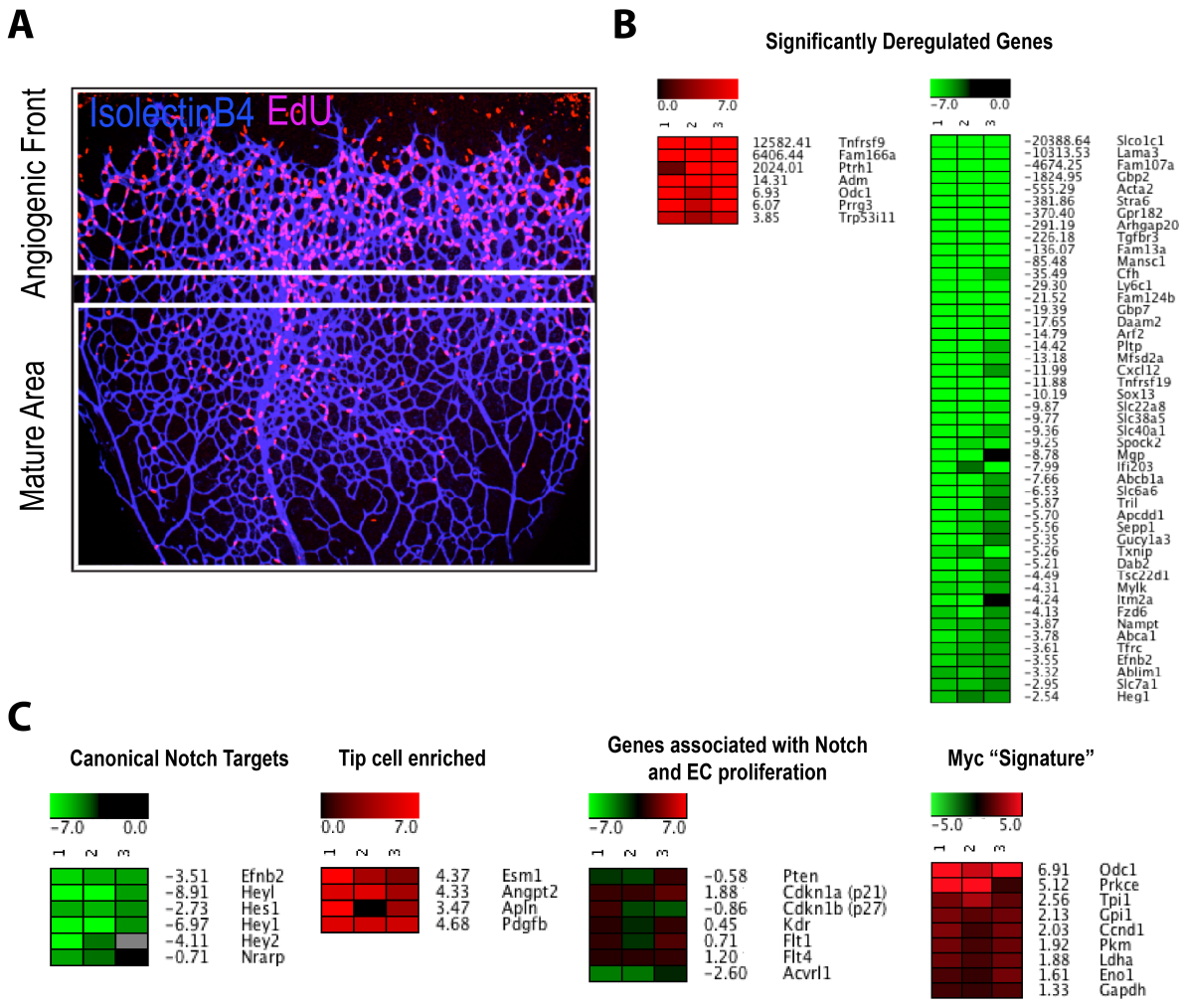

Figure 4.24. *In vivo* transcriptomic analysis of endothelial cells after Notch inhibition during angiogenesis. A, Representative confocal micrograph of the P6 retinal vasculature (IsolectinB4+, blue), showing the location of EdU+ endothelial cells (pink nuclei) at the angiogenic front and in the mature area. White boxes indicate the two areas that were microdissected before FACS of EC populations for downstream RNAseq analysis. **B, C,** Heatmaps of three independent experiments showing the individual and average gene-expression fold-change in control vs anti-Dll4 treated ECs from the angiogenic front **B,** List of all upregulated (Left) or downregulated (Right) genes that passed the Benjamini-Hochberg FDR with $p<0.05$. **C** List of Canonical Notch target genes, tip cell enriched genes, several genes previously associated with the Notch function in EC proliferation, and previously reported Myc-controlled genes.

Due to the low input and variability among triplicates, we found relatively few deregulated genes that passed the established significance threshold with adjusted p-values (Fig. 4.24 B). However canonical Notch target genes showed the expected pattern of downregulation (Fig. 4.24 C). Moreover, several tip-cell enriched genes also appeared upregulated in line with previous results. However, several genes previously implicated in Notch-regulated EC proliferation (Benedito and Hellstrom, 2013; Dou *et al.,* 2008; Nicoli *et al.,* 2012; Noseda *et al.,* 2004; Potente *et al.,* 2011; Serra *et al.,* 2015) were only slightly altered (Fig. 4.24 C).

One of the most significantly upregulated genes was Odc1, which is highly expressed in normal angiogenic ECs, and is upregulated 7-fold after Notch inhibition. Odc1 expression has been shown to be controlled by Myc genes (Bello-Fernandez, Packham, and Cleveland, 1993). Recent publications have shown that the Myc gene can also regulate EC proliferation during angiogenesis (Wilhelm *et al.,* 2016) and we found additional upregulated genes that have been previously included in a Myc-controlled transcriptional signature (Zeller *et al.*, 2003) that would further implicate that Notch could be controlling EC proliferation during angiogenesis through Myc and Odc1 regulation, even though Myc mRNA levels were not significantly deregulated.

For this reason, we further analyzed the role of these two genes in angiogenesis and their functional interaction with Notch. Particularly Odc1, as its function during angiogenesis has not been studied in detail.

4.16 Odc1 expression is repressed by Notch and partially promoted by Myc in ECs during angiogenesis

Odc1 is the rate-limiting enzyme in polyamine biosynthesis, and is one of the most rapidly turned over proteins in cells, being critically controlled during phases of cellular expansion *(Auvinen et al.,* 1992). Its expression and activity is tightly regulated during the cell-cycle, peaking at the G1/S and G2/M transitions, and markedly decreasing in quiescent cells. Polyamines are small positively charged amines required for proper DNA replication, and are thus particularly important for G1/S phase transition and S-phase (Alm and Oredsson, 2009).

To validate that Odc1 expression is indeed increased after Notch inhibition we used the *Odc1-LacZ* mouse line. These mice have a LacZ gene encoding β-galactosidase (b-Gal) inserted between exons 6 and 7 of the Odc1 gene, that is spliced-in after Exon 6. Thus b-Gal expression in these animals recapitulates the endogenous expression and regulation of the Odc1 gene.

We treated these animals with control IgG or aDll4 at P5 and 48h later, at P7, retinas were immunostained for IsolectinB4 and b-Gal.

We saw that the pattern of expression of Odc1 was very similar to that of pERK. During normal angiogenesis in control animals b-Gal was strongly express in tip-cells but not in other vascular areas of the retina. After Notch inhibition the expression pattern expanded to occupy most of the vasculature at the angiogenic front, further indicating that Notch repress Odc1 expression, particularly in stalk cells *In vivo* (Fig. 4.25 A).

Analysis of the Odc1 promoter region showed that the Odc1 CpG island contains two binding sites for the canonical endothelial Notch targets and downstream effectors Hey1 and Hey2 (Fig. 4.25 B). These sites were conserved both in mouse and humans. Hey1 and Hey2 are two transcription factors (TFs) that execute a great part of the Notch downstream transcriptional program and activity since Hey1/Hey2 double KO embryos have vascular defects similar to endothelial-specific Notch mutants (Krebs *et al.*, 2000; Duarte *et al.*, 2004).

To evaluate if the Odc1 gene could be repressed by these TFs, we performed a luciferase assay using the mouse Odc1 minimal promoter containing these regions. This minimal promoter was cloned upstream of the of the firefly luciferase gene, and after luciferase assays were performed in human HEK293 cells, with or without overexpression of the Hey1 and Hey2 genes.

We found that forced expression of Hey transcription factors in HEK293 cells decreases luciferase activity from Odc1 minimal promoter (Fig. 4.25 B), indicating that, consistent with previous reports (Heisig *et al.*, 2012), Notch could be repressing Odc1 activity through the upregulation of Hey1 and Hey2.

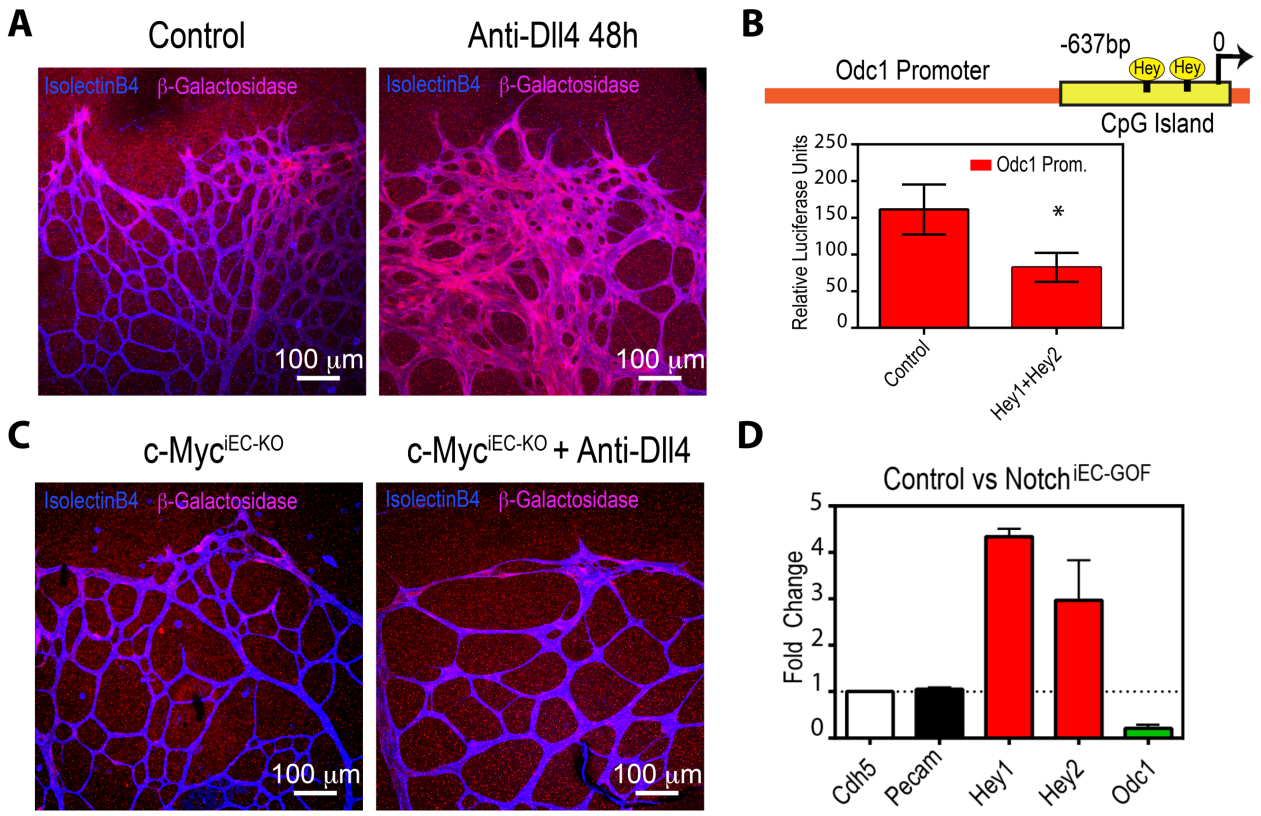

Figure 4.25. Regulation of Odc1 expression by Notch and Myc during angiogenesis. A, Immunostaining of IsolectinB4 and b-Gal, encoded by the lacZ gene knocked-in downstream of the Odc1 promoter in the *Odc1*$^{tm1a(EUCOMM)Hmgu}$ transgene, in P7 retinas from animals treated with Control IgG or aDLl4 at P5, 48 h before dissection. **B**, Mouse and human Odc1 promoters have two conserved binding sites for the Hey transcriptional repressors in the CpG island. Quantification of Relative Luciferase activity from HEK293 cells transfected with control or Hey1 and Hey2 expressing plasmids. Errors bars indicate SEM. *p=0.0288 with a one tailed t-test. **C**, Immunostaining of IsolectinB4 and b-Gal in P7 retinas from Myc$^{Floxed/floxed}$ animals injected with tamoxifen once a day from P1 to P3 and treated with Control IgG or aDLl4 at P5, 48 h before dissection. **D**, qRT-PCR analysis of isolated retinal ECs overexpressing NICD. Errors bars indicate SEM.

Myc has been described as one of the most important activators of Odc1 expression in different tumor models (Nilsson *et al.* 2005; Annibali *et al.* 2014). As we saw that Notch inhibition induces the overexpression of several other Myc-related genes, we analyzed if Odc1 expression also depends on Myc activity in ECs during angiogenesis.

We bred Myc floxed animals (de Alboran *et al.,* 2001) carrying the Cdh5-(PAC)-CreERT2 allele with *Odc1-LacZ* mice and induced recombination from P1 to P3 to delete the Myc gene. At P5 these animals were injected with Control IgG or aDll4 and retinas were analyzed for b-Gal expression at P7, 48h after Notch inhibition.

We found reduced levels of b-Gal expression in $Myc^{iEC\text{-}KO}$ retinal vasculatures (Fig. 4.25 C left), suggesting that Myc also regulates Odc1 during angiogenesis. However, Odc1-lacZ expression was not completely abrogated, indicating that basal Odc1 expression can occur in the absence of Myc.

Notch inhibition did not increase b-Gal expression as strongly in $Myc^{iEC\text{-}KO}$ animals as in wildtype animals (Fig. 4.25 C right), suggesting that, although Odc1 expression could be directly regulated by Hey proteins, Myc is still required to reach high Odc1 expression levels after Notch LOF.

To evaluate *In vivo* the repression of Odc1 by Notch in ECs we analyzed by qRT-PCR the expression of the Odc1 gene in retinal ECs with increased Notch activity. We found that these cells, which show increased expression of Hey1 and Hey2, also downregulate Odc1 (Fig. 4.25 D), further indicating that Notch activity repress Odc1 expression.

4.17 Odc1 down regulation phenocopies Notch overactivation in ECs during angiogenesis

To evaluate the role of Odc1 during angiogenesis we first generated a new mouse line, $Oaz1^{GOF}$, with which is possible to induce the simultaneous expression of H2B-Cerulean and the gene Oaz1 (Fig. 4.26 A). Oaz1 is a very specific negative regulator of Odc1 function, inducing its degradation (Kahana, 2009). Thus in these mice, by overexpressing Oaz1, we can evaluate how Odc1 degradation in ECs affects angiogenesis.

We bred these mice with the Cdh5-(PAC)-CreERT2 line, induced recombination from P1 to P3 and evaluated retinal vascular phenotypes and S-phase ratios as before at P6.

We saw that retinas with a high number of recombined cells, expressing H2B-Cerulean, have a considerably altered vascular network, with a reduced number of ERG+ endothelial cells and S-phase ratios, presumably indicating a defect in proliferation (Fig. 4.26 B, E, F).

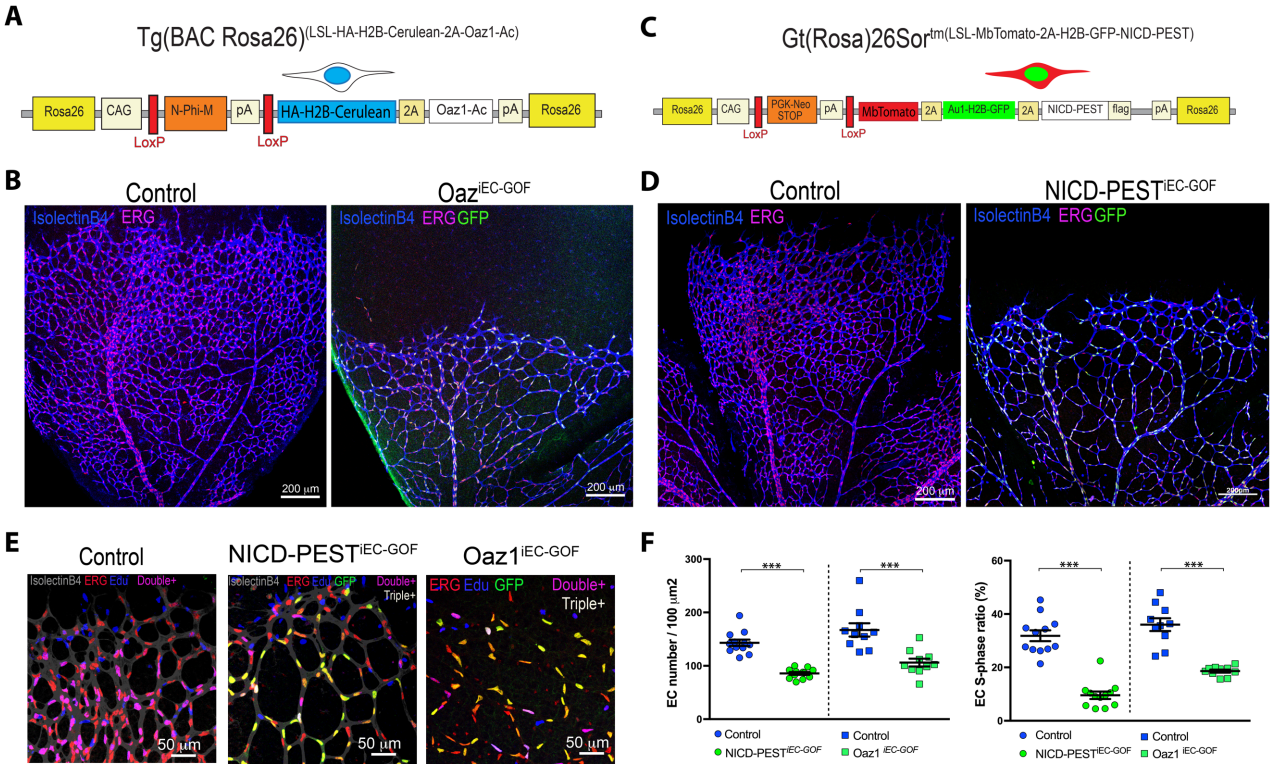

Figure 4.26. Vascular defects in retinas with Odc1 inhibition or Notch overactivation. A, Diagram of the DNA construct generated to decrease Odc1 activity by overexpressing the Odc1 inhibitor Oaz1 after Cre recombination. Recombined cells also express H2B-Cerulean. For endothelial specific recombination these animals were bred with Cdh5-CreERT2 line (Oaz1$^{iEC\text{-}GOF}$). **B,** Confocal micrographs of retinal vasculature from P6 control or Oaz1$^{iEC\text{-}GOF}$ animals injected with tamoxifen once a day from P1-P3. Retinas were immunostained for IsolectinB4, ERG and Cerulean. **C,** Diagram of the DNA construct generated to increase Notch activity by overexpressing a NICD-PEST after Cre recombination. Recombined cells also express H2B-GFP. For endothelial specific recombination these animals were bred with Cdh5-CreERT2 line (NICD-PEST$^{iEC\text{-}GOF}$). **D** Confocal micrographs of retinal vasculature from P6 control or NICD-PEST$^{iEC\text{-}GOF}$ animals injected with tamoxifen once a day from P1-P3. Retinas were immunostained for IsolectinB4, ERG and GFP. **E**, Higher magnification of angiogenic fronts from control, Oaz1$^{iEC\text{-}GOF}$ and NICD-PEST$^{iEC\text{-}GOF}$ retinas immunostained for IsolectinB4, ERG, GFP and EdU. **F,** Quantification of endothelial nuclei density (ERG+ nuclei per vascular area) and S-phase ratio (% of EdU+ERG+ among all ERG+ EC nuclei per field) in the angiogenic front of these animals. Error bars indicate SEM; *** p<0.0005 with a t-test.

Because we have seen that Odc1 expression is negatively correlated with Notch signaling we evaluated if overactivation of Notch signaling could also lead to a similar phenotype, as it would reduce Odc1 expression. Although there are available mouse lines to overactivate Notch signaling in a specific and inducible manner, they are based in a very high expression of a constitutively active NICD without its native PEST domain (Murtaugh *et al*., 2003), which leads to a very strong and non-physiological upregulation of Notch signaling

To evaluate the role of a more physiological Notch activation we generated a new mouse line, NICD-PEST^{GOF}, in which the NICD includes the native PEST degradation domain that allows for a more moderate overactivation of Notch signaling. Furthermore, in this line NICD-PEST overexpression is also directly associated with expression at equimolar levels (due to the 2A peptide) of the fluorescent reporters H2B-GFP and Mb-tomato (Fig. 4.26 C).

We bred these mice with the Cdh5-(PAC)-CreERT2 line, induced recombination from P1 to P3 and evaluated retinal vascular phenotypes and S-phase ratios as before at P6.

Retinas from these mice showed very similar phenotypes to those resulting from the inhibition of Odc1, with reduced ERG+ endothelial cell number and S-phase ratio, (Fig. 4.26 D-F), further suggesting a functional relationship between Notch signaling and Odc1 and a requirement of moderate Notch signaling activation and Odc1 activity in ECs to undergo normal proliferation during angiogenesis.

4.18 Odc1 deletion blocks EC proliferation and also prevents EC expansion after Notch inhibition

To further evaluate the relationship between Notch and Odc1during angiogenesis we decided to inhibit Notch in mice that have induced alterations in Odc1 expression in endothelial cells. We crossed the Odc1$^{flox/flox}$ or the Oaz1^{GOF} lines with the Cdh5-(PAC)-CreERT2 line to induce deletion of the Odc1 gene (*Odc1*$^{iEC\text{-}KO}$) or induce its degradation (*Oaz1*$^{iEC\text{-}GOF}$*).* At P5 these animals were injected with Control IgG or aDll4 and retinas were analyzed at P7, 48h after Notch inhibition.

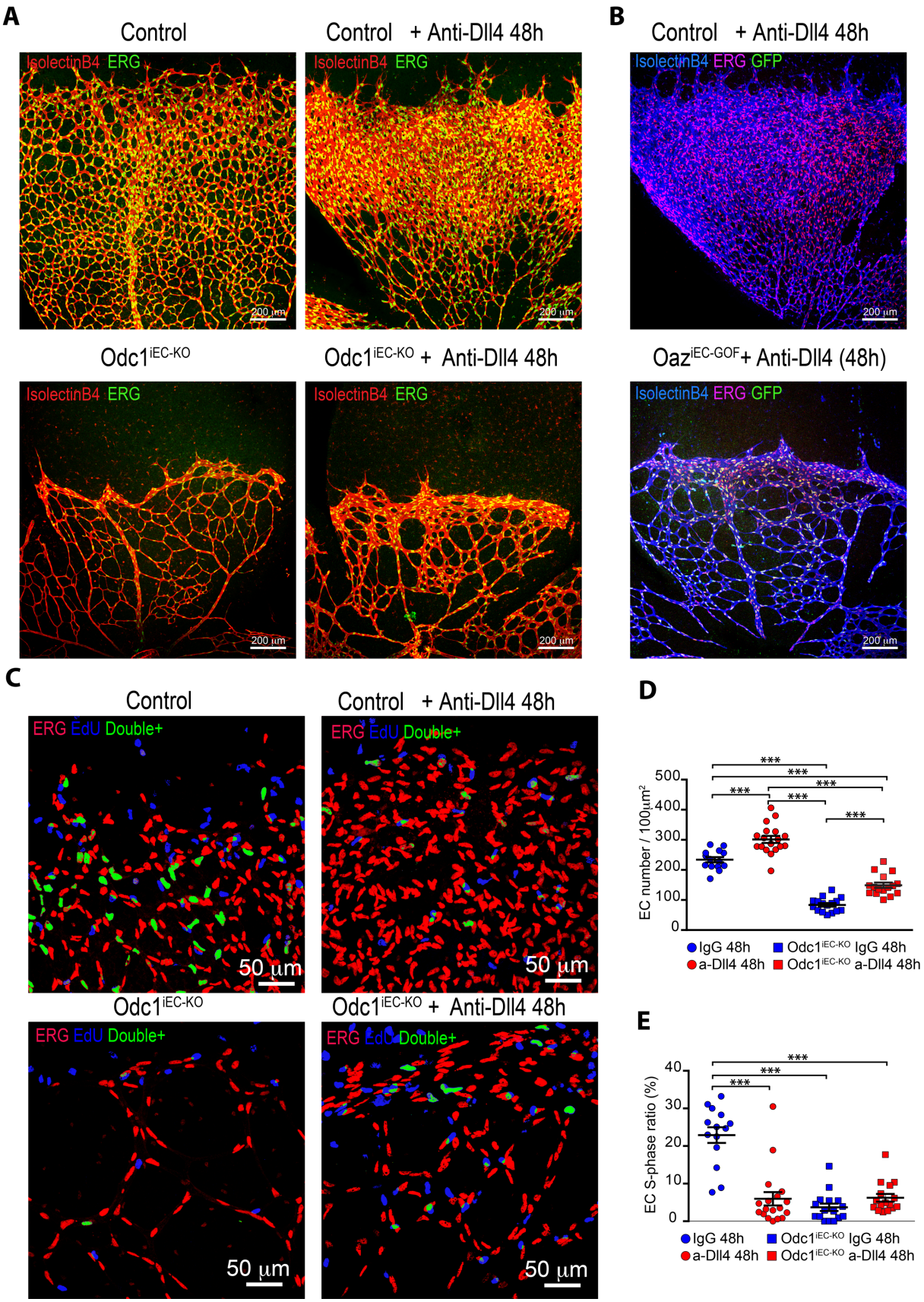
A
Control
Control + Anti-Dll4 48h
IsolectinB4 ERG
200 µm
B
Control + Anti-Dll4 48h
IsolectinB4 ERG GFP
200 µm
Odc1iEC-KO
Odc1iEC-KO + Anti-Dll4 48h
Oaziec-GOF+ Anti-Dll4 (48h)
C
Control
Control + Anti-Dll4 48h
ERG EdU Double+
50 µm
Odc1iEC-KO
Odc1iEC-KO + Anti-Dll4 48h
D
EC number / 100µm2
IgG 48h
Odc1iEC-KO IgG 48h
a-Dll4 48h
Odc1iEC-KO a-Dll4 48h
E
EC S-phase ratio (%)

Figure 4.27. Functional interaction between Odc1 and Notch during angiogenesis. A, Confocal micrographs of retinas from P7 control or Odc1^{iEC-KO} animals injected with tamoxifen once a day from P1 to P3 and treated with Control IgG or aDll4 at P5, 48h before dissection. Odc1^{iEC-KO} animals harbor the Cdh5-CreERT2 transgene. Retinas were immunostained for IsolectinB4 and ERG. **B**, Confocal micrographs of retinas from P7 control or Oaz1$^{iEC-GOF}$ animals injected with tamoxifen once a day from P1 to P3 and treated with Control IgG or aDll4 at P5, 48h before dissection. Oaz1$^{iEC-GOF}$ animals harbor the Cdh5-CreERT2 transgene. Retinas were immunostained for IsolectinB4, ERG and GFP.**C**, Confocal micrographs of P7 retinal vasculature fronts from control or Odc1^{iEC-KO} animals treated with Control IgG or aDll4 at P5, 48 hours before dissection. ERG in red, EdU in blue and Double positive cell in Green. **D, E**, Quantification of endothelial nuclei density (ERG+ nuclei per vascular area) and S-phase ratio (% of EdU+ERG+ among all ERG+ EC nuclei per field) in the angiogenic front of these animals. Error bars indicate SEM; NS, non-significant; ** p<0.01; *** p<0.001; with ANOVA.

Similarly to what we saw in *Oaz1$^{iEC-GOF}$* animals, retinas with Odc1 deletion showed a very strong vascular phenotype, with reduced number of ECs and very low S-phase ratios (Fig. 4.27 A, C, D). However, this phenotype was even stronger than the one observed in *Oaz1$^{iEC-GOF}$* animals, probably due to the total absence of endogenous functional protein.

More importantly, both Odc1 deletion or functional reduction partially prevented the characteristic vascular hyperplastic phenotypes induced after Notch inhibition (Fig. 4.27 A, B). Still, patches of vasculature at the angiogenic front had more vascular and cellular density compared with animals with Odc1 deletion only. These areas had, in the *Oaz1$^{iEC-GOF}$ + aDll4* retinas, a higher number of non-recombined, H2B-Cerulean negative ECs (Fig. 4.27 B), in which Odc1 function could still be normally regulated by Notch.

Nevertheless, retinas with both Notch inhibition and Odc1 deletion showed a decreased number of ECs at the angiogenic front compared with retinas only treated with aDll4 (Fig. 4.27 C, D) indicating that Odc1 deletion precludes excessive EC proliferation after the loss of Notch signaling. These findings could indicate that Odc1 is a protein essential for normal EC proliferation during angiogenesis and cells without Odc1 activity cannot respond to further Notch regulation.

4.19 Myc deletion phenocopies Odc1 deletion during angiogenesis

As previously mentioned, Odc1 is a canonical target of Myc. Myc is a TF that is important for the control of cell cycle progression and metabolism (Dang, 2012). Previous studies have shown that Odc1 is a fundamental driver of Myc-induced cell cycle regulation in tumors (Nilsson *et al.,* 2005; Annibali *et al.,* 2014) Moreover, Myc has also been implicated in proliferation and metabolic regulation during angiogenesis (Wilhelm *et al.,* 2016) and is essential for normal vascular development (Baudino *et al.,* 2002).

As we detected an increase in Myc regulated genes in the RNAseq analysis, we decided to evaluate the functional relationship between Myc and Notch in EC cell cycle regulation during angiogenesis. We crossed the Myc^{floxed} line with the Cdh5-(PAC)-CreERT2 line and induced recombination from P1 to P3. At P5 these animals were injected with Control IgG or aDll4 and retinas were analyzed at P7, 48h after Notch inhibition.

Retinal vascular phenotypes in $Myc^{iEC\text{-}KO}$ were very similar to those observed in $Odc1^{iEC\text{-}KO}$ animals, with a dramatic decrease in EC number and a reduction in the S-phase ratio of these cells (Fig. 4.28) indicating an essential role of Myc for normal cell cycle progression in ECs. Notch inhibition in $Myc^{iEC\text{-}KO}$ animals could not elicit the same proliferative response seen in wild type animals treated with aDll4, which is similar to the functional interaction observed in Odc1 mutants.

The $Myc^{iEC\text{-}KO}$ retinas seem to have even lower number of ECs and a stronger reduction in the S-phase ratio than $Odc1^{iEC\text{-}KO}$ retinas, suggesting a more important role for Myc in the control of EC proliferation, as it could be expected considering that Odc1 would not be the only Myc-regulated gene controlling cell cycle. These data suggest that Myc is also required for ECs to be responsive to Notch inhibition.

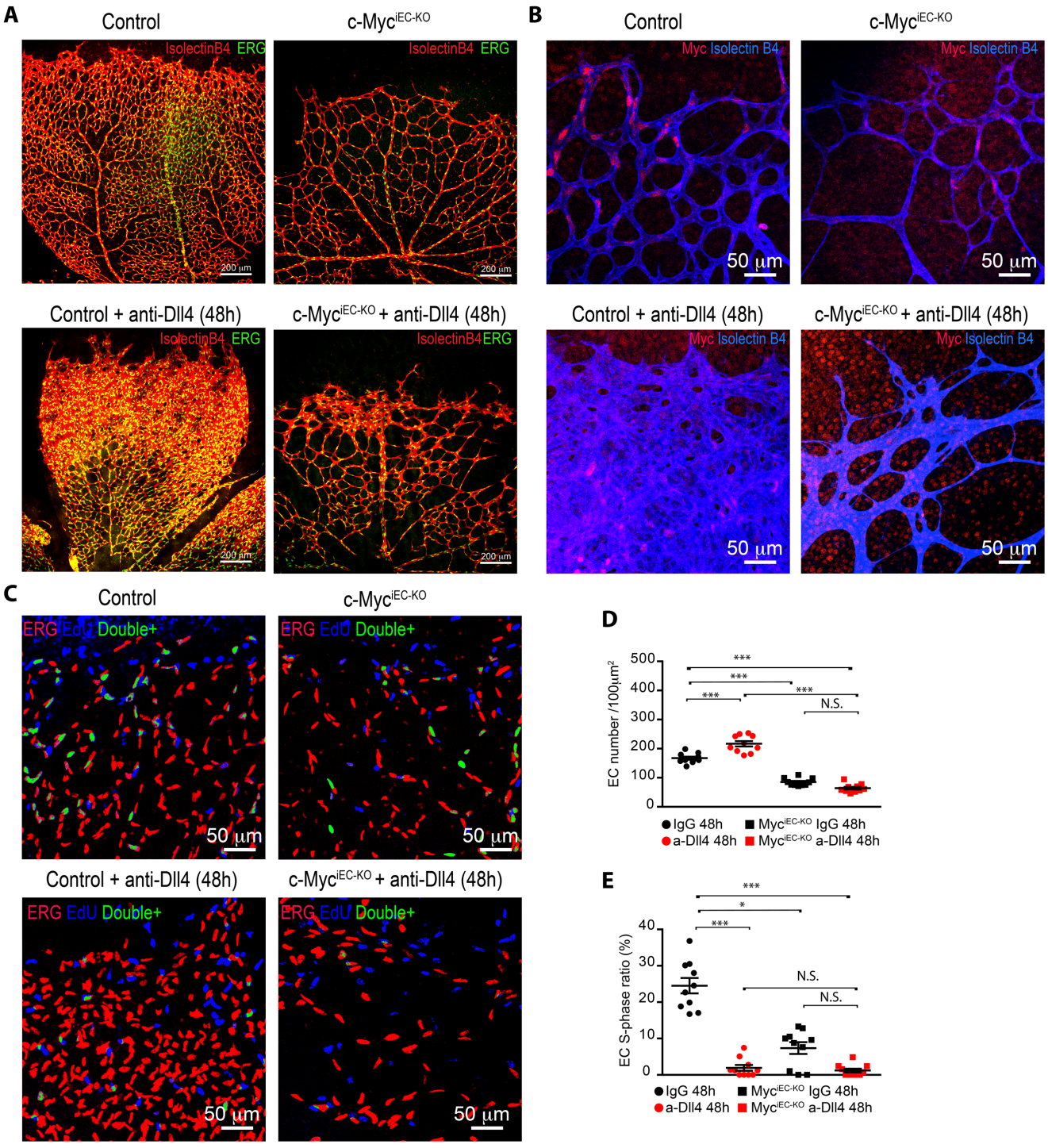
A
Control
c-Myc iEC-KO
IsolectinB4 ERG
200 μm
Control + anti-Dll4 (48h)
c-Myc iEC-KO + anti-Dll4 (48h)
B
Control
c-Myc iEC-KO
Myc Isolectin B4
50 μm
Control + anti-Dll4 (48h)
c-Myc iEC-KO + anti-Dll4 (48h)
C
Control
c-Myc iEC-KO
ERG EdU Double+
50 μm
Control + anti-Dll4 (48h)
c-Myc iEC-KO + anti-Dll4 (48h)
D
EC number /100μm²
500
400
300
200
100
0
***
***
***
***
N.S.
IgG 48h
Myc iEC-KO IgG 48h
a-Dll4 48h
Myc iEC-KO a-Dll4 48h
E
EC S-phase ratio (%)
40
30
20
10
0
***
*
***
N.S.
N.S.
IgG 48h
Myc iEC-KO IgG 48h
a-Dll4 48h
Myc iEC-KO a-Dll4 48h

Figure 4.28. Functional interaction between Myc and Notch during angiogenesis. A, Confocal micrographs of retinas from P7 control or $Myc^{iEC\text{-}KO}$ animals injected with tamoxifen once a day from P1 to P3 and treated with Control IgG or aDll4 at P5, 48h before dissection. $Myc^{iEC\text{-}KO}$ animals harbor the Cdh5-CreERT2 transgene. Retinas were immunostained for IsolectinB4 and ERG. **B**, Confocal micrographs of P7 retinal vasculature fronts from control or $Myc^{iEC\text{-}KO}$ animals treated with Control IgG or aDll4 at P5, 48 hours before dissection immunostained for Myc in red and IsolectinB4 in blue. **C**, Confocal micrographs of P7 retinal vasculature fronts from control or $Myc^{iEC\text{-}KO}$ animals treated with Control IgG or aDll4 at P5, 48 hours before dissection immunostained for ERG in red, EdU in blue showing double positive cell in Green. **D, E**, Quantification of endothelial nuclei density (ERG+ nuclei per vascular area) and S-phase ratio (% of EdU+ERG+ among all ERG+ EC nuclei per field) in the angiogenic front of these animals. Error bars indicate SEM; NS, non-significant; *p<0.05; *** p<0.001; with ANOVA.

4.20 Hypoplastic vascular phenotypes are associated with high p21 expression

The previous results showed that either genetic deletion of pro-proliferative genes (Myc, Odc1) or genetic overexpression of anti-proliferative genes (Notch) in ECs during angiogenesis lead to similar retinal vascular phenotypes characterized by a strong decrease in EC number and a strong reduction in the S-phase ratio in ECs, indicative of an absence of proliferation in mutant cells. As we have seen before, p21 can be induced by excessive mitogenic stimuli and mediate cell-cycle arrest during angiogenesis.

We decided to evaluate if the defects in EC proliferation observed in $Odc1^{iEC\text{-}KO}$, $Myc^{iEC\text{-}KO}$ and $NICD^{iEC\text{-}GOF}$ were also associated with p21 expression. We found that a very high percentage of ECs throughout the whole retina vasculature of these mutant animals were expressing p21 (Fig. 4.29). The intensity in p21 protein immunostaining levels in these mutants were much higher than the one seen in tip-cells during normal angiogenesis or after Notch inhibition (Compare with Fig. 4.19), suggesting a stronger cell cycle arrest after these genetic manipulations. These results suggest that $Odc1^{iEC\text{-}KO}$, $Myc^{iEC\text{-}KO}$ and $NICD^{iEC\text{-}GOF}$ ECs may be or irreversibly arrested. More studies will be required to answer this question properly.

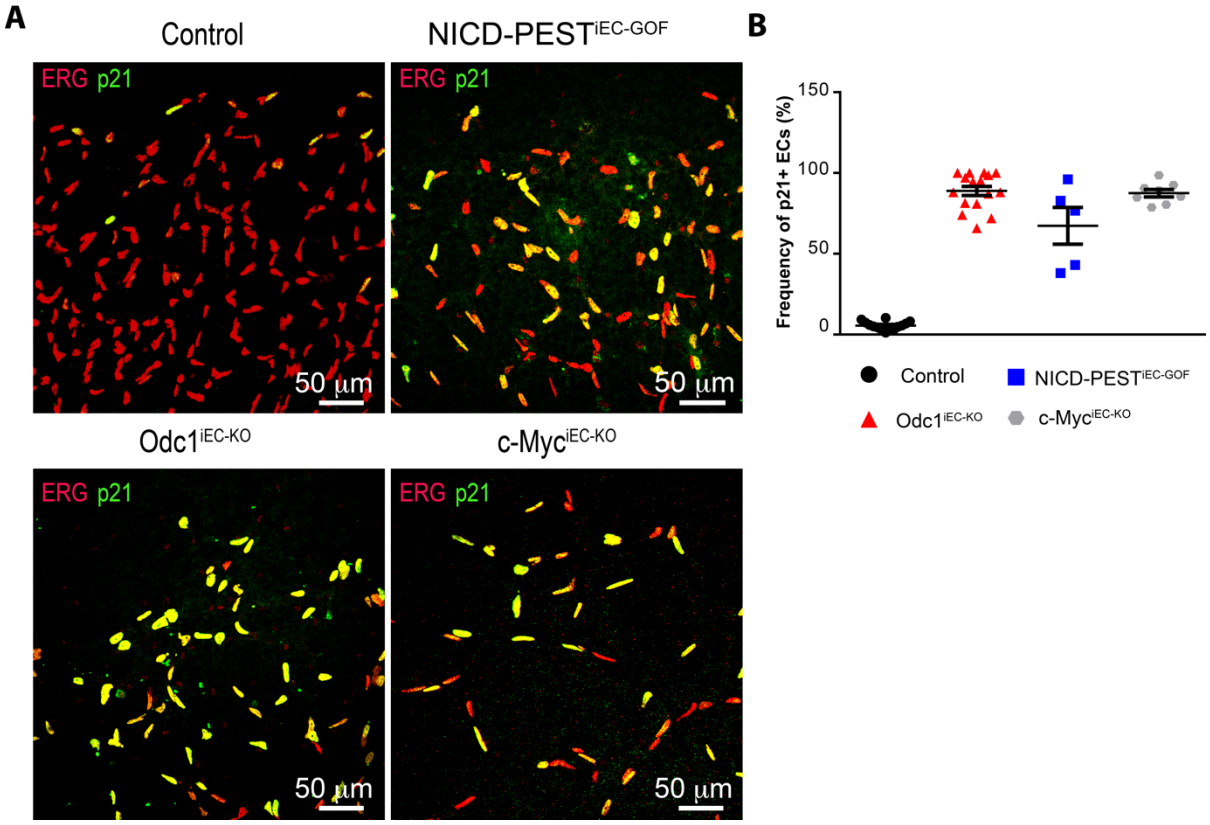

Figure 4.29. Expression of p21 in ECs mutant for signaling pathways controlling proliferation. A, Confocal micrographs of P7 retinal vasculature fronts of control, NICD-PEST$^{iEC-GOF}$, Odc1^{iEC-KO} and Myc^{iEC-KO} from different independent experiments. Retinas were immunostained for ERG in red and p21 in Green. **B,** Quantification of the frequency of p21-expressing ECs at the angiogenic front of these retinas. Errors indicate SEM.

DISCUSSION

5 DISCUSSION

Angiogenesis is a complex morphogenetic process in which endothelial cells have to carefully orchestrate different cellular behaviors. These include responsiveness to angiogenic signals, migration, proliferation, differentiation, maturation and stabilization within the vasculature. The proper coordination of each of these processes, among each other and among different ECs, is essential to generate a functional vascular network. For this reason, specific mechanisms must exist that precisely regulate the temporal and spatial transitions between different endothelial cell states during angiogenesis.

One of the current models describing endothelial cell behavior during angiogenic sprouting is based on the transient and dynamic specification of two endothelial cell states denominated tip and stalk cells (Gerhardt *et al.*, 2003). These two types of endothelial cells have distinct morphological and molecular characteristics that are thought to give rise to different cellular behaviors. These characteristics are normally said to be highly conserved, but differences may exist between different vascular beds and modes of sprouting. Indeed, in zebrafish it seems that different types of vessels use different modulations of the Notch and VEGF receptors to regulate EC sprouting (Siekmann, Affolter, and Belting, 2013)

In this work, I will discuss models proposed based on data obtained mainly on the retina angiogenesis system, that has been extensively studied by different research groups, and considered to represent how angiogenesis is generally regulated also in other organs, even though there might exist tissue or organ specific signals that may change the characteristics of this regulation. In general, tip cells appear closest to hypoxic avascular areas, receiving and responding to proangiogenic signals and are characterized for having a migratory phenotype, extending filopodia and expressing genes involved in ECM remodeling and cell migration (Gerhardt *et al.*, 2003; Strasser, Kaminker, and Tessier-Lavigne, 2010). An initial analysis with relatively low cellular/nuclei resolution, suggested that tip cells do not proliferate or proliferate weakly (Hellström *et al.*, 2007), however several groups demonstrated after that tip cells can proliferate during vascular development in zebrafish (Siekmann and Lawson, 2007). Stalk cells

constitute a population of endothelial cells forming an immature vasculature just behind tip cells and in the case of the retina, they are actively proliferating to generate new ECs for the growing vascular network (Gerhardt *et al.,* 2003; Fruttiger, 2007).

VEGF and Notch signaling pathways have been shown to be central in controlling angiogenic progression and the stalk-tip cell switch (Blanco and Gerhardt, 2013). Based on endothelial specific loss of function studies for components of these pathways a model has been proposed in which VEGF will induce the specification of tip cells and the expression of the Notch ligand Dll4 in vivo (Suchting *et al.*, 2007; Lobov *et al.*, 2007) and in vitro *(*Liu *et al.,* 2003; Williams *et al.*, 2006). Notch activation in adjacent cells would repress tip cell specification. The way how it transcriptionally controls the repression of tip cell specification is still under debate and controversy. Some groups suggested that Notch represses the tip cell fate by repressing the expression of VEGF receptors, mainly VEGFR2 (Taylor, Henderson, and Hughes, 2002; Liu *et al.,* 2003; Gerhardt *et al.*, 2003; Siekmann, Covassin, and Lawson, 2008), whereas more recent data and our own data shows that the transcription of VEGFRs is not significantly deregulated after Notch LOF during angiogenesis *in vivo* (Benedito *et al.*, 2012; del Toro *et al.*, 2010; Lobov *et al.*, 2007). Nonetheless, it is generally considered that the regulation of the number of sprouting tip cells is achieved through Notch dependent lateral inhibition of tip cell specification (Bentley, Gerhardt, and Bates, 2008). However, Notch is also known to block EC proliferation *(Noseda et al.*, 2004), which is a characteristic of actively migrating and sprouting tip cells.

The interdependence of EC sprouting and proliferation dynamics by VEGF and Notch have been difficult to adjust to a model where sprouting ECs do not proliferate, and proliferating ECs do not sprout. The phenotype caused by Notch inhibition, or increase in VEGF signaling, has been described as a result of simultaneous hypersprouting and hyperproliferation (Gerhardt *et al.*, 2003; Suchting *et al.*, 2007)which is not compatible with a model where sprouting tip cells do not proliferate well.

In this work we have explored in more detail this issue, specifically how Notch signaling controls endothelial proliferation during angiogenesis, with high temporal and cellular resolution. We have developed new genetic tools to perform inducible multispectral clonal analysis of cells with

different Notch and VEGF signaling levels and determine its effect on endothelial cell proliferation. We have also functionally characterized new putative Notch target genes that control EC proliferation during angiogenesis.

5.1 The Dual ifgMosaic strategy enables the generation of high resolution functional genetic mosaics in mice

All previous studies that have evaluated the effect of different genes on endothelial cell proliferation are based on global, tissue-level deletion of Dll4, RBPJ, VEGFR2 (Benedito *et al.*, 2012) and 3 (Tammela *et al.*, 2008), Jagged (Benedito *et al.*, 2009) or pharmacological inhibition (Suchting *et al.*, 2007; Hellström *et al.*, 2007; Lobov *et al.*, 2007). However, the available genetic strategies to generate and perform functional genetic mosaics in mice were limited.

With our Dual ifgMosaic strategy, we were able to generate a high resolution fluorescent mosaic with the combination of independent, nuclear and membrane localized, fluorescent markers (Fig. 4.1). Moreover, this strategy allows for the co-expression of a gene of interest with the fluorescent marker in equimolar proportions, and we have produced several mESCs and mouse lines where is possible to induce Notch (iChr-Notch-mosaic) and VEGF signaling activity (iMb-Vegfr2-mosaic) mosaics (Fig. 4.2). With this strategy we could compare cellular phenotypes induced by different genetic modifications within the same tissue, and compare it with labelled control cells in the same tissue.

The induction of these mosaics during *in vitro* endothelial cell differentiation revealed changes in the dynamics of differentiation, proliferation or survival of the recombined EC with alterations of Notch or VEGF signaling (Fig. 4.3), confirming that the functional genetic cassettes modify Notch and VEGF signaling when expressed.

In addition, we saw *in vivo* that these functional modifications induce the downstream molecular alterations anticipated from modifications of the Notch and VEGF signaling pathways. However, they also produced some unexpected single-cell derived clonal phenotypes.

Induction of the Notch mosaics during embryonic neurogenesis showed the expected alterations in the neuronal differentiation dynamics (Louvi and Artavanis-Tsakonas, 2006), with Notch Loss-of-Function cells preferentially committing to differentiation, while Gain-of-function cells remained undifferentiated (Fig. 4.4). Endothelial cells having more Vegfr2 activity in iMb-Vegfr2-Mosaic mice, had more pERK activity (Fig. 4.5), as expected, but showed defects in proliferation during retinal angiogenesis (Fig. 4.16 and 4.17).

Importantly, since the mutant mice are mosaic, they do not have severe developmental problems, which enables long-term phenotypic analysis of cells with different signaling status. With these new mouse lines, we were able to evaluate the effects of Notch and VEGF alterations on endothelial cell proliferation at the single cell level in short-term or long-term *in vivo* assays. Moreover, we have used this strategy to perform combinatorial and multiple single cell epistasis analysis by inducing cells with different combinations of Notch and VEGF signaling impairments, as will be further discussed below.

5.2 Notch inhibition in endothelial cells has opposite effects on EC proliferation at different temporal scales.

Based on previous studies and the current model of Notch function in angiogenesis, Notch inhibition increases the proliferative capacity of endothelial cells during angiogenesis (Lobov *et al.,* 2007; Hellström *et al.* ,2007; Benedito *et al.*, 2012; Ridgway *et al.*, 2006; Noguera-Troise *et al.*, 2006) leading to an increase in endothelial cell number. This led us to expect that mosaic induction of cells with a decrease in Notch signaling during early vascular development would produce phenotypes associated with the expansion of these cells, that would presumably outcompete the adjacent control ECs.

However, the induction of the iChr-Notch-mosaic in endothelial cells early during development, with the Tie2-Cre driver, was not embryonically lethal. This allowed us to evaluate the long-term contribution of cells with different Notch activities to the adult vasculature.

We found that the vasculatures of different organs were composed mostly of cells that did not have any Notch functional alteration. (Fig. 4.9) Compared with the predicted recombination ratios, cells with reduced Notch activity were underrepresented suggesting that they had a long-term competitive disadvantage with respect to unmodified cells, in contrast with previous models proposed with data obtained mainly after short-term Notch LOF experiments (Benedito *et al.*, 2012). In agreement with published studies, short-term clonal analysis of retinal endothelial cells expressing the iChr-Notch-mosaic showed that single-cell derived clones of ECs with reduced Notch activity expanded slightly more than wild type clones over a period of three days. (Fig 4.6). Cells with Notch overactivation were clearly unable to proliferate in both short-term (Fig. 4.6) and long-term (Fig.4.9) mosaic experiments being completely absent of the vasculature of adult mice.

Thus, this data indicates that Notch inhibition can initially and transiently increase the proliferation rate of endothelial cells during angiogenesis, but later these cells lose their proliferative capacity when compared to wild type endothelial cells.

5.3 Inhibition of Dll4-dependent Notch signaling during angiogenesis induces rapid endothelial cell cycle progression followed by arrest

The evaluation of global and acute inhibition of Dll4-induced Notch signaling during retinal angiogenesis revealed similar temporal-dependent effects on endothelial cell proliferation.

Notch inhibition induced the expansion of the vascular area after just 24h. This expansion was associated with an increase in endothelial cell number after 24 and 48 hours of Notch inhibition (Figs. 4.11-4.12).

However, this increase in EC number was not associated to a concomitant increase in the frequency of Ki67+ or EdU+ proliferating ECs (Figs. 4.12; 4.13 and 4.14). On the contrary, 48h after Notch inhibition very few ECs were proliferating (Fig. 4.12 and 4.14). This halt in EC proliferation was maintained at later time points (72h) (Fig. 4.13).

The cell-cycle marker Ki67, was already expressed by 96% of ECs at the angiogenic front (Fig. 4.14), and that frequency could not obviously significantly increase after Notch LOF. We and other groups never detected apoptotic ECs at the angiogenic front of control retinas. The fact that we observed an increase in EC number, without an increase in the frequency of proliferation or a change in apoptosis rates, suggest that the increase in cell number could only be due to a faster progression through the cell cycle. This may be due to faster G1/S or other cell-cycle checkpoints transitions, or a shorter s-phase, since the EdU labeling index never changed at 12h and 24h, even though more ECs were being generated.

After this initial increase in the speed of cell cycle, at 48h after Notch inhibition, 96% of ECs at the angiogenic front had Ki67+ staining, whereas normally 10% of angiogenic front ECs are KI67+, indicating that there was a pronounced cell cycle arrest of these ECs (Fig. 4.14).

Our data shows that sustained inhibition of Notch during angiogenesis does indeed induce a global blockade of cell cycle progression, however it is associated with a faster completion of the ongoing cell cycle, which initially increases the EC number. This also explains the effects we observed in ECs with Notch inhibition in the long-term genetic mosaics.

Remarkably the effects of Notch inhibition were also context-dependent, as mature areas of the retinas, in which ECs are normally non-proliferative, showed an increase in the population of endothelial cells positive for Ki67 and EdU, as well as an increase in EC number (Figs. 4.12; 4.13 and 4.14).

This suggest that quiescent endothelial cells in mature vasculatures respond differently to Notch inhibition and enter cell cycle, in line with previous studies showing the formation of vascular neoplasms in adult mice after aDll4 treatment (Yan *et al.*, 2010; Cuervo *et al.*, 2016). It has been published that VEGFR2 and VEGFR3 levels are downregulated during maturation in a Notch dependent manner (Ehling *et al.*, 2013) thus cell cycle entry in this cells could be cause by increase activation of VEGF signaling.

5.4 Endothelial tip-cells have limited proliferative capacity in mouse postnatal retinal angiogenesis

As said before, endothelial tip cells have been shown to have low expression of Notch target genes and are believed to constitute a population with low Notch activation (Hellström *et al.*, 2007; Phng *et al.*, 2009).

Ki67 staining in Esm1-HA-H2B-Cerulean+ tip cells, the cells with highest VEGF signaling activation, showed that these cells were more frequently out of cycle, when compared with surrounding stalk cells, further indicating that physiological Notch activation is important to maintain the proliferation of angiogenic endothelial stalk cells (Fig. 4.18).

Previous studies have characterized the phenotype of Notch inhibition as having an increase number of tip cells. We similarly saw that Notch inhibition causes and increase in the expression of Esm1 (Fig. 4.18)., Angpt2 and Apln (Fig. 4.24), which are tip cell enriched genes (del Toro *et al.,* 2010; Strasser, Kaminker, and Tessier-Lavigne, 2010).

This data indicates that Notch activation maintains endothelial cells in a proliferative, undifferentiated state at the angiogenic front. Reduction in Notch activation would induce a differentiation switch to tip cell that is associated with rapid completion of the ongoing cell cycle and cell cycle arrest.

However, clonal analysis of tip cell progeny showed that most cells (almost 80%, Fig. 4.18 E) that expressed Esm1 can divide at least once in a four-day period. Because tip cell specification is a dynamic process (Jakobsson *et al.*, 2010) this results could mean that when tip cells leave the tip cell position, and maybe increase their Notch activation, they can reenter cell cycle. Esm1-derived clone size distribution was smaller than stalk cells (Compare Red distribution in figures 4.6 F with Blue in Figure 4.18 E), which indicates that tip cells have limited proliferation capacity, but they can divide, or can reenter cell-cycle after being arrested, for example when moving to a stalk position, more distant from the VEGF source.

This hypothesis can be further supported by the reduction in the Esm1+-derived clone size after Dll4/Notch blockade (Fig 4.18 E), where most Esm1-derived clones are formed by only 1 cell, which means that these cells were prevented from entering cell cycle after Notch/Dll4 inhibition, presumably because they are blocked from switching to a more proliferative stalk cell phenotype.

5.5 Strong activation of the MAPK pathway is associated with cell-cycle arrest during angiogenesis

Tip cells have high activation of VEGFR2 which is associated with downstream activation of the MAPK pathway through phosphorylation of ERK (Fig. 4.5) (Gille *et al.*, 2001).Activation of this receptor is associated with positive angiogenic responses thus it is widely accepted that VEGFR2 activation promotes proliferation and migration of endothelial cells, processes that are both required for angiogenesis.

Moreover, endothelial deletion of the two main effectors of the MAPK pathway, ERK1 and ERK2, in mice causes embryonic lethality associated with defective vascular organization (Srinivasan *et al.,* 2009) and reduction in the proliferation and migration of ECs. However, studies in zebrafish suggest that the activation of the ERK pathway is not necessary for endothelial cells to proliferate (Shin *et al.* 2016), and that ERK activation may only have a role in sprouting or migration during angiogenesis.

Our data shows that ERK activation is prominent in the migratory endothelial cells at the tip of the sprouts during normal retinal angiogenesis and is strongly upregulated in stalk endothelial cells after Notch inhibition (Fig. 4.15). In both these endothelial populations with strong ERK activation we have seen a lower frequency of cells in s-phase or KI67+ (FIgs. 4.14 and 4.18). Forced activation of VEGFR2 (VEGFR2$^{Ac.}$) signaling in the iMb-VEGFR2-Mosaic line also results in strong phosphorylation of ERK proteins (Fig. 4.5). The vascular defects observed in retinas with a high number of VEGFR2^{AC-} cells (Fig. 4.16) and the decrease in proliferation and clonal expansion of these cells (Figs. 4.7; 4.10 and 4.17) further imply an inhibitory effect of strong ERK activation on endothelial cell proliferation.

Yet, our data on cells with reduced VEGFR2 activation (VEGFR2^{TK-}) also suggest that physiological VEGFR2 activation is required for EC proliferation (Figs. 4.7; 4.10 and 4.17). We have also seen that the reduced proliferation of VEGFR2^{TK-} cells is partially reversed by Notch inhibition (Figs. 4.8 and 4.17). and we also showed that Notch inhibition has different effects in the proliferation of angiogenic or quiescent endothelial cells, which also have low expression of VEGFR2 and VEGFR3 (Ehling *et al.*, 2013)(Figs. 4.12 and 4.14).

Both, VEGFR2 activation and Notch inhibition promote ERK phosphorylation, thus endothelial cell proliferation could be controlled by the integration of these two signals at the level of ERK activation. During angiogenesis, the activation levels of the pro-mitogenic MAPK pathway, independently controlled by Notch and VEGFR2, seem to promote proliferation only within a specified range of signaling activity, and both very low or very high ERK activation prevents cell cycle progression.

To test the requirement of ERK activation for endothelial cell proliferation, we inhibited ERK phosphorylation during angiogenesis using a MEK inhibitor. We indeed saw a reduction in DNA synthesis after 24h of MEK inhibition in the angiogenic EC population. However, we did not see differences in endothelial cell density or number (Fig 4.22)

As ERK activity has been shown to be required for the transition through G1 to S-phase (For a review of different mechanisms of ERK-controlled G1/S transition see Chambard *et al.*, 2007) these results could indicate that the cells that were already past the G1/S transition were able to divide normally. Cells that were in G1 before MEK inhibition and the newly formed cells after 24h would not be able to progress through cell cycle thus reducing S-phase labelling. Accordingly, a significant effect in endothelial cell number might not be detected until later stages, in which the population that was in G1, and it is blocked by MEK inhibition, would have had time to progress and divide.

Our data also reflected the role of ERK in promoting cell cycle entry (Rodríguez *et al.*, 2010), as the increase in proliferation in quiescent endothelial cells after Notch inhibition was completely lost in the absence of normal ERK phosphorylation(Fig. 4.23).

Interestingly, the angiogenic front after MEK inhibition is blunt and devoid of sprouts (Figs. 4.21 and 4.22), indicating that high ERK phosphorylation is required to activate the sprouting and migratory behavior in tip cells as shown before (Shin *et al.,* 2016; Mavria *et al.,* 2006).

Therefore, ERK seems to be, at relatively low levels, a pro-mitogenic signal that is required for transitioning through the different cell-cycle phases in stalk cells, whereas at high levels is an anti-mitogenic and pro-sprouting signal that is required for tip cell migration. This could be a simple mechanism to establish differences among proliferative stalk cells and migratory tip cell populations during angiogenesis.

5.6 Expression of the cell cycle inhibitor p21 is regulated by Notch and VEGF signaling

The cell cycle inhibitor p21 has been described to be activated in response to high mitogenic signaling, particularly through the MAPK pathway (Pumiglia and Decker, 1997; Balmanno and Cook, 1999). This has been described as a mechanism to avoid excessive proliferation that could lead to tumorigenesis.

We detected high p21 expression in tip cells, VEGFR2AC+ cells and cells with Notch LOF (Fig. 4.19). All these ECs have high pERK levels, suggesting that the cell cycle arrest seen in these EC populations could be mediated by a pERK dependent induction of p21 expression. However, our experiments indicate that blocking ERK activity for 24h does not reverse/downregulate the expression of existing p21 in tip cells, even though it is required for the full *de novo* stalk-cell upregulation of p21 after Notch-inhibition (Fig. 4.22) These results indicate that both VEGF activation and Notch inhibition induce the expression of p21, and at least partially through pERK dependent mechanisms. The fact that p21 protein does not decrease in tip cells after pERK inhibition, and that is still partially induced in the absence of Notch and pERK signaling suggest that there may exist alternative mechanisms to regulate maximal expression of p21 in tip cells and stalk cells with Notch LOF.

Furthermore, analysis of normal angiogenesis in p21 full knockout animals (Fig. 4.20) suggest (Fig 4.20) that p21 has a minor role on stalk-cell EC proliferation, which is consistent with the fact that is mainly expressed by tip cells. However, it is a significant modulator of EC proliferation in vessels with low Notch signaling, which upregulate p21, and become more sensitive to the loss of this cell-cycle inhibitor. However, p21 loss only partially reversed the cell cycle exit induced by loss of Notch signaling, arguing for additional molecular regulators controlling cell cycle speed and exit after Notch downregulation. Other cell-cycle inhibitors, such as p27, may also compensate for the loss of p21. Indeed, p27 loss was already shown to be able to partially modulate the Notch response in zebrafish ECs (Nicoli *et al.*, 2012).

5.7 Notch represses the expression of several cell cycle regulators

To identify and characterize other molecular mechanisms that may be regulated by Notch during angiogenesis, we performed comparative RNAseq analyses of angiogenic endothelial cells 24 hours after Notch inhibition. This analysis showed the expected increase in previously described tip-cell enriched genes (Strasser, Kaminker, and Tessier-Lavigne, 2010)(Fig. 4.24).

In contrast to previous studies indicating that Notch effects on angiogenesis could be due to regulation of the VEGF receptors (Gerhardt *et al.,* 2003; Suchting *et al.,* 2007; Ridgway *et al.,* 2006), we did not observe clear changes in their mRNA expression in our RNAseq analysis of angiogenic vessels. This supports the notion that the proliferative effects seen after Notch inhibition would be independent of VEGFRs transcriptional regulation, as has been previously published (Benedito *et al.,* 2012). Our epistasis analysis with Notch and VEGFR2 combinatorial mosaics also reveal that VEGFR2 is only partially required for the proliferation of ECs with lower Notch signaling. The PI3K/Akt pathway has also been previously connected to the control of proliferation exerted by Notch through the upregulation of PTEN (Serra *et al.*, 2015). However, we could not find clear differences in the mRNA levels of PTEN arguing for and alternative regulation mechanism.

Instead, the RNAseq analysis revealed that Notch activation is associated with the repression of several Myc downstream target genes and in particular Odc1, which are strongly associated with cell cycle progression and proliferation (Auvinen *et al.*, 1992; Bretones, Delgado, and León 2015).

These results argue for an anti-proliferative effect of Notch activity, required for maintaining controlled and sustained proliferation and avoid a mitogen-induced cell cycle exit response during angiogenesis. This effect does not seem to be mediated by transcriptional control of upstream regulators of pro-mitogenic signaling like VEGFRs or PTEN but could instead be realized through the regulation of downstream effectors of those pathways like ERK, directly at the transcriptional (through Myc) or further down at the direct regulatory (Odc1 and polyamines) levels of cell cycle regulation

5.8 Odc1 expression is repressed by Notch and promoted by Myc in ECs during angiogenesis

Synthesis of polyamines by Odc1 is absolutely required for normal cell cycle progression (Oredsson, 2003). Moreover, alterations of polyamine levels are associated with changes in cell cycle speed (Nasizadeh *et al.,* 2005). Thus, polyamine-dependent increase in the speed of cell cycle after Notch inhibition could explain the rapid increase in endothelial cell numbers we have observed.

Our data indicates that Notch can control the expression of the Odc1 gene through Hey1/2 repression suggesting direct control of Odc1 and polyamine synthesis by the Notch pathway (Fig. 4.25), which has been already reported before *In vitro* (Heisig *et al.,* 2012). However Odc1 expression and polyamine regulation has been strongly associated with Myc activity (Auvinen *et al.*, 2003; Wagner *et al.,* 1993) and our data show that Notch inhibition is associated with the upregulation of several Myc controlled genes suggesting that Notch could be controlling Odc1 through Myc. Odc1 expression is indeed promoted by Myc during angiogenesis, although it does not seem to be fully necessary for Odc1 expression in ECs (Fig 4.25 C). Overall our data suggest that Notch could be controlling both Odc1 expression directly and indirectly through alterations of Myc function. Even though we could not detect changes in Myc expression in our RNAseq our

this does not reject that myc activity could be controlled by Notch post transcriptionally.

5.9 The activities of Odc1 and Myc are necessary for normal endothelial cell proliferation during angiogenesis

Suppression of Odc1 activity, either by inhibition or deletion of Odc1, as well as Myc deletion, lead to very similar vascular phenotypes, characterized by strong reduction in vascular and cellular densities and EC was very reduced in these retinas strongly suggesting that minimal activity of Myc and Odc1 is required for normal cell cycle progression (Figs.4.26-4.28).

As we have shown ERK activation seem to be essential for normal endothelial cell cycle progression. ERK has been shown to promote Myc activity to induce the G1/S transition through the regulation of cyclin D (Seth *et al.*, 1991; Daksis *et al.*, 1994). Thus, the strong effect of Notch inhibition on ERK phosphorylation could be the driver of Myc and Odc1 upregulation in combination with the reduction of the direct Hey-mediated inhibition.

Moreover a recent study have shown that notch effects during angiogenesis could be mediated by direct regulation of endothelial VEGF expression (Pitulescu *et al.,* 2017), which in turn would increase MAPK signaling and Myc activity. Further analysis of the effect of Notch on cell cycle dynamics would require the evaluation of the relative weight of ERK-Myc mediated or Hey mediated control of Odc1 expression

5.10 Endothelial cells defective for genes essential in cell cycle progression enter a permanent non-proliferative state

The similar phenotypes obtained after Odc1 and Myc deletion or Notch overactivation suggest a common effect of cell cycle arrest due to the reduction of the signals required for cell cycle progression.

This arrest was associated with strong p21 expression in all cases (Fig. 4.29) indicating that this cell cycle inhibitor could be a general mediator of endothelial cell cycle arrest in the endothelium. A recent study (Muñoz-Espín *et al.*, 2013) have shown that p21 mediates the

induction developmentally programed senescence. These effects could be explained by a reduction in polyamines levels as it has been previously shown that their absence can induce senescence-like phenotypes (Kramer *et al.*, 2001).

These arrested ECs, with Myc or Odc1 deletion, were unable to respond to the hyperproliferative signal caused by inhibition of Notch, while surrounding, non-recombined cells (in the case of Odc downregulation in the $Oaz^{iEC\text{-}GOF}$) present the typical hyperplasic response.

This data indicates that the pro-mitogenic signals increased after Notch inhibition cannot reverse the state of permanent cell cycle arrest associated with strong p21 expression, in contrast with the temporal cell cycle exit in tip cells associated with transient p21 upregulation

5.11 The role of Notch on endothelial cell proliferation during angiogenesis.

The data presented in this thesis contributes to clarify the dynamics and regulation of endothelial cell cycle progression during angiogenesis. Endothelial cell proliferation is essential to produce the cells required to form new blood vessel. However, proliferation has to be coordinated with the directed migration of endothelial cells towards avascular areas.

VEGF is the most important molecule that induces angiogenesis. This is achieved by the activation of endothelial cells in existing vessels.

However, this activation is restricted to only a few cells along the vessels receiving the angiogenic stimuli. This restriction seems to be necessary for the formation of new functional vessels. Our data shows that the activation of tip cell is mediated by strong phosphorylation of ERK. The activation of the MAPK pathway seems to be necessary to confer migratory properties to tip cells. Yet, we have seen that this strong MAPK activation in tip cells also blocks cell cycle progression and proliferation. This seems to be mediated by p21 in a characteristic mitogen-induced cell cycle arrest.

Notch activation would constitute a mechanism to reduce MAPK signaling to levels that permit endothelial cell proliferation. This inhibition is associated with a reduction in Myc transcriptional

responses, including the Odc1 gene. Well-adjusted levels of these molecules are necessary to establish a cellular state that is capable of normal and continuous proliferation.

When Notch is inhibited this repression is released, leading to an increase in ERK phosphorylation, and the expression of Odc1 and other Myc related genes. This induces a fast completion of cell cycle due to the increase of pro-proliferative signals. However, it also leads to a blockade of cell proliferation as al ECs at the angiogenic front acquire the tip cell phenotype.

Nonetheless, our data shows that the effect of Notch is context dependent. In mature areas, which do not receive the same VEGF stimuli as angiogenic areas, Notch completely blocks cell cycle, not allowing the pro-mitogenic signals to reach the threshold required for cell cycle entry. When Notch is inhibited in these quiescent cells they reenter cell cycle, maybe permanently

On the other hand, excessive Notch activation or elimination of genes essential for cell cycle progression, like Myc and Odc1, induce the entry in a permanent non-proliferative state associated with high p21 expression. Cells in this state are not responsive to pro-mitogenic signals and are not able to proliferate even after Notch inhibition.

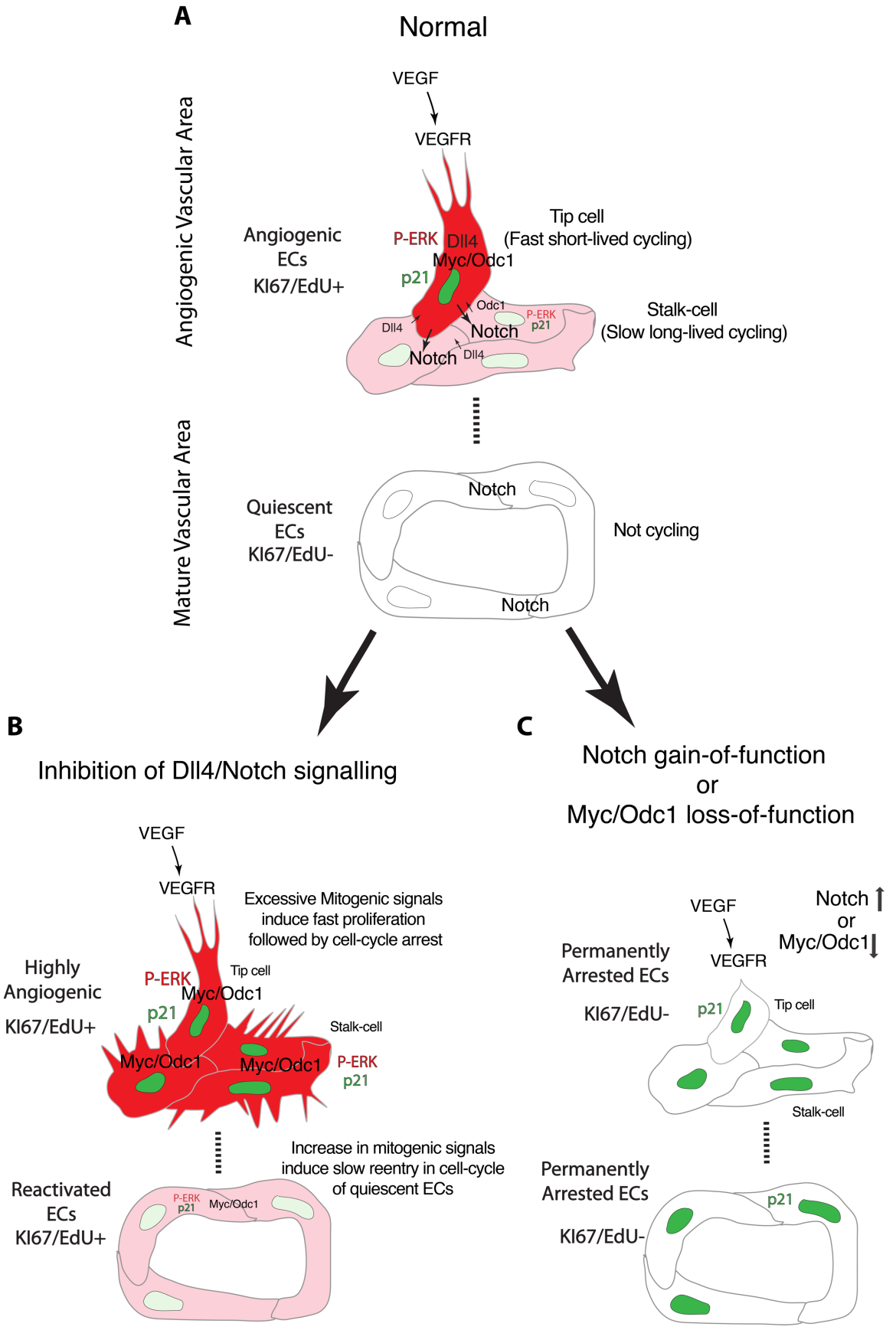
A
Normal
Angiogenic Vascular Area
VEGF
VEGFR
Angiogenic ECs KI67/EdU+
P-ERK
Dll4
Myc/Odc1
p21
Tip cell (Fast short-lived cycling)
Odc1
P-ERK
p21
Dll4
Notch
Notch
Dll4
Stalk-cell (Slow long-lived cycling)
Mature Vascular Area
Quiescent ECs KI67/EdU-
Notch
Notch
Not cycling
B
Inhibition of Dll4/Notch signalling
VEGF
VEGFR
Excessive Mitogenic signals induce fast proliferation followed by cell-cycle arrest
Highly Angiogenic KI67/EdU+
P-ERK
Myc/Odc1
p21
Tip cell
Stalk-cell
Myc/Odc1
Myc/Odc1
P-ERK
p21
Increase in mitogenic signals induce slow reentry in cell-cycle of quiescent ECs
Reactivated ECs KI67/EdU+
P-ERK
p21
Myc/Odc1
C
Notch gain-of-function
or
Myc/Odc1 loss-of-function
VEGF
VEGFR
Notch
or
Myc/Odc1
Permanently Arrested ECs
KI67/EdU-
p21
Tip cell
Stalk-cell
Permanently Arrested ECs
KI67/EdU-
p21

Figure 5.1. Summary of the data on the control of endothelial proliferation by Notch. Illustration showing the distinct angiogenic and mature vascular areas. Intensity of color and size of letter indicates strength of signal or expression. (**A)** At the angiogenic front, endothelial tip cells receive a higher stimulus provided by VEGF. This induces the high expression of Dll4 and ERK phosphorylation. Dll4 strongly activates Notch receptors on adjacent stalk endothelial cells. These cells also express Dll4 ligands, but at lower level, which leads to relatively weaker activation of Notch receptors in adjacent tip cells or other cells with higher Dll4. Higher Notch signaling in stalk-cells represses the transcription of Odc1, and attenuates the activation of ERK. This leads to a relatively slower, but longer-lived cell-cycle of stalk-cells, when compared with the adjacent tip cells, that have lower Notch signaling and cycle faster when they commit for proliferation. However, at the same time, many of these fast-cycling endothelial tip cells also have higher levels of p21, a cell senescence marker that can induce premature cell-cycle arrest of these highly angiogenic cells. Unlike stalk-cells, the majority of tip cells that experience high VEGF signaling exit cell-cycle (KI67-). Most ECs in the more mature vascular area already exited cell-cycle (KI67/EdU-), but still have active Notch signaling that is important to keep them quiescent. Compared with angiogenic ECs, these cells are exposed to less VEGF and have lower Odc1 expression, lower P-ERK levels and the p21 protein is undetectable. The large majority of these cells are in G0, but show no signs of senescence. (**B)** The blockade of Dll4/Notch signaling releases endothelial stalk-cells from the cell-to-cell lateral inhibition. After this pharmacological treatment, stalk-cells display a tip-cell like profile and upregulate the expression of Odc1 and pERK. This leads to a significant increase in the speed of EC proliferation, however, it also leads to upregulation of the cell cycle inhibitor p21 and premature cell-cycle exit. Impairment of Dll4/Notch in more mature and quiescent ECs produces a distinct effect. Here, the increase in P-ERK and Odc1 levels after Dll4/Notch inhibition induces cell-cycle reentry. **C)** Overactivation of Notch, or impairment of Odc1 or Myc function, in angiogenic ECs, induces a very strong cell-cycle arrest (KI67/EdU-), and most cells strongly and permanently upregulate p21.

CONCLUSIONS/ CONCLUSIONES

6 CONCLUSIONS

1. The dual ifgMosaic genetic strategy used to induce functional genetic mosaics allowed high resolution single-cell clonal analysis of EC proliferation during angiogenesis.
2. Physiological Notch activity during angiogenesis maintains angiogenic endothelial cells in a balanced proliferative state.
3. Angiogenic tip cells have a low proliferative capacity associated with high p21 expression and ERK phosphorylation.
4. Inhibition of Notch activity induces tip cell specification that is associated with accelerated cell cycle progression and premature cell cycle exit.
5. High VEGF signaling drives excessive ERK activation and arrests angiogenesis.
6. Balanced ERK activation during angiogenesis is required for normal cell cycle progression.
7. Physiological Notch activity represses the expression of genes involved in cell cycle progression during angiogenesis.
8. Odc1, an enzyme involved in polyamine metabolism, is regulated by Notch during angiogenesis and it is essential for normal EC proliferation and angiogenesis.
9. Myc is a strong regulator of Odc1 expression and required for the expansion of ECs
10. The cell cycle inhibitor p21 is induced by excessive mitogenic stimuli and arrests angiogenesis.
11. Activation of Notch or ablation of genes essential for cell-cycle progression induces strong p21 upregulation, which may lead to developmental cellular senescence.

7 CONCLUSIONES

1. La estrategia de modificación genética ifgMosaic dual para generar mosaicos funcionales permite realizar análisis clonal de la proliferación de células endoteliales durante angiogénesis con gran resolución.
2. La activación de Notch en niveles fisiológicos durante la angiogénesis mantiene a las células endoteliales en un estado proliferativo estable.
3. Las células *tip* angiogénicas tiene una capacidad proliferativa limitada asociada con elevados niveles de fosforilación de ERK y elevada expresión de p21..
4. La inhibición de la actividad de Notch promueve la especificación a células *tip*, que está asociada con una aceleración y posterior detención del ciclo celular.
5. Una alta activación de la vía de VEGF promueve la excesiva activación de ERK, bloqueando la angiogénesis.
6. El correcto avance a través del ciclo celular requiere de una activación controlada de ERK.
7. La activación de Notch reprime la expresión de genes que están implicados en el en el avance a través del ciclo celular.
8. La expresión de Odc1, una enzima relacionada con el metabolismo de poliaminas, está regulada por la activación de Notch y es esencial para mantener una proliferación normal durante la angiogénesis.
9. La proteína Myc es un potente regulador de Odc1 y es necesaria para la proliferación de células endoteliales
10. El inhibidor del ciclo celular p21 interviene en la detención de la angiogénesis inducida por un exceso de señales mitogénicas.
11. La activación de Notch o la eliminación de genes esenciales para la proliferación produce una fuerte sobreexpresión de p21, que podría conducir a un estado de senescencia celular.

BIBLIOGRAPHY

BIBLIOGRAPHY

de Alboran, I. M., O'Hagan, R. C., Gärtner, F., Malynn, B., Davidson, L., Rickert, R., Rajewsky, K., DePinho, R. A. and Alt, F. W. (2001) 'Analysis of C-MYC function in normal cells via conditional gene-targeted mutation.', *Immunity*, 14(1), pp. 45–55. doi: 10.1016/S1074-7613(01)00088-7.

Alm, K. and Oredsson, S. (2009) 'Cells and polyamines do it cyclically.', *Essays in biochemistry*, 46, pp. 63–76. doi: 10.1042/bse0460005.

Annibali, D., Whitfield, J. R., Favuzzi, E., Jauset, T., Serrano, E., Cuartas, I., Redondo-Campos, S., Folch, G., Gonzàlez-Juncà, A., Sodir, N. M., Massó-Vallés, D., Beaulieu, M.-E., Swigart, L. B., Mc Gee, M. M., Somma, M. P., Nasi, S., Seoane, J., Evan, G. I. and Soucek, L. (2014) 'Myc inhibition is effective against glioma and reveals a role for Myc in proficient mitosis.', *Nature communications*, 5(4632), p. 4632. doi: 10.1038/ncomms5632.

Auvinen, M., Paasinen, A., Andersson, L. C. and Hölttä, E. (1992) 'Ornithine decarboxylase activity is critical for cell transformation.', *Nature*, 360(6402), pp. 355–8. doi: 10.1038/360355a0.

Auvinen, M., Järvinen, K., Hotti, A., Okkeri, J., Laitinen, J., Jänne, O. A., Coffino, P., Bergman, M., Andersson, L. C., Alitalo, K. and Hölttä, E. (2003) 'Transcriptional regulation of the ornithine decarboxylase gene by c-Myc/Max/Mad network and retinoblastoma protein interacting with c-Myc.', *The international journal of biochemistry & cell biology*, 35(4), pp. 496–521. doi: 10.1016/S1357-2725(02)00305-9.

Balmanno, K. and Cook, S. J. (1999) 'Sustained MAP kinase activation is required for the expression of cyclin D1, p21Cip1 and a subset of AP-1 proteins in CCL39 cells.', *Oncogene*, 18(20), pp. 3085–97. doi: 10.1038/sj.onc.1202647.

Baudino, T. A., McKay, C., Pendeville-Samain, H., Nilsson, J. A., Maclean, K. H., White, E. L., Davis, A. C., Ihle, J. N. and Cleveland, J. L. (2002) 'c-Myc is essential for vasculogenesis and angiogenesis during development and tumor progression.', *Genes & development*, 16(19), pp. 2530–43. doi: 10.1101/gad.1024602.

Bello-Fernandez, C., Packham, G. and Cleveland, J. L. (1993) 'The ornithine decarboxylase gene is a transcriptional target of c-Myc.', *Proceedings of the National Academy of Sciences of the United States of America*, 90(16), pp. 7804–8.

Benedito, R., Roca, C., Sörensen, I., Adams, S., Gossler, A., Fruttiger, M. and Adams, R. H. (2009) 'The notch ligands Dll4 and Jagged1 have opposing effects on angiogenesis.', *Cell*, 137(6), pp. 1124–35. doi: 10.1016/j.cell.2009.03.025.

Benedito, R., Rocha, S. F., Woeste, M., Zamykal, M., Radtke, F., Casanovas, O., Duarte, A., Pytowski, B. and Adams, R. H. (2012) 'Notch-dependent VEGFR3 upregulation allows angiogenesis without VEGF-VEGFR2 signalling.', *Nature*, 484(7392), pp. 110–4. doi: 10.1038/nature10908.

Benedito, R. and Hellström, M. (2013) 'Notch as a hub for signaling in angiogenesis.', *Experimental cell research*, 319(9), pp. 1281–8. doi: 10.1016/j.yexcr.2013.01.010.

Bentley, K., Gerhardt, H. and Bates, P. A. (2008) 'Agent-based simulation of notch-mediated tip cell selection in angiogenic sprout initialisation.', *Journal of theoretical biology*, 250(1), pp. 25–36. doi: 10.1016/j.jtbi.2007.09.015.

Besson, A., Dowdy, S. F. and Roberts, J. M. (2008) 'CDK inhibitors: cell cycle regulators and beyond.', *Developmental cell*, 14(2), pp. 159–69. doi: 10.1016/j.devcel.2008.01.013.

Blanco, R. and Gerhardt, H. (2013) 'VEGF and Notch in tip and stalk cell selection.', *Cold Spring Harbor perspectives in medicine*, 3(1), p. a006569. doi: 10.1101/cshperspect.a006569.

Blanpain, C. and Simons, B. D. (2013) 'Unravelling stem cell dynamics by lineage tracing.', *Nature reviews. Molecular cell biology*. Nature Publishing Group, 14(8), pp. 489–502. doi: 10.1038/nrm3625.

Boward, B., Wu, T. and Dalton, S. (2016) 'Concise Review: Control of Cell Fate Through Cell Cycle and Pluripotency Networks.', *Stem cells (Dayton, Ohio)*, 34(6), pp. 1427–36. doi: 10.1002/stem.2345.

Bray, S. J. (2006) 'Notch signalling: a simple pathway becomes complex.', *Nature reviews. Molecular cell biology*, 7(9), pp. 678–89. doi: 10.1038/nrm2009.

Bray, S. J. (2016) 'Notch signalling in context.', *Nature reviews. Molecular cell biology*. Nature Publishing Group, 17(11), pp. 722–735. doi: 10.1038/nrm.2016.94.

Bretones, G., Delgado, M. D. and León, J. (2015) 'Myc and cell cycle control.', *Biochimica et biophysica acta*. Elsevier B.V., 1849(5), pp. 506–16. doi: 10.1016/j.bbagrm.2014.03.013.

Briscoe, J. and Small, S. (2015) 'Morphogen rules: design principles of gradient-mediated embryo patterning.', *Development (Cambridge, England)*, 142(23), pp. 3996–4009. doi: 10.1242/dev.129452.

Brugarolas, J., Chandrasekaran, C., Gordon, J. I., Beach, D., Jacks, T. and Hannon, G. J. (1995) 'Radiation-induced cell cycle arrest compromised by p21 deficiency.', *Nature*, 377(6549), pp. 552–7. doi: 10.1038/377552a0.

Buckingham, M. E. and Meilhac, S. M. (2011) 'Tracing cells for tracking cell lineage and clonal behavior.', *Developmental cell*, 21(3), pp. 394–409. doi: 10.1016/j.devcel.2011.07.019.

Burri, P. H., Hlushchuk, R. and Djonov, V. (2004) 'Intussusceptive angiogenesis: its emergence, its characteristics, and its significance.', *Developmental dynamics : an official publication of the American Association of Anatomists*, 231(3), pp. 474–88. doi: 10.1002/dvdy.20184.

Carmeliet, P., Ferreira, V., Breier, G., Pollefeyt, S., Kieckens, L., Gertsenstein, M., Fahrig, M., Vandenhoeck, A., Harpal, K., Eberhardt, C., Declercq, C., Pawling, J., Moons, L., Collen, D., Risau, W. and Nagy, A. (1996) 'Abnormal blood vessel development and lethality in embryos lacking a single VEGF allele.', *Nature*, 380(6573), pp. 435–9. doi: 10.1038/380435a0.

Carmeliet, P. and Jain, R. K. (2011) 'Molecular mechanisms and clinical applications of angiogenesis.', *Nature*, 473(7347), pp. 298–307. doi: 10.1038/nature10144.

Chambard, J.-C., Lefloch, R., Pouysségur, J. and Lenormand, P. (2007) 'ERK implication in cell cycle regulation.', *Biochimica et biophysica acta*, 1773(8), pp. 1299–310. doi: 10.1016/j.bbamcr.2006.11.010.

Chappell, J. C., Taylor, S. M., Ferrara, N. and Bautch, V. L. (2009) 'Local guidance of emerging vessel sprouts requires soluble Flt-1.', *Developmental cell*. Elsevier Ltd, 17(3), pp. 377–86. doi: 10.1016/j.devcel.2009.07.011.

Chevalier, C., Nicolas, J.-F. and Petit, A.-C. (2014) 'Preparation and delivery of 4-hydroxy-tamoxifen for clonal and polyclonal labeling of cells of the surface ectoderm, skin, and hair follicle.', *Methods in molecular biology (Clifton, N.J.)*, 1195(February), pp. 239–45. doi: 10.1007/7651_2013_63.

Chung, A. S. and Ferrara, N. (2011) 'Developmental and pathological angiogenesis.', *Annual review of cell and developmental biology*, 27, pp. 563–84. doi: 10.1146/annurev-cellbio-092910-154002.

Claesson-Welsh, L. (2016) 'VEGF receptor signal transduction - A brief update.', *Vascular pharmacology*. Elsevier B.V., 86(112), pp. 14–17. doi: 10.1016/j.vph.2016.05.011.

Coultas, L., Chawengsaksophak, K. and Rossant, J. (2005) 'Endothelial cells and VEGF in vascular development.', *Nature*, 438(7070), pp. 937–45. doi: 10.1038/nature04479.

Cuervo, H., Nielsen, C. M., Simonetto, D. A., Ferrell, L., Shah, V. H. and Wang, R. A. (2016) 'Endothelial notch signaling is essential to prevent hepatic vascular malformations in mice.', *Hepatology (Baltimore, Md.)*, 64(4), pp. 1302–1316. doi: 10.1002/hep.28713.

Daksis, J. I., Lu, R. Y., Facchini, L. M., Marhin, W. W. and Penn, L. J. (1994) 'Myc induces cyclin D1 expression in the absence of de novo protein synthesis and links mitogen-stimulated signal transduction to the cell cycle.', *Oncogene*, 9(12), pp. 3635–45.

Dang, C. V (2012) 'MYC on the path to cancer.', *Cell*, 149(1), pp. 22–35. doi: 10.1016/j.cell.2012.03.003.

Dosch, D. D. and Ballmer-Hofer, K. (2010) 'Transmembrane domain-mediated orientation of receptor monomers in active VEGFR-2 dimers.', *FASEB journal : official publication of the Federation of American Societies for Experimental Biology*, 24(1), pp. 32–8. doi: 10.1096/fj.09-132670.

Dou, G.-R., Wang, Y.-C., Hu, X.-B., Hou, L.-H., Wang, C.-M., Xu, J.-F., Wang, Y.-S., Liang, Y.-M., Yao, L.-B., Yang, A.-G. and Han, H. (2008) 'RBP-J, the transcription factor downstream of Notch receptors, is essential for the maintenance of vascular homeostasis in adult mice.', *FASEB journal : official publication of the Federation of American Societies for Experimental Biology*, 22(5), pp. 1606–17. doi: 10.1096/fj.07-9998com.

Drake, C. J. and Fleming, P. a (2000) 'Vasculogenesis in the day 6.5 to 9.5 mouse embryo.', *Blood*, 95(5), pp. 1671–9.

Duarte, A., Hirashima, M., Benedito, R., Trindade, A., Diniz, P., Bekman, E., Costa, L., Henrique, D. and Rossant, J. (2004) 'Dosage-sensitive requirement for mouse Dll4 in artery development.', *Genes & development*, 18(20), pp. 2474–8. doi: 10.1101/gad.1239004.

Dumont, D. J., Jussila, L., Taipale, J., Lymboussaki, A., Mustonen, T., Pajusola, K., Breitman, M. and Alitalo, K. (1998) 'Cardiovascular failure in mouse embryos deficient in VEGF receptor-3.', *Science (New York, N.Y.)*, 282(5390), pp. 946–9. doi: 10.1126/science.282.5390.946.

Ehling, M., Adams, S., Benedito, R. and Adams, R. H. (2013) 'Notch controls retinal blood vessel maturation and quiescence.', *Development (Cambridge, England)*, 140(14), pp. 3051–61. doi: 10.1242/dev.093351.

Ellertsdóttir, E., Lenard, A., Blum, Y., Krudewig, A., Herwig, L., Affolter, M. and Belting, H.-G. (2010) 'Vascular morphogenesis in the zebrafish embryo.', *Developmental biology*, 341(1), pp. 56–65. doi: 10.1016/j.ydbio.2009.10.035.

Feraud, O., Cao, Y. and Vittet, D. (2001) 'Embryonic stem cell-derived embryoid bodies development in collagen gels recapitulates sprouting angiogenesis.', *Laboratory investigation; a journal of technical methods and pathology*, 81(12), pp. 1669–81. doi: 10.1038/labinvest.3780380.

Ferrara, N., Carver-Moore, K., Chen, H., Dowd, M., Lu, L., O'Shea, K. S., Powell-Braxton, L., Hillan, K. J. and Moore, M. W. (1996) 'Heterozygous embryonic lethality induced by targeted inactivation of the VEGF gene.', *Nature*, 380(6573), pp. 439–42. doi: 10.1038/380439a0.

Fong, G. H., Rossant, J., Gertsenstein, M. and Breitman, M. L. (1995) 'Role of the Flt-1 receptor tyrosine kinase in regulating the assembly of vascular endothelium.', *Nature*, 376(6535), pp. 66–70. doi: 10.1038/376066a0.

Fruttiger, M. (2007) 'Development of the retinal vasculature.', *Angiogenesis*, 10(2), pp. 77–88. doi: 10.1007/s10456-007-9065-1.

Funahashi, Y., Shawber, C. J., Vorontchikhina, M., Sharma, A., Outtz, H. H. and Kitajewski, J. (2010) 'Notch regulates the angiogenic response via induction of VEGFR-1.', *Journal of angiogenesis research*, 2(1), p. 3. doi: 10.1186/2040-2384-2-3.

George, S. H. L., Gertsenstein, M., Vintersten, K., Korets-Smith, E., Murphy, J., Stevens, M. E., Haigh, J. J. and Nagy, A. (2007) 'Developmental and adult phenotyping directly from mutant embryonic stem cells.', *Proceedings of the National Academy of Sciences of the United States of America*, 104(11), pp. 4455–60. doi: 10.1073/pnas.0609277104.

Gerhardt, H., Golding, M., Fruttiger, M., Ruhrberg, C., Lundkvist, A., Abramsson, A., Jeltsch, M., Mitchell, C., Alitalo, K., Shima, D. and Betsholtz, C. (2003) 'VEGF guides angiogenic sprouting utilizing endothelial tip cell filopodia.', *The Journal of cell biology*, 161(6), pp. 1163–77. doi: 10.1083/jcb.200302047.

Gille, H., Kowalski, J., Li, B., LeCouter, J., Moffat, B., Zioncheck, T. F., Pelletier, N. and Ferrara, N. (2001) 'Analysis of biological effects and signaling properties of Flt-1 (VEGFR-1) and KDR (VEGFR-2). A reassessment using novel receptor-specific vascular endothelial growth factor mutants.', *The Journal of biological chemistry*, 276(5), pp. 3222–30. doi: 10.1074/jbc.M002016200.

Gridley, T. (2010) 'Notch signaling in the vasculature.', *Current topics in developmental biology*, 92(10), pp. 277–309. doi: 10.1016/S0070-2153(10)92009-7.

Guerra, C., Mijimolle, N., Dhawahir, A., Dubus, P., Barradas, M., Serrano, M., Campuzano, V. and Barbacid, M. (2003) 'Tumor induction by an endogenous K-ras oncogene is highly dependent on cellular context.', *Cancer cell*, 4(2), pp. 111–20. doi: 10.1016/S1535-6108(03)00191-0.

Harashima, H., Dissmeyer, N. and Schnittger, A. (2013) 'Cell cycle control across the eukaryotic kingdom.', *Trends in cell biology*. Elsevier Ltd, 23(7), pp. 345–56. doi: 10.1016/j.tcb.2013.03.002.

Harrington, L. S., Sainson, R. C. A., Williams, C. K., Taylor, J. M., Shi, W., Li, J.-L. and Harris, A. L. (2008) 'Regulation of multiple angiogenic pathways by Dll4 and Notch in human umbilical vein endothelial cells.', *Microvascular research*, 75(2), pp. 144–54. doi: 10.1016/j.mvr.2007.06.006.

Hasan, S. S., Tsaryk, R., Lange, M., Wisniewski, L., Moore, J. C., Lawson, N. D., Wojciechowska, K., Schnittler, H. and Siekmann, A. F. (2017) 'Endothelial Notch signalling limits angiogenesis via control of artery formation.', *Nature cell biology*, 19(8), pp. 928–940. doi: 10.1038/ncb3574.

Heisig, J., Weber, D., Englberger, E., Winkler, A., Kneitz, S., Sung, W.-K., Wolf, E., Eilers, M., Wei, C.-L. and Gessler, M. (2012) 'Target gene analysis by microarrays and chromatin immunoprecipitation identifies HEY proteins as highly redundant bHLH repressors.', *PLoS genetics*, 8(5), p. e1002728. doi: 10.1371/journal.pgen.1002728.

Hellström, M., Phng, L.-K., Hofmann, J. J., Wallgard, E., Coultas, L., Lindblom, P., Alva, J., Nilsson, A.-K., Karlsson, L., Gaiano, N., Yoon, K., Rossant, J., Iruela-Arispe, M. L., Kalén, M., Gerhardt, H. and Betsholtz, C. (2007) 'Dll4 signalling through Notch1 regulates formation of tip cells during angiogenesis.', *Nature*, 445(7129), pp. 776–80. doi: 10.1038/nature05571.

Hirashima, M., Kataoka, H., Nishikawa, S., Matsuyoshi, N. and Nishikawa, S. (1999) 'Maturation of embryonic stem cells into endothelial cells in an in vitro model of vasculogenesis.', *Blood*, 93(4), pp. 1253–63.

Iso, T., Kedes, L. and Hamamori, Y. (2003) 'HES and HERP families: multiple effectors of the Notch signaling pathway.', *Journal of cellular physiology*, 194(3), pp. 237–55. doi: 10.1002/jcp.10208.

Jakobsson, L., Franco, C. a, Bentley, K., Collins, R. T., Ponsioen, B., Aspalter, I. M., Rosewell, I., Busse, M., Thurston, G., Medvinsky, A., Schulte-Merker, S. and Gerhardt, H. (2010) 'Endothelial cells dynamically compete for the tip cell position during angiogenic sprouting.', *Nature cell biology*. Nature Publishing Group, 12(10), pp. 943–53. doi: 10.1038/ncb2103.

Kahana, C. (2009) 'Regulation of cellular polyamine levels and cellular proliferation by antizyme and antizyme inhibitor.', *Essays in biochemistry*, 46, pp. 47–61. doi: 10.1042/bse0460004.

Kaldis, P. and Richardson, H. E. (2012) 'When cell cycle meets development.', *Development (Cambridge, England)*, 139(2), pp. 225–30. doi: 10.1242/dev.073288.

Kearney, J. B., Kappas, N. C., Ellerstrom, C., DiPaola, F. W. and Bautch, V. L. (2004) 'The VEGF receptor flt-1 (VEGFR-1) is a positive modulator of vascular sprout formation and branching morphogenesis.', *Blood*, 103(12), pp. 4527–35. doi: 10.1182/blood-2003-07-2315.

Kisanuki, Y. Y., Hammer, R. E., Miyazaki, J., Williams, S. C., Richardson, J. a and Yanagisawa, M. (2001) 'Tie2-Cre transgenic mice: a new model for endothelial cell-lineage analysis in vivo.', *Developmental biology*, 230(2), pp. 230–42. doi: 10.1006/dbio.2000.0106.

Kopan, R. and Ilagan, M. X. G. (2009) 'The canonical Notch signaling pathway: unfolding the activation mechanism.', *Cell*, 137(2), pp. 216–33. doi: 10.1016/j.cell.2009.03.045.

Kramer, D. L., Chang, B. D., Chen, Y., Diegelman, P., Alm, K., Black, A. R., Roninson, I. B. and Porter, C. W. (2001) 'Polyamine depletion in human melanoma cells leads to G1 arrest associated with induction of p21WAF1/CIP1/SDI1, changes in the expression of p21-regulated genes, and a senescence-like phenotype.', *Cancer research*, 61(21), pp. 7754–62.

Kranz, A., Fu, J., Duerschke, K., Weidlich, S., Naumann, R., Stewart, A. F. and Anastassiadis, K. (2010) 'An improved Flp deleter mouse in C57Bl/6 based on Flpo recombinase.', *Genesis (New York, N.Y. : 2000)*, 48(8), pp. 512–20. doi: 10.1002/dvg.20641.

Krebs, L. T., Xue, Y., Norton, C. R., Shutter, J. R., Maguire, M., Sundberg, J. P., Gallahan, D., Closson, V., Kitajewski, J., Callahan, R., Smith, G. H., Stark, K. L. and Gridley, T. (2000) 'Notch signaling is essential for vascular morphogenesis in mice.', *Genes & development*, 14(11), pp. 1343–52. doi: 10.1101/gad.14.11.1343.

Krebs, L. T., Shutter, J. R., Tanigaki, K., Honjo, T., Stark, K. L. and Gridley, T. (2004) 'Haploinsufficient lethality and formation of arteriovenous malformations in Notch pathway mutants.', *Genes & development*, 18(20), pp. 2469–73. doi: 10.1101/gad.1239204.

Kretzschmar, K. and Watt, F. M. (2012) 'Lineage tracing.', *Cell*. Elsevier Inc., 148(1–2), pp. 33–45. doi: 10.1016/j.cell.2012.01.002.

Krock, B. L., Skuli, N. and Simon, M. C. (2011) 'Hypoxia-induced angiogenesis: good and evil.', *Genes & cancer*, 2(12), pp. 1117–33. doi: 10.1177/1947601911423654.

Krueger, J., Liu, D., Scholz, K., Zimmer, A., Shi, Y., Klein, C., Siekmann, A., Schulte-Merker, S., Cudmore, M., Ahmed, A. and le Noble, F. (2011) 'Flt1 acts as a negative regulator of tip cell formation and branching morphogenesis in the zebrafish embryo.', *Development (Cambridge, England)*, 138(10), pp. 2111–20. doi: 10.1242/dev.063933.

Lawson, N. D., Scheer, N., Pham, V. N., Kim, C. H., Chitnis, a B., Campos-Ortega, J. a and Weinstein, B. M. (2001) 'Notch signaling is required for arterial-venous differentiation during embryonic vascular development.', *Development (Cambridge, England)*, 128(19), pp. 3675–83.

Leslie, J. D., Ariza-McNaughton, L., Bermange, A. L., McAdow, R., Johnson, S. L. and Lewis, J. (2007) 'Endothelial signalling by the Notch ligand Delta-like 4 restricts angiogenesis.', *Development (Cambridge, England)*, 134(5), pp. 839–44. doi: 10.1242/dev.003244.

Liang, D., Xu, X., Chin, A. J., Balasubramaniyan, N. V, Teo, M. A. L., Lam, T. J., Weinberg, E. S. and Ge, R. (1998) 'Cloning and characterization of vascular endothelial growth factor (VEGF) from zebrafish, Danio rerio.', *Biochimica et biophysica acta*, 1397(1), pp. 14–20. doi: 10.1016/S0167-4781(97)00233-9.

Limbourg, A., Ploom, M., Elligsen, D., Sörensen, I., Ziegelhoeffer, T., Gossler, A., Drexler, H. and Limbourg, F. P. (2007) 'Notch ligand Delta-like 1 is essential for postnatal arteriogenesis.', *Circulation research*, 100(3), pp. 363–71. doi: 10.1161/01.RES.0000258174.77370.2c.

Limbourg, F. P., Takeshita, K., Radtke, F., Bronson, R. T., Chin, M. T. and Liao, J. K. (2005) 'Essential role of endothelial Notch1 in angiogenesis.', *Circulation*, 111(14), pp. 1826–32. doi: 10.1161/01.CIR.0000160870.93058.DD.

Liu, J., Willet, S. G., Bankaitis, E. D., Xu, Y., Wright, C. V. E. and Gu, G. (2013) 'Non-parallel recombination limits Cre-LoxP-based reporters as precise indicators of conditional genetic manipulation.', *Genesis (New York, N.Y. : 2000)*, 51(6), pp. 436–42. doi: 10.1002/dvg.22384.

Liu, Z., Shirakawa, T., Li, Y., Soma, A., Oka, M., Dotto, G. P., Fairman, R. M., Velazquez, O. C. and Herlyn, M. (2003) 'Regulation of Notch1 and Dll4 by vascular endothelial growth factor in arterial endothelial cells: implications for modulating arteriogenesis and angiogenesis.', *Molecular and cellular biology*, 23(1), pp. 14–25. doi: 10.1128/MCB.23.1.14.

Livet, J., Weissman, T. a, Kang, H., Draft, R. W., Lu, J., Bennis, R. a, Sanes, J. R. and Lichtman, J. W. (2007) 'Transgenic strategies for combinatorial expression of fluorescent proteins in the nervous system.', *Nature*, 450(7166), pp. 56–62. doi: 10.1038/nature06293.

Lobov, I. B., Renard, R. A., Papadopoulos, N., Gale, N. W., Thurston, G., Yancopoulos, G. D. and Wiegand, S. J. (2007) 'Delta-like ligand 4 (Dll4) is induced by VEGF as a negative regulator of angiogenic sprouting.', *Proceedings of the National Academy of Sciences of the United States of America*, 104(9), pp. 3219–24. doi: 10.1073/pnas.0611206104.

Long, M. A. and Rossi, F. M. V (2009) 'Silencing inhibits Cre-mediated recombination of the Z/AP and Z/EG reporters in adult cells.', *PloS one*, 4(5), p. e5435. doi: 10.1371/journal.pone.0005435.

Louvi, A. and Artavanis-Tsakonas, S. (2006) 'Notch signalling in vertebrate neural development.', *Nature reviews. Neuroscience*, 7(2), pp. 93–102. doi: 10.1038/nrn1847.

Madisen, L., Zwingman, T. A., Sunkin, S. M., Oh, S. W., Zariwala, H. A., Gu, H., Ng, L. L., Palmiter, R. D., Hawrylycz, M. J., Jones, A. R., Lein, E. S. and Zeng, H. (2010) 'A robust and high-throughput Cre reporting and characterization system for the whole mouse brain.', *Nature neuroscience*. Nature Publishing Group, 13(1), pp. 133–40. doi: 10.1038/nn.2467.

Maillard, I., Weng, A. P., Carpenter, A. C., Rodriguez, C. G., Sai, H., Xu, L., Allman, D., Aster, J. C. and Pear, W. S. (2004) 'Mastermind critically regulates Notch-mediated lymphoid cell fate decisions.', *Blood*, 104(6), pp. 1696–702. doi: 10.1182/blood-2004-02-0514.

Marcelo, K. L., Goldie, L. C. and Hirschi, K. K. (2013) 'Regulation of endothelial cell differentiation and specification.', *Circulation research*, 112(9), pp. 1272–87. doi: 10.1161/CIRCRESAHA.113.300506.

Mavria, G., Vercoulen, Y., Yeo, M., Paterson, H., Karasarides, M., Marais, R., Bird, D. and Marshall, C. J. (2006) 'ERK-MAPK signaling opposes Rho-kinase to promote endothelial cell survival and sprouting during angiogenesis.', *Cancer cell*, 9(1), pp. 33–44. doi: 10.1016/j.ccr.2005.12.021.

Milde, F., Lauw, S., Koumoutsakos, P. and Iruela-Arispe, M. L. (2013) 'The mouse retina in 3D: quantification of vascular growth and remodeling.', *Integrative biology : quantitative biosciences from nano to macro*, 5(12), pp. 1426–38. doi: 10.1039/c3ib40085a.

Muñoz-Chápuli, R. and Pérez-Pomares, J. M. (2010) 'Origin of the Vertebrate Endothelial Cell Lineage', in *Heart Development and Regeneration*. Elsevier, pp. 465–486. doi: 10.1016/B978-0-12-381332-9.00022-0.

Muñoz-Espín, D., Cañamero, M., Maraver, A., Gómez-López, G., Contreras, J., Murillo-Cuesta, S., Rodríguez-Baeza, A., Varela-Nieto, I., Ruberte, J., Collado, M. and Serrano, M. (2013) 'Programmed cell senescence during mammalian embryonic development.', *Cell*, 155(5), pp. 1104–18. doi: 10.1016/j.cell.2013.10.019.

Murtaugh, L. C., Stanger, B. Z., Kwan, K. M. and Melton, D. A. (2003) 'Notch signaling controls multiple steps of pancreatic differentiation.', *Proceedings of the National Academy of Sciences of the United States of America*, 100(25), pp. 14920–5. doi: 10.1073/pnas.2436557100.

Nasizadeh, S., Myhre, L., Thiman, L., Alm, K., Oredsson, S. and Persson, L. (2005) 'Importance of polyamines in cell cycle kinetics as studied in a transgenic system.', *Experimental cell research*, 308(2), pp. 254–64. doi: 10.1016/j.yexcr.2005.04.027.

Nicoli, S., Knyphausen, C.-P., Zhu, L. J., Lakshmanan, A. and Lawson, N. D. (2012) 'miR-221 is required for endothelial tip cell behaviors during vascular development.', *Developmental cell*. Elsevier Inc., 22(2), pp. 418–29. doi: 10.1016/j.devcel.2012.01.008.

Nilsson, J. A., Keller, U. B., Baudino, T. A., Yang, C., Norton, S., Old, J. A., Nilsson, L. M., Neale, G., Kramer, D. L., Porter, C. W. and Cleveland, J. L. (2005) 'Targeting ornithine decarboxylase in Myc-induced lymphomagenesis prevents tumor formation.', *Cancer cell*, 7(5), pp. 433–44. doi: 10.1016/j.ccr.2005.03.036.

Noguera-Troise, I., Daly, C., Papadopoulos, N. J., Coetzee, S., Boland, P., Gale, N. W., Lin, H. C., Yancopoulos, G. D. and Thurston, G. (2006) 'Blockade of Dll4 inhibits tumour growth by promoting non-productive angiogenesis.', *Nature*, 444(7122), pp. 1032–7. doi: 10.1038/nature05355.

Noseda, M., Chang, L., McLean, G., Grim, J. E., Clurman, B. E., Smith, L. L. and Karsan, A. (2004) 'Notch activation induces endothelial cell cycle arrest and participates in contact inhibition: role of p21Cip1 repression.', *Molecular and cellular biology*, 24(20), pp. 8813–22. doi: 10.1128/MCB.24.20.8813-8822.2004.

Oellerich, M. F. and Potente, M. (2012) 'FOXOs and sirtuins in vascular growth, maintenance, and aging.', *Circulation research*, 110(9), pp. 1238–51. doi: 10.1161/CIRCRESAHA.111.246488.

Ohnuma, S. and Harris, W. A. (2003) 'Neurogenesis and the cell cycle.', *Neuron*, 40(2), pp. 199–208. doi: 10.1016/S0896-6273(03)00632-9.

Okabe, K., Kobayashi, S., Yamada, T., Kurihara, T., Tai-Nagara, I., Miyamoto, T., Mukouyama, Y., Sato, T. N., Suda, T., Ema, M. and Kubota, Y. (2014) 'Neurons limit angiogenesis by titrating VEGF in retina.', *Cell*. Elsevier Inc., 159(3), pp. 584–96. doi: 10.1016/j.cell.2014.09.025.

Olsson, A.-K., Dimberg, A., Kreuger, J. and Claesson-Welsh, L. (2006) 'VEGF receptor signalling - in control of vascular function.', *Nature reviews. Molecular cell biology*, 7(5), pp. 359–71. doi: 10.1038/nrm1911.

Oredsson, S. M. (2003) 'Polyamine dependence of normal cell-cycle progression.', *Biochemical Society transactions*, 31(2), pp. 366–70. doi: 10.1042/.

Papadopoulos, N., Martin, J., Ruan, Q., Rafique, A., Rosconi, M. P., Shi, E., Pyles, E. A., Yancopoulos, G. D., Stahl, N. and Wiegand, S. J. (2012) 'Binding and neutralization of vascular endothelial growth factor (VEGF) and related ligands by VEGF Trap, ranibizumab and bevacizumab.', *Angiogenesis*, 15(2), pp. 171–85. doi: 10.1007/s10456-011-9249-6.

Phng, L.-K., Potente, M., Leslie, J. D., Babbage, J., Nyqvist, D., Lobov, I., Ondr, J. K., Rao, S., Lang, R. A., Thurston, G. and Gerhardt, H. (2009) 'Nrarp coordinates endothelial Notch and Wnt signaling to control vessel density in angiogenesis.', *Developmental cell*, 16(1), pp. 70–82. doi: 10.1016/j.devcel.2008.12.009.

Pitulescu, M. E., Schmidt, I., Benedito, R. and Adams, R. H. (2010) 'Inducible gene targeting in the neonatal vasculature and analysis of retinal angiogenesis in mice.', *Nature protocols*. Nature Publishing Group, 5(9), pp. 1518–34. doi: 10.1038/nprot.2010.113.

Pitulescu, M. E., Schmidt, I., Giaimo, B. D., Antoine, T., Berkenfeld, F., Ferrante, F., Park, H., Ehling, M., Biljes, D., Rocha, S. F., Langen, U. H., Stehling, M., Nagasawa, T., Ferrara, N., Borggrefe, T. and Adams, R. H. (2017) 'Dll4 and Notch signalling couples sprouting angiogenesis and artery formation', *Nature Cell Biology*, 19(8), pp. 915–927. doi: 10.1038/ncb3555.

Pontes-Quero, S., Heredia, L., Casquero-García, V., Fernández-Chacón, M., Luo, W., Hermoso, A., Bansal, M., Garcia-Gonzalez, I., Sanchez-Muñoz, M. S., Perea, J. R., Galiana-Simal, A., Rodriguez-Arabaolaza, I., Del Olmo-Cabrera, S., Rocha, S. F., Criado-Rodriguez, L. M., Giovinazzo, G. and Benedito, R. (2017) 'Dual ifgMosaic: A Versatile Method for Multispectral and Combinatorial Mosaic Gene-Function Analysis.', *Cell*, 170(4), p. 800–814.e18. doi: 10.1016/j.cell.2017.07.031.

Potente, M., Gerhardt, H. and Carmeliet, P. (2011) 'Basic and therapeutic aspects of angiogenesis.', *Cell*. Elsevier Inc., 146(6), pp. 873–87. doi: 10.1016/j.cell.2011.08.039.

Potente, M. and Mäkinen, T. (2017) 'Vascular heterogeneity and specialization in development and disease.', *Nature reviews. Molecular cell biology*. Nature Publishing Group, 18(8), pp. 477–494. doi: 10.1038/nrm.2017.36.

Pumiglia, K. M. and Decker, S. J. (1997) 'Cell cycle arrest mediated by the MEK/mitogen-activated protein kinase pathway.', *Proceedings of the National Academy of Sciences of the United States of America*, 94(2), pp. 448–52. doi: 10.1073/pnas.94.2.448.

Quillien, A., Moore, J. C., Shin, M., Siekmann, A. F., Smith, T., Pan, L., Moens, C. B., Parsons, M. J. and Lawson, N. D. (2014) 'Distinct Notch signaling outputs pattern the developing arterial system.', *Development (Cambridge, England)*, 141(7), pp. 1544–52. doi: 10.1242/dev.099986.

Rafii, S., Butler, J. M. and Ding, B.-S. (2016) 'Angiocrine functions of organ-specific endothelial cells.', *Nature*, 529(7586), pp. 316–25. doi: 10.1038/nature17040.

Rhind, N. and Russell, P. (2012) 'Signaling pathways that regulate cell division.', *Cold Spring Harbor perspectives in biology*, 4(10), pp. a005942–a005942. doi: 10.1101/cshperspect.a005942.

Ridgway, J., Zhang, G., Wu, Y., Stawicki, S., Liang, W.-C., Chanthery, Y., Kowalski, J., Watts, R. J., Callahan, C., Kasman, I., Singh, M., Chien, M., Tan, C., Hongo, J.-A. S., de Sauvage, F., Plowman, G. and Yan, M. (2006) 'Inhibition of Dll4 signalling inhibits tumour growth by deregulating angiogenesis.', *Nature*, 444(7122), pp. 1083–7. doi: 10.1038/nature05313.

Risau, W. (1997) 'Mechanisms of angiogenesis.', *Nature*, 386(6626), pp. 671–4. doi: 10.1038/386671a0.

Risau, W. and Flamme, I. (1995) 'Vasculogenesis.', *Annual review of cell and developmental biology*, 11, pp. 73–91. doi: 10.1146/annurev.cb.11.110195.000445.

Rocha, S. F., Schiller, M., Jing, D., Li, H., Butz, S., Vestweber, D., Biljes, D., Drexler, H. C. a, Nieminen-Kelhä, M., Vajkoczy, P., Adams, S., Benedito, R. and Adams, R. H. (2014) 'Esm1 modulates endothelial tip cell behavior and vascular permeability by enhancing VEGF bioavailability.', *Circulation research*, 115(6), pp. 581–90. doi: 10.1161/CIRCRESAHA.115.304718.

Rodríguez, J., Calvo, F., González, J. M., Casar, B., Andrés, V. and Crespo, P. (2010) 'ERK1/2 MAP kinases promote cell cycle entry by rapid, kinase-independent disruption of retinoblastoma-lamin A complexes.', *The Journal of cell biology*, 191(5), pp. 967–79. doi: 10.1083/jcb.201004067.

Ruhrberg, C., Gerhardt, H., Golding, M., Watson, R., Ioannidou, S., Fujisawa, H., Betsholtz, C. and Shima, D. T. (2002) 'Spatially restricted patterning cues provided by heparin-binding VEGF-A control blood vessel branching morphogenesis.', *Genes & development*, 16(20), pp. 2684–98. doi: 10.1101/gad.242002.

Ruijtenberg, S. and van den Heuvel, S. (2016) 'Coordinating cell proliferation and differentiation: Antagonism between cell cycle regulators and cell type-specific gene expression.', *Cell cycle (Georgetown, Tex.)*. Taylor & Francis, 15(2), pp. 196–212. doi: 10.1080/15384101.2015.1120925.

Sakurai, Y., Ohgimoto, K., Kataoka, Y., Yoshida, N. and Shibuya, M. (2005) 'Essential role of Flk-1 (VEGF receptor 2) tyrosine residue 1173 in vasculogenesis in mice.', *Proceedings of the National Academy of Sciences of the United States of America*, 102(4), pp. 1076–81. doi: 10.1073/pnas.0404984102.

Schindelin, J., Arganda-Carreras, I., Frise, E., Kaynig, V., Longair, M., Pietzsch, T., Preibisch, S., Rueden, C., Saalfeld, S., Schmid, B., Tinevez, J.-Y., White, D. J., Hartenstein, V., Eliceiri, K., Tomancak, P. and Cardona, A. (2012) 'Fiji: an open-source platform for biological-image analysis.', *Nature methods*, 9(7), pp. 676–82. doi: 10.1038/nmeth.2019.

Scott, A., Powner, M. B., Gandhi, P., Clarkin, C., Gutmann, D. H., Johnson, R. S., Ferrara, N. and Fruttiger, M. (2010) 'Astrocyte-derived vascular endothelial growth factor stabilizes vessels in the developing retinal vasculature.', *PloS one*, 5(7), p. e11863. doi: 10.1371/journal.pone.0011863.

Serra, H., Chivite, I., Angulo-Urarte, A., Soler, A., Sutherland, J. D., Arruabarrena-Aristorena, A., Ragab, A., Lim, R., Malumbres, M., Fruttiger, M., Potente, M., Serrano, M., Fabra, À., Viñals, F., Casanovas, O., Pandolfi, P. P., Bigas, A., Carracedo, A., Gerhardt, H., *et al.* (2015) 'PTEN mediates Notch-dependent stalk cell arrest in angiogenesis.', *Nature communications*, 6(Mdc), p. 7935. doi: 10.1038/ncomms8935.

Seth, A., Alvarez, E., Gupta, S. and Davis, R. J. (1991) 'A phosphorylation site located in the NH2-terminal domain of c-Myc increases transactivation of gene expression.', *The Journal of biological chemistry*, 266(35), pp. 23521–4.

Sewing, A., Wiseman, B., Lloyd, A. C. and Land, H. (1997) 'High-intensity Raf signal causes cell cycle arrest mediated by p21Cip1.', *Molecular and cellular biology*, 17(9), pp. 5588–97.

Shalaby, F., Rossant, J., Yamaguchi, T. P., Gertsenstein, M., Wu, X. F., Breitman, M. L. and Schuh, A. C. (1995) 'Failure of blood-island formation and vasculogenesis in Flk-1-deficient mice.', *Nature*, 376(6535), pp. 62–6. doi: 10.1038/376062a0.

Sharma, P., Yan, F., Doronina, V. A., Escuin-Ordinas, H., Ryan, M. D. and Brown, J. D. (2012) '2A peptides provide distinct solutions to driving stop-carry on translational recoding.', *Nucleic acids research*, 40(7), pp. 3143–51. doi: 10.1093/nar/gkr1176.

Shawber, C. J., Funahashi, Y., Francisco, E., Vorontchikhina, M., Kitamura, Y., Stowell, S. A., Borisenko, V., Feirt, N., Podgrabinska, S., Shiraishi, K., Chawengsaksophak, K., Rossant, J., Accili, D., Skobe, M. and Kitajewski, J. (2007) 'Notch alters VEGF responsiveness in human and murine endothelial cells by direct regulation of VEGFR-3 expression.', *The Journal of clinical investigation*, 117(11), pp. 3369–82. doi: 10.1172/JCI24311.

Shin, M., Beane, T. J., Quillien, A., Male, I., Zhu, L. J. and Lawson, N. D. (2016) 'Vegfa signals through ERK to promote angiogenesis, but not artery differentiation.', *Development (Cambridge, England)*, 143(20), pp. 3796–3805. doi: 10.1242/dev.137919.

Siekmann, A. F., Affolter, M. and Belting, H.-G. (2013) 'The tip cell concept 10 years after: new players tune in for a common theme.', *Experimental cell research*. Elsevier, 319(9), pp. 1255–63. doi: 10.1016/j.yexcr.2013.01.019.

Siekmann, A. F., Covassin, L. and Lawson, N. D. (2008) 'Modulation of VEGF signalling output by the Notch pathway.', *BioEssays : news and reviews in molecular, cellular and developmental biology*, 30(4), pp. 303–13. doi: 10.1002/bies.20736.

Siekmann, A. F. and Lawson, N. D. (2007) 'Notch signalling limits angiogenic cell behaviour in developing zebrafish arteries.', *Nature*, 445(7129), pp. 781–4. doi: 10.1038/nature05577.

Simons, M., Gordon, E. and Claesson-Welsh, L. (2016) 'Mechanisms and regulation of endothelial VEGF receptor signalling.', *Nature reviews. Molecular cell biology*. Nature Publishing Group, 17(10), pp. 611–25. doi: 10.1038/nrm.2016.87.

Snippert, H. J., van der Flier, L. G., Sato, T., van Es, J. H., van den Born, M., Kroon-Veenboer, C., Barker, N., Klein, A. M., van Rheenen, J., Simons, B. D. and Clevers, H. (2010) 'Intestinal crypt homeostasis results from neutral competition between symmetrically dividing Lgr5 stem cells.', *Cell*. Elsevier Ltd, 143(1), pp. 134–44. doi: 10.1016/j.cell.2010.09.016.

Sörensen, I., Adams, R. H. and Gossler, A. (2009) 'DLL1-mediated Notch activation regulates endothelial identity in mouse fetal arteries.', *Blood*, 113(22), pp. 5680–8. doi: 10.1182/blood-2008-08-174508.

Srinivas, S., Watanabe, T., Lin, C. S., William, C. M., Tanabe, Y., Jessell, T. M. and Costantini, F. (2001) 'Cre reporter strains produced by targeted insertion of EYFP and ECFP into the ROSA26 locus.', *BMC developmental biology*, 1, p. 4. doi: 10.1186/1471-213X-1-4.

Srinivasan, R., Zabuawala, T., Huang, H., Zhang, J., Gulati, P., Fernandez, S., Karlo, J. C., Landreth, G. E., Leone, G. and Ostrowski, M. C. (2009) 'Erk1 and Erk2 regulate endothelial cell proliferation and migration during mouse embryonic angiogenesis.', *PloS one*, 4(12), p. e8283. doi: 10.1371/journal.pone.0008283.

Stahl, A., Connor, K. M., Sapieha, P., Chen, J., Dennison, R. J., Krah, N. M., Seaward, M. R., Willett, K. L., Aderman, C. M., Guerin, K. I., Hua, J., Löfqvist, C., Hellström, A. and Smith, L. E. H. (2010) 'The mouse retina as an angiogenesis model.', *Investigative ophthalmology & visual science*, 51(6), pp. 2813–26. doi: 10.1167/iovs.10-5176.

Stone, J., Itin, A., Alon, T., Pe'er, J., Gnessin, H., Chan-Ling, T. and Keshet, E. (1995) 'Development of retinal vasculature is mediated by hypoxia-induced vascular endothelial growth factor (VEGF) expression by neuroglia.', *The Journal of neuroscience : the official journal of the Society for Neuroscience*, 15(7 Pt 1), pp. 4738–47.

Strasser, G. A., Kaminker, J. S. and Tessier-Lavigne, M. (2010) 'Microarray analysis of retinal endothelial tip cells identifies CXCR4 as a mediator of tip cell morphology and branching.', *Blood*, 115(24), pp. 5102–10. doi: 10.1182/blood-2009-07-230284.

Suchting, S., Freitas, C., le Noble, F., Benedito, R., Bréant, C., Duarte, A. and Eichmann, A. (2007) 'The Notch ligand Delta-like 4 negatively regulates endothelial tip cell formation and vessel branching.', *Proceedings of the National Academy of Sciences of the United States of America*, 104(9), pp. 3225–30. doi: 10.1073/pnas.0611177104.

Sundaram, M. V (2005) 'The love-hate relationship between Ras and Notch.', *Genes & development*, 19(16), pp. 1825–39. doi: 10.1101/gad.1330605.

Tammela, T., Zarkada, G., Wallgard, E., Murtomäki, A., Suchting, S., Wirzenius, M., Waltari, M., Hellström, M., Schomber, T., Peltonen, R., Freitas, C., Duarte, A., Isoniemi, H., Laakkonen, P., Christofori, G., Ylä-Herttuala, S., Shibuya, M., Pytowski, B., Eichmann, A., *et al.* (2008) 'Blocking VEGFR-3 suppresses angiogenic sprouting and vascular network formation.', *Nature*, 454(7204), pp. 656–60. doi: 10.1038/nature07083.

Tarui, T., Takahashi, T., Nowakowski, R. S., Hayes, N. L., Bhide, P. G. and Caviness, V. S. (2005) 'Overexpression of p27 Kip 1, probability of cell cycle exit, and laminar destination of neocortical neurons.', *Cerebral cortex (New York, N.Y. : 1991)*, 15(9), pp. 1343–55. doi: 10.1093/cercor/bhi017.

Taylor, K. L., Henderson, A. M. and Hughes, C. C. W. (2002) 'Notch activation during endothelial cell network formation in vitro targets the basic HLH transcription factor HESR-1 and downregulates VEGFR-2/KDR expression.', *Microvascular research*, 64(3), pp. 372–83. doi: 10.1006/mvre.2002.2443.

del Toro, R., Prahst, C., Mathivet, T., Siegfried, G., Kaminker, J. S., Larrivee, B., Breant, C., Duarte, A., Takakura, N., Fukamizu, A., Penninger, J. and Eichmann, A. (2010) 'Identification and functional analysis of endothelial tip cell-enriched genes.', *Blood*, 116(19), pp. 4025–33. doi: 10.1182/blood-2010-02-270819.

Trichas, G., Begbie, J. and Srinivas, S. (2008) 'Use of the viral 2A peptide for bicistronic expression in transgenic mice.', *BMC biology*, 6(1), p. 40. doi: 10.1186/1741-7007-6-40.

Udan, R. S., Culver, J. C. and Dickinson, M. E. (2013) 'Understanding vascular development.', *Wiley interdisciplinary reviews. Developmental biology*, 2(3), pp. 327–46. doi: 10.1002/wdev.91.

Vempati, P., Popel, A. S. and Mac Gabhann, F. (2014) 'Extracellular regulation of VEGF: isoforms, proteolysis, and vascular patterning.', *Cytokine & growth factor reviews*. Elsevier Ltd, 25(1), pp. 1–19. doi: 10.1016/j.cytogfr.2013.11.002.

Wagner, A. J., Meyers, C., Laimins, L. A. and Hay, N. (1993) 'c-Myc induces the expression and activity of ornithine decarboxylase.', *Cell growth & differentiation : the molecular biology journal of the American Association for Cancer Research*, 4(11), pp. 879–83.

Wang, Y., Nakayama, M., Pitulescu, M. E., Schmidt, T. S., Bochenek, M. L., Sakakibara, A., Adams, S., Davy, A., Deutsch, U., Lüthi, U., Barberis, A., Benjamin, L. E., Mäkinen, T., Nobes, C. D. and Adams, R. H. (2010) 'Ephrin-B2 controls VEGF-induced angiogenesis and lymphangiogenesis.', *Nature*, 465(7297), pp. 483–6. doi: 10.1038/nature09002.

Weissman, T. A. and Pan, Y. A. (2015) 'Brainbow: new resources and emerging biological applications for multicolor genetic labeling and analysis.', *Genetics*, 199(2), pp. 293–306. doi: 10.1534/genetics.114.172510.

Wilhelm, K., Happel, K., Eelen, G., Schoors, S., Oellerich, M. F., Lim, R., Zimmermann, B., Aspalter, I. M., Franco, C. A., Boettger, T., Braun, T., Fruttiger, M., Rajewsky, K., Keller, C., Brüning, J. C., Gerhardt, H., Carmeliet, P. and Potente, M. (2016) 'FOXO1 couples metabolic activity and growth state in the vascular endothelium.', *Nature*. Nature Publishing Group, 529(7585), pp. 216–20. doi: 10.1038/nature16498.

Williams, C. K., Li, J.-L., Murga, M., Harris, A. L. and Tosato, G. (2006) 'Up-regulation of the Notch ligand Delta-like 4 inhibits VEGF-induced endothelial cell function.', *Blood*, 107(3), pp. 931–9. doi: 10.1182/blood-2005-03-1000.

Xue, Y., Gao, X., Lindsell, C. E., Norton, C. R., Chang, B., Hicks, C., Gendron-Maguire, M., Rand, E. B., Weinmaster, G. and Gridley, T. (1999) 'Embryonic lethality and vascular defects in mice lacking the Notch ligand Jagged1.', *Human molecular genetics*, 8(5), pp. 723–30. doi: 10.1093/hmg/8.5.723.

Yan, M., Callahan, C. A., Beyer, J. C., Allamneni, K. P., Zhang, G., Ridgway, J. B., Niessen, K. and Plowman, G. D. (2010) 'Chronic DLL4 blockade induces vascular neoplasms.', *Nature*. Nature Publishing Group, 463(7282), pp. E6-7. doi: 10.1038/nature08751.

Zambon, A. C. (2010) 'Use of the Ki67 promoter to label cell cycle entry in living cells.', *Cytometry. Part A : the journal of the International Society for Analytical Cytology*, 77(6), pp. 564–70. doi: 10.1002/cyto.a.20890.

Zarkada, G., Heinolainen, K., Makinen, T., Kubota, Y. and Alitalo, K. (2015) 'VEGFR3 does not sustain retinal angiogenesis without VEGFR2.', *Proceedings of the National Academy of Sciences of the United States of America*, 112(3), pp. 761–6. doi: 10.1073/pnas.1423278112.

Zeller, K. I., Jegga, A. G., Aronow, B. J., O'Donnell, K. a and Dang, C. V (2003) 'An integrated database of genes responsive to the Myc oncogenic transcription factor: identification of direct genomic targets.', *Genome biology*, 4(10), p. R69. doi: 10.1186/gb-2003-4-10-r69.

Zhao, W., McCallum, S. A., Xiao, Z., Zhang, F. and Linhardt, R. J. (2012) 'Binding affinities of vascular endothelial growth factor (VEGF) for heparin-derived oligosaccharides.', *Bioscience reports*, 32(1), pp. 71–81. doi: 10.1042/BSR20110077.

Zong, H., Espinosa, J. S., Su, H. H., Muzumdar, M. D. and Luo, L. (2005) 'Mosaic analysis with double markers in mice.', *Cell*, 121(3), pp. 479–92. doi: 10.1016/j.cell.2005.02.012.

Zong, H. (2014) 'Generation and Applications of MADM-Based Mouse Genetic Mosaic System', in *Expert Opinion on Investigational Drugs*, pp. 187–201. doi: 10.1007/978-1-4939-1215-5_10.

SUPPLEMENTARY INFORMATION

SUPPLEMENTARY INFORMATION

Supplementary Table 1

Excel file containing the list of deregulated genes identified by RNA-seq analysis of retinal endothelial cells from 3 control and 3 aDll4 treated animals. All genes analyzed (Sheet 1), downregulated genes (Sheet 2) and upregulated genes (Sheet 3). In sheet 1 genes are listed according to their adjusted p-value. In sheets 2 and 3 genes are listed according to their LogFC.

ACKNOWLEDGEMENTS

This thesis would have not been possible without the contributions of all the members, past and present, of the Molecular Genetics of Angiogenesis laboratory as well as every member of the different CNIC laboratories and technical units that has assisted, in any way, to the generation of the data presented in this work.